

From the Center of Experimental Orthopaedics

Saarland University

Director: Prof. Dr. med. Henning Madry

**rAAV-mediated gene vector incorporated in an alginate-based  
hydrogel for articular cartilage regeneration**

*Dissertation for the degree of Doctor of Medicine and Natural Sciences (MD-PhD)*

Faculty of Medicine

SAARLAND UNIVERSITY

2024

Submitted by:

Wei Liu

born on: March.08.1989 in Nei Mongol, P. R. China

Day of Oral Examination: September.12.2024

Dean of the Faculty: Univ.-Prof. Dr. med. M. D. Menger

Examinants: Prof. Dr. Magali Madry

Prof. Dr. Tim Pohlemann

Prof. Dr. Markus Huber-Lang

## **Declaration**

I hereby declare that this thesis is my own original work and effort. All experiments, except for those specified, were exclusively performed by me. Except for the publications written by myself listed in the publication list, the data presented here have not been submitted anywhere else for any award. Where other sources of information and help that have been used, they have been indicated and acknowledged.

Homburg, March.08.2024

---

Wei Liu

# CONTENT

<b>List of Abbreviations</b> .....	<b>1</b>
<b>List of Figures</b> .....	<b>7</b>
<b>List of Tables</b> .....	<b>8</b>
<b>1. ABSTRACT</b> .....	<b>9</b>
<b>2. ZUSAMMENFASSUNG</b> .....	<b>10</b>
<b>3. INTRODUCTION</b> .....	<b>11</b>
<b>3.1. Articular cartilage</b> .....	<b>11</b>
3.1.1. Microstructure and function .....	11
3.1.2. Macrostructure and function.....	13
3.1.3. Special features.....	14
3.1.4. Injuries and treatments.....	15
<b>3.2. Gene therapy for articular cartilage regeneration</b> .....	<b>16</b>
3.2.1. Gene vectors .....	17
3.2.2. Gene candidates .....	21
<b>3.3. Controlled release for gene therapy applications using alginate</b> .....	<b>27</b>
3.3.1. Alginate.....	28
3.3.2. Alginate hydrogel formation.....	29
3.3.3. Alginate hydrogel dissolution.....	30
3.3.4. Alginate hydrogel features.....	31
3.3.5. Alginate hydrogels for gene therapy applications.....	31
<b>4. HYPOTHESES</b> .....	<b>32</b>
<b>5. MATERIALS</b> .....	<b>33</b>
<b>5.1. Biological materials</b> .....	<b>33</b>
5.1.1. Tissues and cells .....	33
5.1.2. Bacteria and viruses.....	33
5.1.3. Biomolecules .....	33
<b>5.2. Chemicals</b> .....	<b>35</b>
5.2.1. Solid reagents .....	35
5.2.2. Liquid reagents.....	35
5.2.3. Analysis kits.....	36

<b>5.3. Laboratory formulations</b> .....	<b>38</b>
5.3.1. Media.....	38
5.3.2. Buffers.....	38
5.3.3. Solutions.....	39
<b>5.4. Laboratory supplies</b> .....	<b>41</b>
5.4.1. Consumables.....	41
5.4.2. Equipment.....	42
5.4.3. Software.....	43
<b>6. METHODS</b> .....	<b>44</b>
<b>6.1. Study design</b> .....	<b>44</b>
6.1.1. Ethical approvals.....	44
6.1.2. Experimental design.....	44
6.1.3. Research groups.....	46
<b>6.2. Cell culture preparation</b> .....	<b>47</b>
6.2.1. Primary human osteoarthritic articular chondrocytes (hOACs) cultures.....	47
6.2.2. Primary human mesenchymal stromal cells (hMSCs) cultures.....	47
6.2.3. Cell passaging and cell counting.....	48
<b>6.3. Production of rAAV vectors</b> .....	<b>49</b>
6.3.1. AAV-derived plasmids used in the study.....	49
6.3.2. Plasmid transformation and enrichment.....	50
6.3.3. Plasmid isolation and quantification.....	50
6.3.4. Packaging of rAAV vectors.....	51
<b>6.4. Production and manipulation of rAAV/alginate hydrogel systems</b> .....	<b>53</b>
6.4.1. Preparation of alginate hydrogels.....	53
6.4.2. Incorporation of rAAV vectors in alginate hydrogels.....	53
6.4.3. Transduction of the cell targets with the rAAV/alginate hydrogel systems.....	54
<b>6.5. Cell culture processing</b> .....	<b>55</b>
6.5.1. Cell culture fixation.....	55
6.5.2. Cell culture lysis.....	55
<b>6.6. Evaluation of rAAV vector release from the alginate hydrogel systems</b> .....	<b>55</b>
<b>6.7. Detection of transgene expression</b> .....	<b>56</b>
6.7.1. X-Gal staining.....	56
6.7.2. Live fluorescence.....	57
6.7.3. TGF- $\beta$ ELISA.....	57

6.7.4. SOX9 and TGF- $\beta$ immunodetection .....	58
<b>6.8. Biochemical analyses .....</b>	<b>58</b>
6.8.1. Hoechst 33258 assay .....	58
6.8.2. Dimethylmethylene blue (DMMB) assay .....	59
6.8.3. WST-1 assay .....	59
6.8.4. Alcian blue assay .....	60
6.8.5. Bicinchoninic acid (BCA) assay .....	60
<b>6.9. Histological analyses .....</b>	<b>61</b>
6.9.1. Hematoxylin-eosin (H&E) staining .....	61
6.9.2. Toluidine blue staining .....	61
6.9.3. Safranin O staining .....	62
6.9.4. Alizarin red staining .....	62
<b>6.10. Immunocytochemical analysis .....</b>	<b>63</b>
<b>6.11. Histomorphometrically analysis .....</b>	<b>63</b>
<b>6.12. Real-time reverse transcription polymerase chain reaction (RT-PCR) .....</b>	<b>64</b>
<b>6.13. Statistical analysis .....</b>	<b>65</b>
<b>7. RESULTS .....</b>	<b>66</b>
<b>7.1. Ability of alginate-based hydrogels to deliver rAAV vectors in human osteoarthritic articular chondrocytes .....</b>	<b>66</b>
7.1.1. Optimization of rAAV delivery in human osteoarthritic articular chondrocytes via alginate hydrogels .....	66
7.1.2. Kinetics of rAAV vector release from alginate hydrogels .....	68
<b>7.2. Ability of alginate-based hydrogels to deliver therapeutic rAAV vectors in human osteoarthritic articular chondrocytes and in human mesenchymal stromal cells .....</b>	<b>70</b>
7.2.1. Transgene expression .....	70
7.2.2. Effects on the biological and chondroreparative activities .....	76
7.2.3. Effects on the osteogenic, hypertrophic, and mineralization activities .....	82
<b>8. DISCUSSION .....</b>	<b>87</b>
<b>8.1. Ability of alginate-based hydrogels to deliver rAAV vectors in human osteoarthritic articular chondrocytes .....</b>	<b>87</b>
<b>8.2. Ability of alginate-based hydrogels to deliver therapeutic rAAV vectors in human osteoarthritic articular chondrocytes and in human mesenchymal stromal cells .....</b>	<b>89</b>
8.2.1. Transgene expression .....	89
8.2.2. Effects on the biological and chondroreparative activities .....	90

8.2.3. Effects on the osteogenic, hypertrophic, and mineralization activities .....	91
<b>8.3. Limitations and future directions .....</b>	<b>91</b>
<b>8.4. Clinical implications.....</b>	<b>92</b>
<b>9. CONCLUSIONS.....</b>	<b>94</b>
<b>10. REFERENCES.....</b>	<b>95</b>
<b>11. PUBLICATIONS AND PRESENTATIONS .....</b>	<b>113</b>
<b>11.1. Publications .....</b>	<b>113</b>
<b>11.2. Oral presentations.....</b>	<b>113</b>
<b>11.3. Poster presentations.....</b>	<b>114</b>
<b>12. ACKNOWLEDGEMENTS.....</b>	<b>115</b>
<b>13. CURRICULUM VITAE.....</b>	<b>116</b>

## List of Abbreviations

°C	Celsius
3D	three-dimensional
AAV	adeno-associated virus
ABC	avidin-biotin complex
ACAN	aggrecan
ACI	autologous chondrocyte implantation
Ad	adenovirus
ALK-1	activin receptor-like kinase-1
ALK-5	activin receptor-like kinase-5
ALP	alkaline phosphatase
AOD	average optical density
Ba <sup>2+</sup>	barium ion
BCA	bicinchoninic acid
β-gal	β-galactosidase
BMA	bone marrow aspirate
BMP	bone morphogenetic protein
BSA	bovine serum albumin
Ca <sup>2+</sup>	calcium ion
CaCl <sub>2</sub>	calcium chloride
CaCl <sub>2</sub> ·2H <sub>2</sub> O	calcium chloride-dihydrate
<i>cap</i>	capsid (open reading frame, i.e. gene)
Cap	capsid (protein)
Cd <sup>2+</sup>	cadmium ion
cDNA	complementary DNA
cm	centimeter
CMV-IE	cytomegalovirus-immediate early
CO <sub>2</sub>	carbon dioxide
Co <sup>2+</sup>	cobalt ion
Col-I	type-I collagen
Col-II	type-II collagen
Col-X	type-X collagen
COL1A1	type-I collagen (gene)

COL2A1	type-II collagen (gene)
COL10A1	type-X collagen (gene)
COMP	cartilage oligomeric protein
CSPCP	cartilage-specific proteoglycan core protein
Ct	threshold cycle
Cu <sup>2+</sup>	copper ion
CXC motif	chemokines with sequence Cys-X-Cys at C-terminal
DAB	diaminobenzidine
DMEM	Dulbecco's Modified Eagle Medium
DMMB	dimethylmethylene blue
DNA	deoxyribonucleic acid
DNase	deoxyribonuclease
dNTPs	deoxynucleotide triphosphates
<i>E. coli</i>	<i>Escherichia coli</i>
ECM	extracellular matrix
EDTA	ethylenediaminetetraacetic acid
ELISA	enzyme-linked immunosorbent assay
Eu <sup>3+</sup>	europium ion
FBS	fetal bovine serum
FGF-2	basic fibroblast growth factor
fibrin-PCL	fibrin-poly( $\epsilon$ -caprolactone)
fibrin-PU	fibrin-polyurethane
FLAG	FLAG tag
For	forward
G	1,4-linked $\alpha$ -L-guluronic acid
G (needle)	gauge
g	gram
GAGs	glycosaminoglycans
GAPDH	glyceraldehyde-3-phosphate dehydrogenase
GOI	gene of interest
h	hour
H&E	hematoxylin and eosin
H <sub>2</sub> O <sub>2</sub>	hydrogen peroxide
HA	hyaluronic acid
HBS	HEPES-buffered saline

HCl	hydrochloric acid
HEK	human embryonic kidney
HEPES	4-(2-hydroxyethyl)-1-piperazineethanesulfonic acid
hFGF-2	human basic fibroblast growth factor
hIGF-I	human insulin-like growth factor I
HIV	human immunodeficiency virus
HMG	high mobility group
hMSCs	human mesenchymal stromal cells
hOACs	human osteoarthritic articular chondrocytes
HRP	horseradish peroxidase
hsox9	human sex-determining region Y-type high mobility group box 9
HSV	herpes simplex virus
hTGF- $\beta$	human transforming growth factor beta
ICC	immunocytochemistry
IGF-I	insulin-like growth factor I
IgG	immunoglobulin G
IL-1 $\beta$	interleukin 1 beta
ITRs	inverted terminal repeats
K	kilo
kbp	kilobase pair
kg	kilogram
kPa	kilopascal
l	liter
La <sup>3+</sup>	lanthanum ion
<i>lacZ</i>	$\beta$ -galactosidase (gene)
LAP	latency-associated peptide
LB	lysogeny broth
LPL	lipoprotein lipase
M	1,4-linked $\beta$ -D-mannuronic acid
M	molar
MCS	multiple cloning site
mg	milligram
Mg <sup>2+</sup>	magnesium ion
MgCl <sub>2</sub>	magnesium chloride
ml	milliliter

mM	millimolar
MMP-13	matrix metalloproteinase 13
Mn <sup>2+</sup>	manganese ion
MOI	multiplicity of infection
MP	megapixel
MSCs	bone marrow-derived mesenchymal stromal cells
N	normal
N/A	not available
Na <sub>2</sub> HPO <sub>4</sub> -7H <sub>2</sub> O	di-sodium hydrogen phosphate heptahydrate
NaCl	sodium chloride
NaOH	sodium hydroxide
Nd <sup>3+</sup>	neodymium ion
ng	nanogram
Ni <sup>2+</sup>	nickel ion
nm	nanometer
nM	nanomolar
OD	optical density
OA	osteoarthritis
OP	osteopontin
ORFs	open reading frames
Pb <sup>2+</sup>	lead ion
PBA	peripheral blood aspirate
PBE	PBS-EDTA
PBS	phosphate-buffered saline
PCR	polymerase chain reaction
Pen/Strep	penicillin/streptomycin
PEO-PPO-PEO	poly(ethylene oxide)-poly(propylene oxide)-poly(ethylene oxide)
pg	picogram
PGs	proteoglycans
pNaSS-PCL	poly(sodium styrene sulfonate)-poly( $\epsilon$ -caprolactone)
PP	polypropylene
PPARG2	peroxisome proliferator-activated receptor gamma 2
Pr	protein
Pr <sup>3+</sup>	praseodymium ion
Pro	promoter

PS	polystyrene
PTHrP	parathyroid hormone-related protein
QPCR	quantitative polymerase chain reaction
rAAV	recombinant adeno-associated virus
rcf	relative centrifugal force
<i>rep</i>	replication (open reading frame, i.e. gene)
Rep	replication (protein)
Rev	reverse
RFP	red fluorescent protein
RNA	ribonucleic acid
RNase	ribonuclease
rpm	revolution per minute
RT	room temperature
RT-PCR	reverse transcription polymerase chain reaction
RUNX2	runt-related transcription factor 2
SD	standard deviation
SDF-1	stromal cell-derived factor 1
SMAD	mothers against decapentaplegic
SOC-Medium	super optimal medium with catabolic repressor medium
<i>sox9</i>	sex-determining region Y-type high mobility group box 9 (gene)
SOX9	sex-determining region Y-type high mobility group box 9 (protein)
Sr <sup>2+</sup>	strontium ion
ssDNA	single-stranded DNA
SZP	superficial zone protein
TAE	tris-acetate-EDTA
Tb <sup>3+</sup>	terbium ion
TE	Tris-EDTA
TEN	Tris-EDTA-NaCl
TGF-β	transforming growth factor beta
TIMPs	tissue inhibitors of metalloproteinases
TNF-α	tumor necrosis factor alpha
TβRII	type-II transforming growth factor beta receptor
v/v	volume/volume
w/v	weight/volume
Wnt	wingless and int

WST	water-soluble tetrazolium salts
X-Gal	5-bromo-4-chloro-3-indolyl- $\beta$ -D-galactopyranoside
Zn <sup>2+</sup>	zinc ion
$\mu$ g	microgram
$\mu$ l	microliter
$\mu$ M	micromolar
$\mu$ m	micrometer

## List of Figures

<b>Figure 1.</b> Structure of the articular cartilage. ....	11
<b>Figure 2.</b> Structure of AAV and of rAAV vectors and rAAV-mediated transduction.....	21
<b>Figure 3.</b> Alginate components and hydrogel formation. ....	29
<b>Figure 4.</b> Experimental design of the study. ....	45
<b>Figure 5.</b> Experimental evaluations were performed in the study.....	46
<b>Figure 6.</b> rAAV vector production in HEK-293 cells. ....	49
<b>Figure 7.</b> Optimization of rAAV delivery in human osteoarthritic articular chondrocytes via alginate hydrogels.....	68
<b>Figure 8.</b> Kinetics of rAAV release from alginate hydrogels. ....	69
<b>Figure 9.</b> Targeted transgene overexpression from the rAAV/alginate hydrogel systems in human osteoarthritic articular chondrocytes.....	73
<b>Figure 10.</b> Targeted transgene overexpression from the rAAV/alginate hydrogel systems in human mesenchymal stromal cells. ....	76
<b>Figure 11.</b> Effects of the rAAV/alginate hydrogel systems on the biological and chondrogenic activities in human osteoarthritic articular chondrocytes.....	79
<b>Figure 12.</b> Effects of the rAAV/alginate hydrogel systems on the biological and chondrogenic activities in human mesenchymal stromal cells.....	82
<b>Figure 13.</b> Effects of the rAAV/alginate hydrogel systems on the osteogenic, hypertrophic, and mineralization activities in human osteoarthritic articular chondrocytes.....	84
<b>Figure 14.</b> Effects of the rAAV/alginate hydrogel systems on the osteogenic, hypertrophic, and mineralization activities in human mesenchymal stromal cells. ....	86

## List of Tables

<b>Table 1.</b> Gene transfer vectors currently used for articular cartilage repair .....	19
<b>Table 2.</b> Application of <i>sox9</i> to enhance chondroregeneration <i>in vitro</i> .....	23
<b>Table 3.</b> Application of <i>sox9</i> to enhance articular cartilage regeneration <i>in situ</i> .....	24
<b>Table 4.</b> Application of <i>sox9</i> to enhance articular cartilage regeneration <i>in vivo</i> .....	24
<b>Table 5.</b> Application of TGF- $\beta$ to enhance chondroregeneration <i>in vitro</i> .....	26
<b>Table 6.</b> Application of TGF- $\beta$ to enhance articular cartilage regeneration <i>in situ</i> .....	27
<b>Table 7.</b> Application of TGF- $\beta$ to enhance articular cartilage regeneration <i>in vivo</i> .....	27
<b>Table 8.</b> Tissues and cells used in the studies .....	33
<b>Table 9.</b> Bacteria and viruses used in the studies.....	33
<b>Table 10.</b> Nucleic acids used in the studies .....	33
<b>Table 11.</b> Proteins used in the studies .....	34
<b>Table 12.</b> Saccharides used in the studies .....	34
<b>Table 13.</b> Commercial media used in the studies .....	35
<b>Table 14.</b> Solid reagents used in the studies .....	35
<b>Table 15.</b> Liquid reagents used in the studies.....	36
<b>Table 16.</b> Analysis kits used in the studies.....	36
<b>Table 17.</b> Reconstituted media used in the studies .....	38
<b>Table 18.</b> Buffers used in the studies.....	38
<b>Table 19.</b> Solutions used in the studies .....	39
<b>Table 20.</b> Consumables used in the studies .....	41
<b>Table 21.</b> Equipment used in the studies .....	42
<b>Table 22.</b> Software used in the studies .....	43
<b>Table 23.</b> Research groups.....	46
<b>Table 24.</b> Preparation of the rAAV/alginate hydrogel systems.....	53
<b>Table 25.</b> Preparation of the target cells for transduction .....	54
<b>Table 26.</b> Transduction conditions using the rAAV/alginate hydrogel systems .....	54

# 1. ABSTRACT

The articular cartilage has a limited capacity for self-healing and current clinical techniques met limited success to support its regeneration. Recombinant adeno-associated virus (rAAV) vectors emerged as adapted gene vehicles to treat traumatic cartilage defects and osteoarthritic lesions especially when provided via biomaterials to sites of injury. The current work examined the potential of alginate hydrogels for the controlled release of rAAV vectors to activate cartilage-specific reparative activities in human osteoarthritic chondrocytes (hOACs) and in human mesenchymal stromal cells (hMSCs) using highly chondroreparative sex-determining region Y-type high mobility group box 9 (*sox9*) and transforming growth factor beta (TGF- $\beta$ ) gene sequences. The feasibility of administering rAAV/alginate hydrogel systems upon controlled vector release was monitored in human osteoarthritic chondrocytes (this feature has been already successfully reported in human mesenchymal stromal cells) and the capability of therapeutic rAAV (*sox9*, TGF- $\beta$ )/alginate hydrogel systems to enhance chondroregeneration was tested both in human osteoarthritic chondrocytes and human mesenchymal stromal cells. Upon optimization of rAAV delivery via the alginate hydrogel (multiplicity of infection of 80, 0.2% alginate concentration, 1-minute gelation time), successful controlled release of rAAV from the rAAV/alginate hydrogel system was noted over a period of 21 days. As a result of the effective, sustained levels of *sox9* and TGF- $\beta$  overexpression via the rAAV/alginate hydrogel systems, significant enhancements in the levels of cell proliferation and of specific extracellular matrix deposition (glycosaminoglycans, proteoglycans, type-II collagen) with reduced levels of particular unwanted activities (type-I/-X collagen expression, mineralization) were overall reported in the cells. The present work demonstrates the benefits of using alginate hydrogels to control the delivery of therapeutic rAAV vectors as a means to strengthen the chondroreparative potential of human osteoarthritic chondrocytes and human mesenchymal stromal cells, paving the way for a future application of rAAV/alginate hydrogel systems as off-the-shelf treatments to improve the processes of cartilage repair in patients.

## 2. ZUSAMMENFASSUNG

Der Gelenkknorpel verfügt nur über eine begrenzte Selbstheilungskapazität, und die derzeitigen klinischen Therapien zur Unterstützung seiner Regeneration sind nur begrenzt erfolgreich. Rekombinante adeno-assoziierte virale (rAAV) Vektoren haben sich als geeignetes Genvehikel zur Behandlung traumatischer Knorpeldefekte und arthrotischer Läsionen erwiesen, insbesondere wenn sie über Biomaterialien in die Gelenkknorpeldefekte appliziert wurden. Die vorliegende Arbeit untersuchte das Potenzial von Alginat-Hydrogelen für die kontrollierte Freisetzung von rAAV-Vektoren zur Aktivierung knorpelspezifischer reparativer Aktivitäten in humanen arthrotischen Chondrozyten (hOACs) und in humanen mesenchymalen Stromazellen (hMSCs) unter Verwendung von hochchondroreparativen Gensequenzen der geschlechtsbestimmenden Region Y-Typ High Mobility Group Box 9 (*sox9*) und des transformierenden Wachstumsfaktors beta (TGF- $\beta$ ). Die Durchführbarkeit der Applikation von rAAV/Alginat-Hydrogelsystemen nach kontrollierter Freisetzung des Vektors wurde in humanen arthrotischen Chondrozyten überprüft (über diese Eigenschaft wurde bereits erfolgreich in humanen mesenchymalen Stromazellen berichtet), und die Fähigkeit der therapeutischen rAAV (*sox9*, TGF- $\beta$ )/Alginat-Hydrogelsysteme zur Verbesserung der Chondroregeneration wurde sowohl in humanen arthrotischen Chondrozyten als auch in humanen mesenchymalen Stromazellen getestet. Nach der Optimierung der rAAV-Applikation über das Alginat-Hydrogel (Infektionsmultiplikation von 80, 0,2 % Alginatkonzentration, 1 Minute Gelierzeit) wurde eine erfolgreiche kontrollierte Freisetzung von rAAV aus dem rAAV/Alginat-Hydrogelsystem über einen Zeitraum von 21 Tagen festgestellt. Infolge der effektiven, anhaltenden Überexpression von *sox9* und TGF- $\beta$  durch die rAAV/Alginat-Hydrogelsysteme zeigten die Zellen signifikante Steigerungen ihrer Proliferation und der Sekretion spezifischer extrazellulärer Matrixproteine (Glykosaminoglykane, Proteoglykane, Typ-II-Kollagen) mit reduzierten Parametern unerwünschter Aktivitäten (Typ-I/-X-Kollagen-Expression, Mineralisierung). Die vorliegende Arbeit zeigt somit die Vorteile der Verwendung von Alginat-Hydrogelen zur Kontrolle der Zuführung therapeutischer rAAV-Vektoren als Mittel zur Stärkung des chondroreparativen Potenzials von humanen arthrotischen Chondrozyten und humanen mesenchymalen Stromazellen auf. Sie ebnet den Weg für eine künftige Anwendung von rAAV/Alginat-Hydrogelsystemen als zellfreier Ansatz zur Verbesserung der Knorpelreparatur in der Klinik.

### 3. INTRODUCTION

#### 3.1. Articular cartilage

The articular cartilage is the gliding tissue covering the joints (Buckwalter & Mankin, 1998a). It supporting load transmission and translation, shock absorption, and friction reduction in synovial articulations (Anderson & Johnstone, 2017; Orth et al., 2015). The biological structure of the articular cartilage is critical to its functions (Diduch et al., 2000) (**Figure 1**).

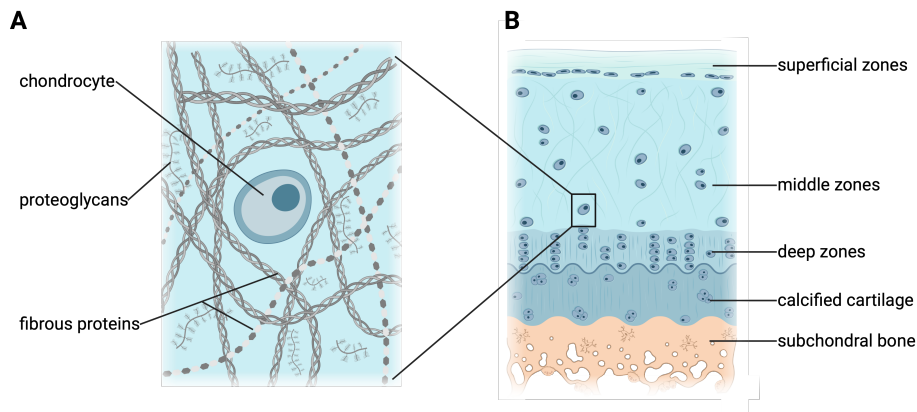


**Figure 1.** Structure of the articular cartilage. (A) Microstructure and (B) macrostructure of the native articular cartilage (created with BioRender).

##### 3.1.1. Microstructure and function

The articular cartilage is composed of chondrocytes that produce and surround themselves with a highly hydrated extracellular matrix (ECM) (Buckwalter & Mankin, 1998a; Oláh & Madry, 2018; Oláh et al., 2021) (**Figure 1A**). The chondrocytes represent the main cell type in the articular cartilage that also includes a population of stem cells (Nelson et al., 2014) or progenitor cells (Dowthwaite et al., 2004; Fellows et al., 2017; Williams et al., 2010). Altogether, these cells contribute only to 5% of the total cartilage volume (Buckwalter & Mankin, 1998a). At the adult age, these cells rarely divide but they maintain an ability to produce and retain this extracellular matrix after skeletal maturity (Coates & Fisher, 2012).

The extracellular matrix is composed of a pericellular, territorial, and interterritorial matrix (Guilak et al., 2018; Wilusz et al., 2014). The extensively studied territorial matrix can be considered as a chondron-surrounding structure consisting of a high concentration of soluble proteoglycans (PGs) with rapid turnover, embedded in a dense meshwork of fibrous proteins with low turnover (Buckwalter & Mankin, 1998a; Caron et al., 2012; Demoor-Fossard et al., 1998;

Ragan et al., 2000; Van Osch et al., 1998a) (**Figure 1A**). Proteoglycans used as a cell cushion consist of a protein core surrounded by long chains of starch-like molecules called glycosaminoglycans (GAGs) (Platt et al., 1997) which can be classified in large, predominant proteoglycans like aggrecan and in small, minor proteoglycans such as decorin, biglycan, asporin, lumican, and fibromodulin (Demoor-Fossard et al., 1998; Grogan et al., 2014; Hauselmann et al., 1994). Glycosaminoglycans include hyaluronic acid (HA), dermatan sulfate, chondroitin sulfate, heparan sulfate, and keratan sulfate (Platt et al., 1997) while the major glycosaminoglycans attached to the core protein include chondroitin-4/6-sulfate and keratan sulfate (Platt et al., 1997) and non-hyaluronic acid glycosaminoglycans interacting with hyaluronic acid lead to proteoglycans form large multi-molecular aggregates (aggregating proteoglycans) (Liu et al., 1998). Aggrecan, also known as the cartilage-specific proteoglycan core protein (CSPCP), or chondroitin-1-sulfate, is a protein encoded by the aggrecan gene in humans (Doege et al., 1991) and is always the major population of synthesized proteoglycans (Hauselmann et al., 1992; Platt et al., 1997). Its size varies depending on the age of the cartilage from which the cells are derived (Hauselmann et al., 1992). Small proteoglycans are represented by decorin and biglycan with leucine-rich regions in their core protein and chondroitin sulfate or dermatan sulfate chains respectively (Demoor-Fossard et al., 1999) and interact with type-II collagen (Demoor-Fossard et al., 1998), taking 1-2% of the total mass of the proteoglycans as essential components of the normal mature articular cartilage (Kokenyesi et al., 2000). Fibrous proteins used to support cells are composed of insoluble structural proteins providing strength and resilience (type-II collagen and other collagens) and elastin and soluble specialized proteins that bind proteoglycans and collagen fibers to receptors on the cell surface (fibronectin, laminin) (Buckwalter & Mankin, 1998a; Caron et al., 2012; Demoor-Fossard et al., 1998; Ragan et al., 2000). Type-II collagen is the basis for the hyaline cartilage formed by homotrimers of type-II collagen alpha 1 chains, representing up to 50% of all proteins and 85-90% of collagens in the tissue (Beekman et al., 1997; Bonaventure et al., 1994; Demoor-Fossard et al., 1999; Domm et al., 2004; Gagne et al., 2000; Hauselmann et al., 1994; Kuettner et al., 1991; Kuettner, 1992; Newman, 1998; Poole et al., 2001; Ragan et al., 2000). Other collagens include smaller amounts of type-VI (Gagne et al., 2000; Hauselmann et al., 1994; Kuettner et al., 1991; Kuettner, 1992; Newman, 1998; Poole et al., 2001), -IX (Beekman et al., 1997; Bonaventure et al., 1994; Demoor-Fossard et al., 1999; Domm et al., 2004; Gagne et al., 2000; Hauselmann et al., 1994; Kuettner et al., 1991; Kuettner, 1992; Newman, 1998; Poole et al., 2001; Ragan et al., 2000), -XI (Beekman et al., 1997; Bonaventure et al., 1994; Demoor-Fossard et al., 1999; Domm et al., 2004; Gagne et al., 2000; Hauselmann et al., 1994; Kuettner et al., 1991; Kuettner, 1992; Newman, 1998; Poole et al., 2001; Ragan et al., 2000), and -XIV collagen (Kuettner et al., 1991; Kuettner, 1992; Newman, 1998; Poole et al., 2001) and few type-

I/-X collagen (Schuurman et al., 2009), playing important roles in the formation and stability of fibrils in the mature articular cartilage (Petit et al., 1996). Compared with the territorial matrix, a variety of matrix molecules such as aggrecan monomers and small aggregates (Poole et al., 1982, 1991), type-VI (Poole et al., 1988, 1992) and -IX collagen (Hu et al., 2006; Poole et al., 1997), hyaluronan (Knudson, 1993; Poole et al., 1991), biglycan (Kavanagh & Ashhurst, 1999), and perlecan (SundarRaj et al., 1995), can be found either exclusively or at higher concentration in the pericellular matrix. Interactions between molecular constituents of the extracellular matrix contribute to its distinct macrostructure. Large quantities of water are confined by proteoglycans, contributing to up to 70-80% of the cartilage wet weight (Newman, 1998), opposing the deformation caused by compressive loading and tensile loading in the joint.

### 3.1.2. Macrostructure and function

The articular cartilage is subdivided in the superficial, middle, and deep zones (Buckwalter & Mankin, 1998a; Oláh & Madry, 2018; Oláh et al., 2021) (**Figure 1B**). The superficial, tangential zone is composed of ellipsoidal cells aligned parallel to the surface (Buckwalter & Mankin, 1998a). In this zone, the chondrocytes have the smallest size (Coates & Fisher, 2012) and the cell density is the most elevated (Coates & Fisher, 2012; Siczkowski & Watt, 1990; Vanderploeg et al., 2008; Wong et al., 1996). The superficial zone represents approximately 10% of the articular cartilage volume (Ulrich-Vinther et al., 2003), with the lowest biosynthetic activity (Wong et al., 1996) and the highest amounts of small proteoglycans (Miosge et al., 1994; Poole et al., 1996) and type-II (Muir et al., 1970) and -I collagen (Hayes et al., 2007) deposition. The deposition of small proteoglycans and type-II collagen decreases with the distance from the superficial zone (Schuurman et al., 2009), while clusterin (Herzog & Federico, 2006; Yamane et al., 2007) and the superficial zone protein (SZP) (Flannery et al., 1999; Schumacher et al., 1994, 1999) are found exclusively in this zone. Collagen fibers are orientated at high densities in bundles parallel to the articulating surface along with the cells, giving the superficial zone the highest ability of tensile stiffness and strength (Bank et al., 1998; Kempson et al., 1973). The middle zone is composed of randomly distributed spherical chondrocytes within a matrix with collagen fibrils arranged in an oblique orientation to the surface (Buckwalter & Mankin, 1998a), displaying a middle size at the lowest cell density (Coates & Fisher, 2012). This zone approximately accounts for 60-70% of the articular cartilage volume (Ulrich-Vinther et al., 2003) with a high deposition of hyaluronic acid (Asari et al., 1994), dermatan sulfate (Asari et al., 1994) and cartilage intermediate layer protein (Maroudas et al., 1969). The deep zone contains the largest cells (Coates & Fisher, 2012) arranged in columns aligned perpendicular to the surface (Buckwalter & Mankin, 1998a) with a

middle-range cell density (Coates & Fisher, 2012). This zone almost occupies 10-15% of the articular cartilage volume (Ulrich-Vinther et al., 2003), with the highest amounts of large proteoglycans (Muir et al., 1970), type-X collagen (Muir et al., 1970), cartilage oligomeric protein (COMP) (DiCesare et al., 1995), and keratan sulfate (Asari et al., 1994; Bayliss et al., 1983) deposition. Chondroitin sulfate has been reported to have either the highest deposition in the deep (Asari et al., 1994) or in the middle zone (Bayliss et al., 1983) depending on methods of evaluation and on the variability of the samples tested. Large proteoglycans are orientated at high density in vertical columns perpendicular to the articulating surface along with the cells, allowing the deep zone to have a higher ability of compressive and resilience (Coates & Fisher, 2012).

Differences in cell morphology, cell densities, cell metabolism, and matrix biochemical composition in each zone are the reasons of the different functions in the zonal articular cartilage (Grogan et al., 2014). The assembly of biomolecules determines the functionally defined cartilage, supporting its ability to transmit load, absorb shock, and reduce friction (Van Osch et al., 1998a), while alterations of any of its components may decrease its ability to withstand loads placed across it (Diduch et al., 2000).

### 3.1.3. Special features

The special biological features of the articular cartilage include its low cellularity, low proliferation, low cell migration, low vascularization, and low nutrition and waste diffusion, overall explaining that the articular cartilage is intrinsically unable to readily regenerate itself (Athanasidou et al., 2001; Buckwalter & Mankin, 1998b; Frenkel & Di Cesare, 1999; Hall et al., 1996; Hunziker, 2002; Mankin, 1982; Muir, 1995; O'Driscoll, 1998; Pearle et al., 2005; Sophia Fox et al., 2009; Stockwell, 1978). As a result, chondrocytes are difficult to obtain in large quantities for instance in implantation protocols in cartilage regeneration (De Ceuninck et al., 2004; Domm et al., 2004; Grunder et al., 2004; Hauselmann et al., 1992; Lemare et al., 1998). In particular, the culture and expansion of chondrocytes *in vitro* remains problematic (Buckwalter & Mankin, 1998b; Mierisch et al., 2003) since these cells differentiate into different phenotypes during expansion culture (Grandolfo et al., 1993; Van Osch et al., 1998b), including via transdifferentiation (hypertrophy/osteoblast expression) (Qin et al., 2020; Wolff & Hartmann, 2019) and dedifferentiation (fibroblast expression) (Charlier et al., 2019; Sandell & Aigner, 2001) relative to the normal differentiation state (original expression). Normally differentiated chondrocytes are found at the early stages of monolayer culture (Shakibaei & De Souza, 1997), with a main deposition of type-II collagen (Hayashi et al., 1986; von der Mark et al., 1976), aggregating proteoglycans (Colowick et al., 1987), and zonal characteristic protein (such as SZP) (Mhanna et al., 2013), accompanied by low levels of alkaline

phosphatase (ALP) activity (Grandolfo et al., 1993). Transdifferentiation chondrocytes are detected in high-density monolayer or organoid cultures (Shakibaei & De Souza, 1997) with a main deposition of type-X collagen (Beekman et al., 1997; Binette et al., 1998; Grandolfo et al., 1993), non-aggregating proteoglycans (Grandolfo et al., 1993; Liu et al., 1998), and osteopontin (OP) (Beekman et al., 1997; Binette et al., 1998; Grandolfo et al., 1993) accompanied by high levels of ALP activity (Grandolfo et al., 1993; Loty et al., 1998), matrix vesicle formation (Grandolfo et al., 1993), and endochondral ossification (Binette et al., 1998) mostly occurring at a fetal stage (Binette et al., 1998). Dedifferentiating chondrocytes are found in low density monolayer culture (majority) (Beekman et al., 1997; Darling & Athanasiou, 2005; Jonitz et al., 2011) with a main deposition of type-I/-III/-V collagen (Bonaventure et al., 1994; Caron et al., 2012; Hicks et al., 2007) and of non-aggregating proteoglycans (Liu et al., 1998; Shakibaei & De Souza, 1997) accompanied by an increase in CD44 fragmentation (Takahashi et al., 2010) and a decrease in the expression of type-II transforming growth factor beta receptor (T $\beta$ RII) and of transforming growth factor beta (TGF- $\beta$ ) response (Bauge et al., 2013) mostly occurring at an adult stage (Binette et al., 1998; Domm et al., 2004; Gagne et al., 2000). The chondrocyte phenotype is affected by factors such as the cell adhesion status and the cell shape, and it differs in monolayer and three-dimensional (3D) culture systems (Liu et al., 1998) indicating that geometric entrapment is essential for the maintenance of the chondrocyte phenotype *in vitro* (Cooke et al., 2017). Suspension with hydrogels seems to be an excellent method of geometric embedment for chondrocytes (Grandolfo et al., 1993; Grunder et al., 2004) likely promoting the retention of the original phenotype (Hauselmann et al., 1996; Heiligenstein et al., 2011a) that is precisely required for articular cartilage regeneration.

#### 3.1.4. Injuries and treatments

Articular cartilage injuries resulting from trauma or osteoarthritis (OA) (Reinhard et al., 2024), affecting more than 60% of examined patients (Widuchowski et al., 2007), may further deteriorate if left untreated (Buckwalter & Brown, 2004; Mankin, 1974). From a macroscopic perspective (morphology), changes affecting the articular cartilage include extended matrix discontinuities, clefts, and erosions, while from a microstructural point of view (pathology), they include chondrocyte hypertrophy, apoptosis, and necrosis, and a loss of proteoglycans (Buckwalter & Mankin, 1998a) that gradually and eventually lead to the formation of large cartilage defects, classified as either chondral defects restricted to the articular cartilage or osteochondral defects that further disrupt the underlying subchondral bone (Madry, et al., 2010, 2011a). The injured articular cartilage has a limited intrinsic capacity for self-healing and the chondrocytes adjacent to

the lesions do not substantially contribute to the reconstruction of the cartilage (Madry et al., 2011a).

Clinical strategies to manage articular cartilage injuries include conservative treatments to reduce pain and/or maintain mobility and surgical treatments to induce repair and/or to replace the damaged (osteo)chondral tissue (Madry et al., 2011a, Madry 2022). Conservative treatments include non-pharmacological interventions (physical therapy) and pharmacological treatments (oral, topical and intra-articular applications) and met contrasted success (Buckwalter & Mankin, 1998a; Madry et al., 2011a). Surgical interventions include marrow stimulation (e.g. microfracture), autologous chondrocyte implantation (ACI), and the transplantation of autologous or allogeneic osteochondral grafts (Madry et al., 2011a). Microfracture is an adapted procedure to repair small (< 2.5 cm<sup>2</sup>) defects, mostly in young patients (< 40) and especially suited to treat defects located in the femoral condyles (Jiang et al., 2020). ACI avoids immune rejection but needs intensive surgery to acquire chondrocytes (Jiang et al., 2020). Osteochondral graft transplantation using non-weight-bearing articular surfaces from the patient is relatively simple to perform, also avoiding immune rejection, but also suited for small defects (Jiang et al., 2020). Yet, none of these options allow to achieve full cartilage regeneration in sites of lesions. Microfracture leads to the development of a fibrocartilaginous repair tissue lacking the original hyaline structure of the native cartilage and unable to withstand mechanical loading (Cucchiariini & Madry, 2014a; Kuettner et al., 1991; Kuettner, 1992; Madry et al., 2011a; Welton et al., 2018). ACI may be complicated by phenotype changes of the chondrocytes (hypertrophy), insufficient regenerative cartilage, and disturbed fusion (Cucchiariini & Madry, 2014a; Kuettner et al., 1991; Kuettner, 1992; Madry et al., 2011a; Welton et al., 2018). Else, osteochondral graft transplantation may be impeded by disease transmission, graft failure, donor site morbidity, donor-to-recipient site incongruity, and hemarthrosis (Cucchiariini & Madry, 2014a; Kuettner et al., 1991; Kuettner, 1992; Madry, et al., 2011a; Welton et al., 2018). Overall, such outcomes show the critical need for improved strategies for cartilage regeneration (Ross et al., 2024).

### **3.2. Gene therapy for articular cartilage regeneration**

Current clinical repair techniques for articular cartilage injuries show limited success in promoting tissue restoration, meanwhile the role of genetic components in cartilage regeneration has been investigated, with findings suggesting that genetic factors contribute significantly to cartilage repair (Goh et al., 2023; Makris et al., 2015; Rai et al., 2012). Thus, gene therapy has emerged as a promising tool for cartilage regeneration, aiming at either overexpress therapeutic factors such as growth or transcription factors or to suppress the expression of genes that support the cartilage

destruction, either as a standalone approach or in combination with surgical interventions (Evans & Huard, 2015; Madry & Cucchiari, 2016; Steinert et al., 2009).

### 3.2.1. Gene vectors

Gene delivery involves introducing foreign or therapeutic gene sequences into target cells to treat specific diseases, providing prolonged expression of the transgene compared with traditional therapeutic products (Madry et al., 2020a; Rey-Rico & Cucchiari, 2016a). Nevertheless, a direct application of therapeutic gene in their recombinant forms is hindered by their short pharmacological half-life (Cucchiari & Madry, 2005) due to the susceptibility of naked deoxyribonucleic acid (DNA) to degradation by nucleases present in biological media and since the hydrophilic polyanionic nature and large size of DNA molecules prevent passive DNA penetration through the cell membrane (Ibraheem et al., 2014; Nam et al., 2009). Therefore, vectors capable of carrying therapeutic molecules in target cells must be paired with DNA (Ibraheem et al., 2014). Gene delivery vectors currently involved in articular cartilage repair include non-viral vectors (Cucchiari et al., 2015; Gelse et al., 2008; Goomer et al., 2000) and viral vehicles (Cucchiari & Madry, 2019; Garza-Veloz et al., 2013; Gelse et al., 2003; Madry et al., 2020a, 2020b; Mbita et al., 2014; Meng et al., 2020; Venkatesan et al., 2020a).

#### 3.2.1.1. *Non-viral vectors*

Gene delivery via non-viral vectors (transfection) is the incorporation of DNA alone (e.g. gene-gun technique) or complexed with plasmids (Measure et al., 2019), peptides (Qadir et al., 2019), cationic (Wang et al., 2018), anionic (Lee & Huang, 1997), ionizable polymers (Vedadghavami et al., 2022), in a target cell population (Bono et al., 2020). The use of niosomes (nioplexes) (Carballo-Pedraes et al., 2021), dendrimers (dendriplexes) (Rai et al., 2019), and gold or carbon nanostructures (Sum et al., 2018) are also more recent approaches. Non-viral vectors are generally considered safe carriers as they do not carry the risk of insertional mutagenesis (non-viral vectors are kept in episomal forms) and have low immunogenicity (non-viral vectors do not have intrinsic viral coding sequences) (Thomas et al., 2003). While, non-viral gene transfer approaches are commonly employed for the *ex vivo* modification of cells (Madry & Cucchiari, 2011) as their gene transfer (transfection) efficacy (up to 40% for primary articular chondrocytes) (Madry & Trippel, 2000) is lower than those achieved with viral vectors (Madry et al., 2003a).

### 3.2.1.2. Viral vectors

Gene delivery via viral vectors (transduction) is dependent on the natural cellular entry pathways of the viruses they are derived from (Madry & Cucchiari, 2016). Adenoviruses (Ad), retroviruses and lentiviruses, herpes simplex virus (HSV), and adeno-associated viruses (AAV) are the most common viruses which have been manipulated so far for gene transfer purposes (Madry et al., 2020b; Robbins et al., 1998).

Adenoviral vectors allow to achieve high transduction efficiencies and elevated transgene expression levels in a variety of cells (between 90% and close to 100% in chondrocytes, in particular human osteoarthritic articular chondrocytes, and up to 80% in human mesenchymal stromal cells) (Baragi et al., 1995; Doherty et al., 1998; Nixon et al., 2000), enabling direct *in vivo* application, but their use is limited by their immunogenicity and decreased transgene expression over time (1-2 weeks), mostly due to the degradation of the transduced cells by cytotoxic T cells (Cucchiari & Madry, 2010; Rey-Rico & Cucchiari, 2016a). Retroviral vectors may integrate into the genome of the host cells, enabling transgene maintenance over prolonged periods of time, but they have low transduction efficiencies (less than 20% in human mesenchymal stromal cells before cell selection) (Allay et al., 1997), do not transduce nondividing cells, and carry a risk of insertional mutagenesis that may lead to tumor gene activation (Glass et al., 2014; Murphy et al., 2003; Rey-Rico & Cucchiari, 2016a). Lentiviral vectors have been used as alternatives as they can modify nondividing cells at higher levels of efficiency (up to 95% in chondrocytes, in particular human osteoarthritic articular chondrocytes, and 70% in MSCs) (Gouze et al., 2002; Meyerrose et al., 2008), but again the problem of mutagenesis upon integration is remaining plus the psychological issues of introducing human immunodeficiency virus (HIV)-derived sequences in the host (Madry & Cucchiari, 2016). Vectors derived from the HSV have high transduction efficiencies and can infect nondividing cells but mediate only very short-term transgene expression (some days) (Rey-Rico & Cucchiari, 2016a, 2016b; Robbins & Ghivizzani, 1998; Wu et al., 2013). In marked contrast, due to their unique properties, rAAV vectors are currently the most adapted vehicles for gene transfer *in vitro* and *in vivo*, the basic details being discussed in the next paragraph. The features of non-viral and viral vectors are summarized in **Table 1**.

**Table 1.** Gene transfer vectors currently used for articular cartilage repair

Class of vectors	Structural features		Functional features		References
	Maintenance	Other features	Efficacy	Other features	
non-viral vectors	episomal	<ul style="list-style-type: none"> <li>• large capacity</li> <li>• no quiescent</li> </ul>	low	<ul style="list-style-type: none"> <li>• low immunogenicity</li> <li>• short expression</li> </ul>	(Madry et al., 2005)
adenoviral vectors	episomal	<ul style="list-style-type: none"> <li>• large capacity</li> <li>• free quiescent</li> </ul>	high	<ul style="list-style-type: none"> <li>• high immunogenicity</li> <li>• short expression</li> </ul>	(Appaiahgari & Vrati, 2015)
retroviral vectors	integrative (mutagenesis)	<ul style="list-style-type: none"> <li>• large capacity</li> <li>• no quiescent</li> </ul>	low	<ul style="list-style-type: none"> <li>• high immunogenicity</li> <li>• long expression</li> </ul>	(Hacein-Bey-Abina et al., 2008)
lentiviral vectors	integrative (mutagenesis)	<ul style="list-style-type: none"> <li>• large capacity</li> <li>• free quiescent</li> </ul>	high	<ul style="list-style-type: none"> <li>• high immunogenicity</li> <li>• long expression</li> </ul>	(Naldini et al., 1996)
HSV vectors	episomal	<ul style="list-style-type: none"> <li>• large capacity</li> <li>• free quiescent</li> </ul>	high	<ul style="list-style-type: none"> <li>• high immunogenicity</li> <li>• short expression</li> </ul>	(Goins et al., 2016)
rAAV vectors	mostly episomal	<ul style="list-style-type: none"> <li>• small capacity</li> <li>• free quiescent</li> </ul>	high	<ul style="list-style-type: none"> <li>• low immunogenicity</li> <li>• long expression</li> </ul>	(Berns & Linden, 1995)

Abbreviations: HSV: herpes simplex virus; rAAV: recombinant adeno-associated virus.

### 3.2.1.3. rAAV vectors

AAV is a replication-defective virus (genus Dependoparvovirus) of the family Parvoviridae, with a diameter of ~ 26 nanometers (nm) and a linear single-stranded DNA (ssDNA) genome of ~ 4.8 kilobase pairs (kbp) (Cucchiariini & Rey-Rico, 2017; Naso et al., 2017; Wu et al., 2010) (**Figure 2A**). The AAV genome comprises inverted terminal repeats (ITRs) at both ends of the DNA strand and the two open reading frames (ORFs, i.e. genes) *rep* (four overlapping RP78, RP68, RP52, and RP40 genes encoding Rep proteins required for the AAV life cycle) and *cap* (overlapping sequences for the VP1, VP2 and VP3 capsid proteins) (Bohenzky et al., 1988; Jay et al., 1981; Kyostio et al., 1994). rAAV vectors were originally created by deleting portions of the AAV *rep* and *cap* genes and replacing these with a transgene cassette composed of a heterologous promoter (Pro), the gene of interest (GOI), and a poly-adenylation signal (pA), demonstrating that only the ITRs are required in *cis* for the replication and packaging of rAAV genomes provided that *rep*, *cap*, and helper virus functions are provided in *trans* (Flotte, 2004). This feature leads to the nonpathogenic ability and low frequency random integration of the rAAV genome into the host genome (Daya & Berns, 2008), to the low immunogenicity of rAAV chiefly restricted to the presence of neutralizing antibodies against the AAV capsid proteins, and to almost no cytotoxicity (Chirmule et al., 1999; Hernandez et al., 1999; Ponnazhagan et al., 1997) (**Figure 2B**). rAAV vectors can infect both quiescent and dividing cells at very high gene transfer efficiencies (up to 95% in chondrocytes, in particular human osteoarthritic articular chondrocytes, and close to 92% in MSCs for at least 150 days) (Cucchiariini et al., 2011; Madry et al., 2003a; Podsakoff et al., 1994;

Rey-Rico et al., 2015a; Wu et al., 2006), with their small size enabling direct *in vivo* gene transfer through the dense extracellular matrix (Cucchiari et al., 2013; Cucchiari & Madry, 2014b; Ulrich-Vinther et al., 2004). Entry of rAAV vectors in target cells include initial receptor binding on the target cell's surface, internalization via endocytosis, escape from the endosomal compartment, localization and unpacking of the episomal genome within the nucleus, subsequent transcription and translation processes, and finally, release of the rAAV transgene product (**Figure 2C**). Overall, rAAV vectors have thus more potential to be engineered as an exclusive tool vector in gene therapy to carry candidate genes for amplifying the efficacy of cartilage regeneration therapies.

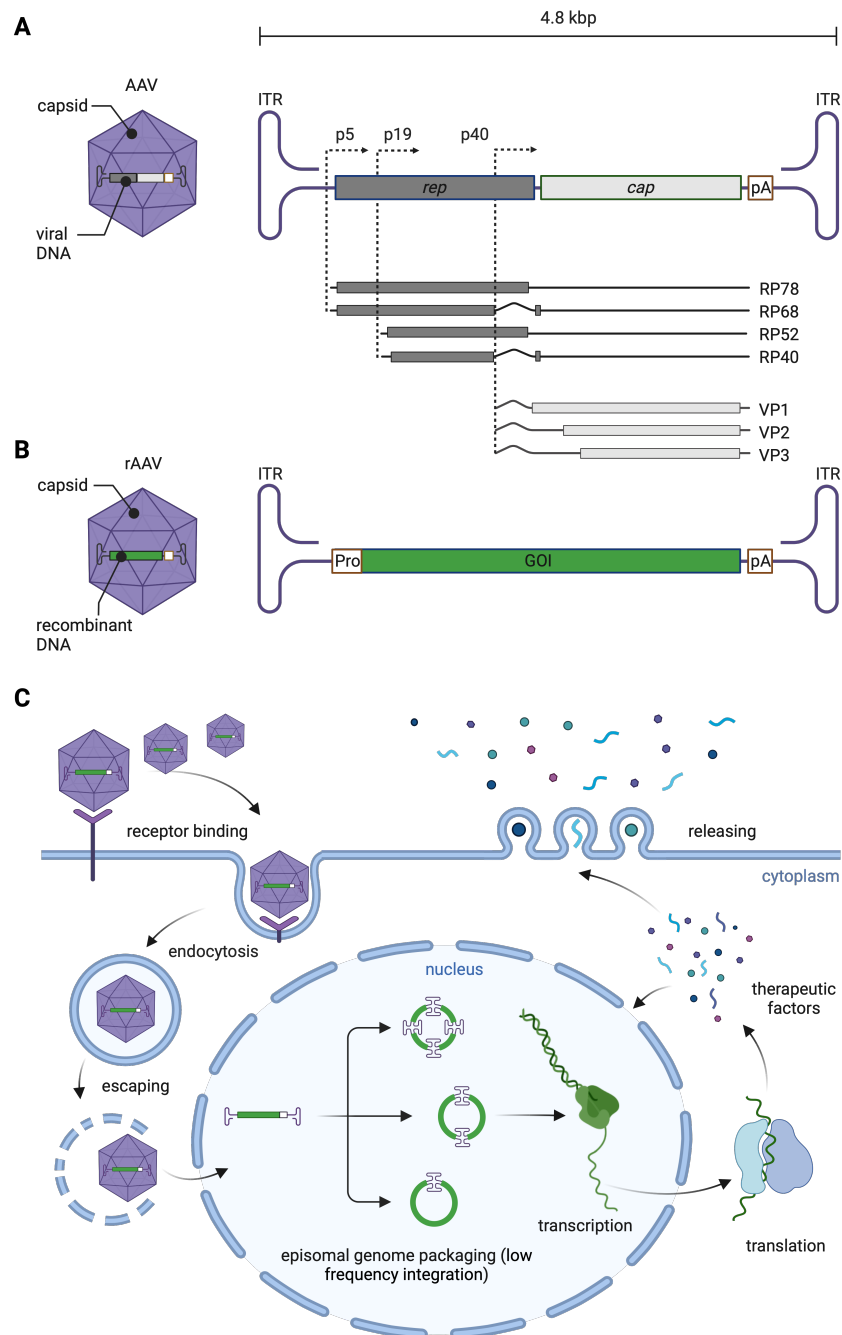


**Figure 2.** Structure of AAV and of rAAV vectors and rAAV-mediated transduction. (A) AAV particle and genome including *rep* and *cap*, (B) rAAV particles and genome including a transgene cassette composed of a heterologous promoter, the gene of interest, and a poly-adenylation signal, (C) and episomal genome packaging of rAAV transfection. Abbreviations: AAV: adeno-associated virus; *cap*: capsid (open reading frame, i.e., gene); Cap: capsid (protein); DNA: deoxyribonucleic acid; GOI: gene of interest; ITRs: inverted terminal repeats; kbp: kilobase pair; pA: poly-adenylation signal; Pro: promoter; rAAV: recombinant adeno-associated virus; *rep*: replication (open reading frame, i.e. gene); Rep: replication (protein) (created with BioRender).

### 3.2.2. Gene candidates

Gene candidates play a crucial role in gene therapy for cartilage regeneration (Hodgkinson et al., 2020; Khalid et al., 2022; Maihofer et al., 2021). Considering the roles of gene candidates for cartilage (chondro-)regeneration (Ashraf et al., 2016; Cheng et al., 2012; Steinert et al., 2009), differentiation (Ashraf et al., 2016; Cheng et al., 2012), signaling pathways (Li et al., 2023; Zhou et al., 2019), immune response (Kwon et al., 2022), network pharmacology (Ye et al., 2020; Zhang et al., 2021), and gene delivery (Frisch et al., 2016a; Yang et al., 2020), the sex-determining region Y-type high mobility group box 9 (*sox9*) and TGF- $\beta$  have been known as exclusive factors contributing to the development of effective gene-based therapies for cartilage regeneration (Cucchiaroni et al., 2013, 2018; Frisch et al., 2016a, 2016b).

#### 3.2.2.1. Structure and functions of *sox9*

The *sox9* gene is located on chromosome 17q24.3 in humans (Jedidi et al., 2018; Murakami et al., 2000; Symon & Harley, 2017). This region is characterized by relatively few genes and a high proportion of non-coding DNA (Huang et al., 2005). A 30-base pair element in the first intron of the *sox9* gene acts as an enhancer, which aids in the regulation of gene expression (Huang et al., 2005). The proximal promoter region is found between 193 and 73 bp from the transcription start site, is crucial for maximal promoter activity (Poree et al., 2008). The protein product, SOX9, has 509 amino acids and four functional domains as a transcription factor, and has the ability to bind to specific DNA sequences and one of the key functional domains of the SOX9 protein is the high mobility group (HMG) box (Chen et al., 2021). The complex structure and regulation pattern is consistent with the significant roles of *sox9* in various developmental processes (Chen et al., 2021). SOX9 is essential for the development and differentiation of skeletal elements, including cartilage, bone, and other connective tissues through the regulation of a cascade of downstream factors in a stage-specific manner (Kozhemyakina et al., 2015; Lefebvre & Dvir-Ginzberg, 2017; Murakami et al., 2000; Symon & Harley, 2017; Whyte et al., 2013). It is particularly important for chondroregeneration, the process by which cartilage is formed (Lefebvre & Dvir-Ginzberg, 2017).

Specifically, SOX9 regulates the expression of several genes involved in chondroregeneration (Bernard & Harley, 2010; Liu et al., 2017; Symon & Harley, 2017), the formation of cartilage during embryonic development (Zhao et al., 1997), the differentiation of mesenchymal cells into chondrocytes (Ikeda et al., 2004; Kozhemyakina et al., 2015; Li et al., 2018; Nishimura et al., 2017, 2018), and the cells that produce and maintain cartilage throughout life (Hattori et al., 2010a). SOX9 is also related to hypertrophic and osteogenic differentiation (Ikeda et al., 2004). The *sox9* gene is also involved in the development of the male reproductive system. In mammals, it is responsible for initiating the differentiation of the gonads into testes, which then leads to the development of male reproductive structures (Wang et al., 2017, 2021). Mutations or dysregulation of the *sox9* gene are associated with various disorders and conditions, including campomelic dysplasia (a skeletal disorder), sex reversal (abnormal development of the reproductive system), and certain forms of cancer (Argentaro et al., 2003; Fan et al., 2023; Knarston et al., 2019; Kobayashi et al., 2005; Matheu et al., 2012; Nelson et al., 2011; Tonni et al., 2013).

### 3.2.2.2. *rAAV-FLAG-hsox9* for articular cartilage regeneration

Transferring a therapeutic *sox9* gene sequence via rAAV carriers is a unique way of gene therapy for cartilage (chondro-)regeneration *in vitro* (**Table 2**), *in situ* (**Table 3**), and *in vivo* (**Table 4**). While delivery of the rAAV-FLAG-tagged human *sox9* (rAAV-FLAG-hsox9) vector has negligible effects on cellular proliferative activities, it may be empowered by an additional use of fibrin-polyurethane (fibrin-PU) scaffolds in a hydrodynamic environment (Venkatesan et al., 2018a), by combined interventions with rAAV-human basic fibroblast growth factor (rAAV-hFGF-2) (Cucchiari et al., 2009) or rAAV-human transforming growth factor beta (rAAV-hTGF- $\beta$ ) (Tao et al., 2016a, 2016b, 2017), or by the manipulation of special biomaterials such as poly(ethylene oxide)-poly(propylene oxide)-poly(ethylene oxide) (PEO-PPO-PEO) (Rey-Rico et al., 2018). Still, rAAV-FLAG-hsox9 delivery led to an increased synthesis of major extracellular matrix components (proteoglycans/glycosaminoglycans and type-II collagen) (Cucchiari et al., 2007, 2009, 2013; Daniels et al., 2019; Meng et al., 2020; Rey-Rico et al., 2018; Tao et al., 2016a, 2016b, 2017; Venkatesan et al., 2012, 2017, 2018a, 2018b, 2020a), reducing the levels of markers of hypertrophy, terminal and osteogenic/adipogenic differentiation (type-I and type-X collagen, ALP, matrix metalloproteinase 13 (MMP-13), and osteopontin with diminished expression of the osteoblast-related transcription factor runt-related transcription factor 2 (RUNX2); lipoprotein lipase (LPL), peroxisome proliferator-activated receptor gamma 2 (PPARG2), as well as their ability to undergo proper osteogenic/adipogenic differentiation (Cucchiari et al., 2013; Daniels et al., 2019; Meng et al., 2020; Rey-Rico et al., 2018; Tao et al., 2016a, 2016b, 2017; Venkatesan et

al., 2012, 2017, 2018a, 2018b, 2020a). These effects are accompanied with decreased levels of  $\beta$ -catenin (a mediator of the wingless and int-1 (Wnt-1) signaling pathway for osteoblast lineage differentiation) and enhanced parathyroid hormone-related protein (PTHrP) expression (an inhibitor of hypertrophic maturation and calcification) via *sox9* treatment (Cucchiari et al., 2013; Venkatesan et al., 2012). Moreover, rAAV-FLAG-*hsox9* can reverse the deleterious effects afforded by the OA cytokines (interleukin 1 beta, IL-1 $\beta$ , or tumor necrosis factor alpha, TNF- $\alpha$ ) (Urich et al., 2020).

**Table 2.** Application of *sox9* to enhance chondroregeneration *in vitro*

Treatments	Targets	Additional interventions	Duration/ Conditions	Proliferation/ Extracellular matrix	References
rAAV-FLAG- <i>hsox9</i>	rabbit normal chondrocytes	alginate incorporation	21 days/ 3D culture	not altered/ enhanced	(Cucchiari et al., 2013)
	human normal/OA chondrocytes	alginate incorporation	26 days/ 3D culture	not altered/ enhanced	(Cucchiari et al., 2007)
	human normal/OA chondrocytes	aggregate culture	21 days/ 3D culture	not altered/ enhanced	(Daniels et al., 2019)
	rabbit normal MSCs	N/A	21 days/ monolayer culture	not altered/ enhanced	(Cucchiari et al., 2013)
	human normal MSCs	aggregate culture	21 days/ 3D culture	not altered/ enhanced	(Venkatesan et al., 2012)
	human normal MSCs	aggregate culture/ fibrin-PU/ bioreactors	21 days/ 3D culture	enhanced/ enhanced	(Venkatesan et al., 2018a)
	minipig normal BMA	N/A	21 days/ monolayer culture	not altered/ enhanced	(Frisch et al., 2016a)
	human normal BMA	fibrin/ bioreactors	28 days/ monolayer culture	not altered/ enhanced	(Venkatesan et al., 2017)
rAAV-FLAG- <i>hsox9</i> / rAAV-hFGF-2	human normal/OA chondrocytes	alginate incorporation	26 days/ 3D culture	enhanced/ enhanced	(Cucchiari et al., 2009)
	human normal/OA chondrocytes	N/A	21 days/ monolayer culture	enhanced/ N/A	(Tao et al., 2016b)
rAAV-FLAG- <i>hsox9</i> / rAAV-hTGF- $\beta$	human normal MSCs	aggregate culture	21 days/ 3D culture	enhanced/ enhanced	(Tao et al., 2016a)
	human normal BMA	N/A	21 days/ monolayer culture	enhanced/ enhanced	(Tao et al., 2017)
	human OA chondrocytes	N/A	10 days/ monolayer culture	enhanced/ enhanced	(Rey-Rico et al., 2018)
rAAV-FLAG- <i>hsox9</i> / PEO-PPO-PEO	human OA chondrocytes	N/A	10 days/ monolayer culture	enhanced/ enhanced	(Rey-Rico et al., 2018)
rAAV-FLAG- <i>hsox9</i> / carbon dots	human normal MSCs	N/A	21 days/ monolayer culture	not altered/ enhanced	(Meng et al., 2020)
rAAV-FLAG- <i>hsox9</i> / pNaSS-PCL	human normal BMA	N/A	21 days/ monolayer culture	not altered/ enhanced	(Venkatesan et al., 2020a)

Abbreviations: 3D: three-dimensional; BMA: bone marrow aspirate; fibrin-PCL: fibrin-poly( $\epsilon$ -caprolactone); fibrin-PU: fibrin-polyurethane; FLAG: FLAG tag; hFGF-2: human basic fibroblast growth factor; hsox9: human sex-determining region Y-type high mobility group box 9; hTGF- $\beta$ : human transforming growth factor beta; MSCs: bone marrow-derived mesenchymal stromal cells; N/A: not available; OA: osteoarthritis; PEO-PPO-PEO: poly(ethylene oxide)-poly(propylene oxide)-poly(ethylene oxide); pNaSS-PCL: poly(sodium styrene sulfonate)-poly( $\epsilon$ -caprolactone); rAAV: recombinant adeno-associated virus.

**Table 3.** Application of sox9 to enhance articular cartilage regeneration *in situ*

Treatments	Targets	Additional interventions	Duration/ Conditions	Proliferation/ Extracellular matrix	References
rAAV-FLAG-hsox9	human normal/OA cartilage	N/A	10 days	not altered/enhanced	(Cucchiari et al., 2007)
rAAV-FLAG-hsox9/ rAAV-hFGF-2	human normal/OA cartilage	N/A	10 days	enhanced/enhanced	(Cucchiari et al., 2009)
rAAV-FLAG-hsox9/ rAAV-hTGF- $\beta$	human normal/OA cartilage	N/A	21 days	N/A/enhanced	(Tao et al., 2016b)
rAAV-FLAG-hsox9/ PEO-PPO-PEO	human OA cartilage	N/A	10 days	enhanced/enhanced	(Rey-Rico et al., 2018)

Abbreviations: FLAG: FLAG tag; hFGF-2: human basic fibroblast growth factor; hsox9: human sex-determining region Y-type high mobility group box 9; hTGF- $\beta$ : human transforming growth factor beta; N/A: not available; OA: osteoarthritis; PEO-PPO-PEO: poly(ethylene oxide)-poly(propylene oxide)-poly(ethylene oxide); rAAV: recombinant adeno-associated virus.

**Table 4.** Application of sox9 to enhance articular cartilage regeneration *in vivo*

Treatments	Species	Targets	Duration/ Conditions	Proliferation/ Extracellular matrix	References
rAAV-FLAG-hsox9	rabbit	normal osteochondral defect	16 weeks	not altered/enhanced	(Cucchiari et al., 2013)
rAAV-FLAG-hsox9	sheep	normal osteochondral defect	24 weeks	not altered/enhanced	(Lange et al., 2021)
rAAV-FLAG-hsox9/ PEO-PPO-PEO	minipig	normal chondral defect	4 weeks	enhanced/enhanced	(Madry et al., 2020a)

Abbreviations: FLAG: FLAG tag; hsox9: human sex-determining region Y-type high mobility group box 9; PEO-PPO-PEO: poly(ethylene oxide)-poly(propylene oxide)-poly(ethylene oxide); rAAV: recombinant adeno-associated virus.

### 3.2.2.3. Structure and functions of TGF- $\beta$

The TGF- $\beta$  genes are encoded by three separate genes (TGF $\beta$ 1, TGF $\beta$ 2, and TGF $\beta$ 3) in humans. Each of these genes produces a different type of TGF- $\beta$  protein (TGF- $\beta$ 1, TGF- $\beta$ 2, and TGF- $\beta$ 3 respectively) (Komai et al., 2018; Tominaga & Suzuki, 2019). All TGF- $\beta$  types are encoded as large protein precursors (Tominaga & Suzuki, 2019). TGF- $\beta$ 1 contains 390 amino acids, while TGF- $\beta$ 2 and TGF- $\beta$ 3 each contain 412 amino acids (Tominaga & Suzuki, 2019). Each TGF- $\beta$  protein has

an N-terminal signal peptide of 20-30 amino acids required for secretion from a cell, a pro-region named latency-associated peptide (LAP), and a 112-114 amino acid C-terminal region that becomes the mature TGF- $\beta$  molecule following its release from the pro-region by proteolytic cleavage (Dallas et al., 2002; Tominaga & Suzuki, 2019). TGF- $\beta$  proteins perform many cellular functions during metabolism (Goncalves Junior et al., 2016; Huang et al., 2020; Lee, 2018; Tominaga & Suzuki, 2019). TGF- $\beta$  controls cell proliferation, differentiation, and apoptosis (programmed cell death) in a wide range of cell types (Kwon et al., 2011). TGF- $\beta$  is crucial for embryonic development and tissue morphogenesis, and plays a role in regulating inflammation and immune responses (Liu et al., 2021). TGF- $\beta$  stimulates the synthesis of extracellular matrix components by regulating the homeostasis between extracellular matrix synthesis and degradation (Hu et al., 2022; Zou et al., 2021). TGF- $\beta$  also stimulates the migration and proliferation of fibroblasts, which are responsible for producing the extracellular matrix and promoting tissue regeneration (Blaney Davidson et al., 2009; Chen et al., 2012; Wu et al., 2008). TGF- $\beta$  signaling interacts with numerous other signaling pathways, such as the Wnt, Notch, bone morphogenetic protein (BMP) and mothers against decapentaplegic (SMAD) pathways and dysregulation of TGF- $\beta$  signaling has been implicated in various diseases, including OA-like disease characterized by severe cartilage degeneration and chondrocyte hypertrophy and other disease like cancer, fibrosis, autoimmune disorders, and cardiovascular disorder (Hasson et al., 2010; Honda et al., 2017; Hu et al., 2022; Kwon et al., 2011; Oliveira Silva et al., 2020; Remst et al., 2014; Shen et al., 2013; Su et al., 2019; Thielen et al., 2019; Tu et al., 2021; Van der Kraan, 2017; Yang et al., 2022).

#### 3.2.2.4. *rAAV-hTGF- $\beta$ for articular cartilage regeneration*

Genetic modification using TGF- $\beta$  may provide a valuable strategy for cartilage (chondro-)regeneration *in vitro* (**Table 5**), *in situ* (**Table 6**), and *in vivo* (**Table 7**). The expression of TGF- $\beta$  achieved via rAAV gene transfer enhances both the proliferative via activation of the stromal cell-derived factor 1 (SDF-1)/chemokine (chemokines with sequence Cys-X-Cys at C-terminal, CXC motif) receptor 4 pathway (Asen et al., 2018) and cartilage matrix deposition (proteoglycans/glycosaminoglycans and type-II collagen) (Venkatesan et al., 2013) via stimulation of the critical *sox9* chondroregenerative pathway (Frisch et al., 2014), which may be reinforced with combined interventions using rAAV-human insulin-like growth factor I (hIGF-I) (Morscheid et al., 2019a) or rAAV-FLAG-h*sox9* (Tao et al., 2016a, 2016b, 2017), or using special biomaterials such as PEO-PPO-PEO (Rey-Rico et al., 2017), carbon dots (Meng et al., 2020), or poly(sodium styrene sulfonate)-poly( $\epsilon$ -caprolactone) (pNaSS-PCL) (Venkatesan et al., 2021). Notably,

sustained rAAV production of TGF- $\beta$  reduces the expression of chondrocyte hypertrophic and osteogenic and terminal differentiation (type-I collagen, type-X collagen, MMP-13, PTHrP,  $\beta$ -catenin) while increasing that of protective tissue inhibitors of metalloproteinases (TIMPs) and of the TGF- $\beta$  receptor I in a manner that restores a favorable activin receptor-like kinase-1/activin receptor-like kinase-5 (ALK1/ALK5) balance (Frisch et al., 2016b; Meng et al., 2020; Morscheid et al., 2019a, 2019b; Rey-Rico et al., 2017; Tao et al., 2016a, 2016b, 2017; Venkatesan et al., 2013, 2021). Strikingly, in the conditions applied elsewhere, hypertrophy and osteogenic differentiation events may also be activated by rAAV-hTGF- $\beta$  in association with enhanced levels of  $\beta$ -catenin and Indian hedgehog and decreased PTHrP expression (Cucchiari et al., 2018; Frisch et al., 2014, 2017). Translation of the current approach may yet need to regulate TGF- $\beta$  expression (Cucchiari et al., 2018; Frisch et al., 2014, 2017).

**Table 5.** Application of TGF- $\beta$  to enhance chondroregeneration *in vitro*

Treatments	Targets	Additional interventions	Duration/ Conditions	Proliferation/ Extracellular matrix	References
rAAV-hTGF- $\beta$	human normal/OA chondrocytes	N/A	21 days/ monolayer culture	enhanced/ enhanced	(Venkatesan et al., 2013)
	human normal MSCs	N/A	21 days/ monolayer culture	enhanced/ enhanced	(Frisch et al., 2014)
	human normal MSCs	aggregate culture	21 days/ 3D culture	enhanced/ enhanced	(Frisch et al., 2014)
	minipig normal BMA	N/A	21 days/ monolayer culture	enhanced/ enhanced	(Frisch et al., 2016a)
	human normal BMA	N/A	21 days/ monolayer culture	enhanced/ enhanced	(Frisch et al., 2016b)
	human normal PBA	N/A	21 days/ monolayer culture	enhanced/ enhanced	(Frisch et al., 2017)
rAAV-hTGF- $\beta$ / rAAV-hIGF-I	human normal MSCs	aggregate culture	21 days/ 3D culture	enhanced/ enhanced	(Morscheid et al., 2019a)
rAAV-hTGF- $\beta$ / rAAV-FLAG-hsox9	human normal/OA chondrocytes	N/A	21 days/ monolayer culture	enhanced/ N/A	(Tao et al., 2016b)
	human normal MSCs	aggregate culture	21 days/ 3D culture	enhanced/ enhanced	(Tao et al., 2016a)
	human normal BMA	N/A	21 days/ monolayer culture	enhanced/ enhanced	(Tao et al., 2017)
rAAV-hTGF- $\beta$ / PEO-PPO-PEO	human OA chondrocytes	N/A	10 days/ monolayer culture	enhanced/ enhanced	(Rey-Rico et al., 2017)
rAAV-hTGF- $\beta$ / carbon dots	human normal MSCs	N/A	21 days/ monolayer culture	enhanced/ enhanced	(Meng et al., 2020)
rAAV-hTGF- $\beta$ / pNaSS-PCL	human normal BMA	N/A	21 days/ monolayer culture	enhanced/ enhanced	(Venkatesan et al., 2021)

Abbreviations: 3D: three-dimensional; BMA: bone marrow aspirate; FLAG: FLAG tag; hIGF-I: human insulin-like growth factor I; hsox9: human sex-determining region Y-type high mobility group box 9; hTGF- $\beta$ : human transforming growth factor beta; MSCs: bone marrow-derived mesenchymal stromal cells; N/A: not available; OA: osteoarthritis; PBA: peripheral blood aspirate; PEO-PPO-PEO: poly(ethylene oxide)-poly(propylene oxide)-poly(ethylene oxide); pNaSS-PCL: poly(sodium styrene sulfonate)-poly( $\epsilon$ -caprolactone); rAAV: recombinant adeno-associated virus.

**Table 6.** Application of TGF- $\beta$  to enhance articular cartilage regeneration *in situ*

Treatments	Targets	Additional interventions	Duration/ Conditions	Proliferation/ Extracellular matrix	References
rAAV-hTGF- $\beta$	human normal/OA cartilage	N/A	90 days	enhanced/ enhanced	(Venkatesan et al., 2013)
rAAV-hTGF- $\beta$ / rAAV-hIGF-I	human OA cartilage	aggregated MSCs	21 days	enhanced/ enhanced	(Morscheid et al., 2019b)
rAAV-hTGF- $\beta$ / rAAV-FLAG-hsox9	human normal/OA cartilage	N/A	21 days	N/A/ enhanced	(Tao et al., 2016b)
rAAV-hTGF- $\beta$ / PEO-PPO-PEO	human OA cartilage	N/A	10 days	enhanced/ enhanced	(Rey-Rico et al., 2017)

Abbreviations: FLAG: FLAG tag; hIGF-I: human insulin-like growth factor I; hsox9: human sex-determining region Y-type high mobility group box 9; hTGF- $\beta$ : human transforming growth factor beta; MSCs: bone marrow-derived mesenchymal stromal cells; N/A: not available; OA: osteoarthritis; PEO-PPO-PEO: poly(ethylene oxide)-poly(propylene oxide)-poly(ethylene oxide); rAAV: recombinant adeno-associated virus.

**Table 7.** Application of TGF- $\beta$  to enhance articular cartilage regeneration *in vivo*

Treatments	Species	Targets	Duration/ Conditions	Proliferation/ Extracellular matrix	References
rAAV-hTGF- $\beta$	minipig	normal osteochondral defect	4 weeks	enhanced/ enhanced	(Cucchiariini et al., 2018)

Abbreviations: hTGF- $\beta$ : human transforming growth factor beta; rAAV: recombinant adeno-associated virus.

### 3.3. Controlled release for gene therapy applications using alginate

Gene therapy of rAAV-FLAG-hsox9 and rAAV-hTGF- $\beta$  has shown promise for cartilage regeneration (Cucchiariini & Madry, 2005, 2019; Madry & Cucchiariini, 2016; Madry et al., 2020a). Yet, an adapted application of rAAV-therapeutic gene candidate in the clinical situation is still restricted by possible immune responses in the recipient including a pre-existence of neutralizing antibodies against the AAV capsid proteins in the human population (Rey-Rico et al., 2016a), which may be addressed by a controlled release of rAAV vectors from biomaterials to protect the viral capsids against such neutralization while enhancing the spatial and temporal availability of therapeutic gene in a defined target (Madry et al., 2020a; Meng et al., 2020; Rey-Rico et al., 2015b, 2017, 2018; Venkatesan et al., 2021, 2020a). While encouraging data are reported, none

of the tested biomaterials gave thus far full satisfaction in terms of complete tissue repair (Cucchiariini & Madry, 2019), supporting the concept of testing novel biological material for the controlled release of therapeutic rAAV vectors in an improved manner (Xu et al., 2024).

Alginate has been used as a biocompatible material that can easily form hydrogels under mild conditions with a lack of immunogenicity and of inflammatory responses, making it a promising system for various tissue engineering approaches (Glukhova et al., 2021; Liu et al., 2022), especially as an experimental controlled release platform.

### 3.3.1. Alginate

Alginates are an unbranched linear copolymers composed of 1,4-linked  $\beta$ -D-mannuronic acid (M) and 1,4-linked  $\alpha$ -L-guluronic acid (G) with regions exclusively composed of one unit or of the other (consecutive M block/residues, consecutive G block/residues) or with regions where the monomers approximate an alternating sequence (alternating MG block/residues) (Li et al., 2019; Loredo et al., 1996), which can be isolated from brown algae (Saltz & Kandalam, 2016; Van Susante et al., 1995) that belong to phaeophyceae (seaweeds) (Loredo et al., 1996; Yang et al., 2013) or are extracted from bacteria such as *Pseudomonas* or *Azotobacter* (Sun & Tan, 2013) (**Figures 3A-3C**). Alginate can be of nonbiomedical- or biomedical-grade quality (mostly employed) (Heiligenstein et al., 2011a), of low (commonly used), medium, or high viscosity (Heiligenstein et al., 2011a), and of low or high molecular weight (also termed polymer chain length) (Loredo et al., 1996). Alginate is hydrophilic, water-soluble, and thickening in neutral conditions, and can form hydrogel when present in polyvalent cations (Homicz et al., 2003; Madry et al., 2014).

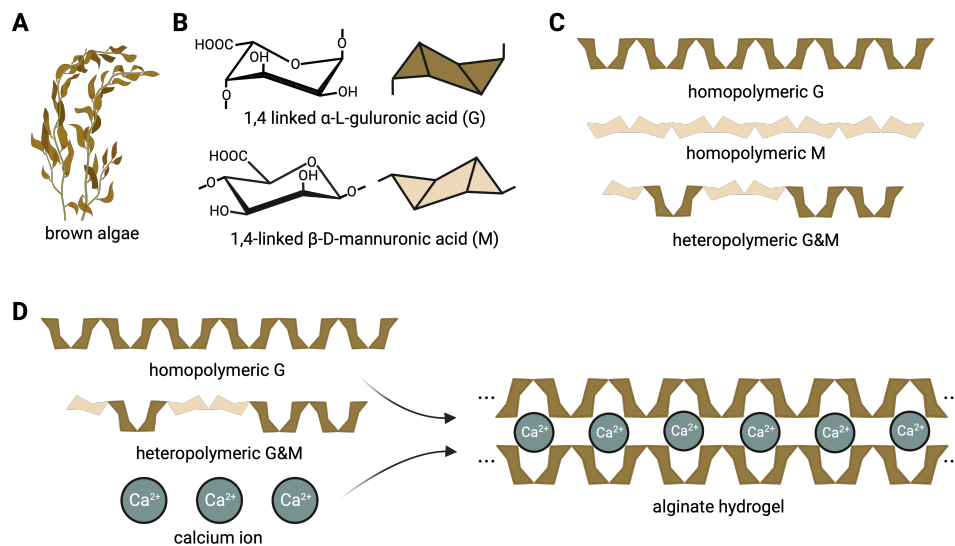


**Figure 3.** Alginate components and hydrogel formation. (A-B) Alginate components include G and M, (C) and their combination termed homopolymeric G, homopolymeric M, and homopolymeric G&M, (D) and alginate gelation via ionic bridges formation between homopolymeric G and calcium ion. Abbreviations: Ca<sup>2+</sup>: calcium ion; G: 1,4-linked  $\alpha$ -L-guluronic acid; M: 1,4-linked  $\beta$ -D-mannuronic acid (created with BioRender).

### 3.3.2. Alginate hydrogel formation

Gelation occurs when polyvalent cations cooperatively interact with blocks of M/G monomers to form ionic bridges (Loredo et al., 1996; Paige & Vacanti, 1995; Sun & Tan, 2013) followed by the formation of the 3D hydrogel network via Van der Waals forces between alginate segments (Gaumann et al., 2000; Khan & Ahmad, 2013) (**Figure 3D**). Cations that crosslink with alginate hydrogels include divalent cations (calcium ion-Ca<sup>2+</sup>, barium ion-Ba<sup>2+</sup>, strontium ion-Sr<sup>2+</sup>, cadmium ion-Cd<sup>2+</sup>, cobalt ion-Co<sup>2+</sup>, copper ion-Cu<sup>2+</sup>, manganese ion-Mn<sup>2+</sup>, nickel ion-Ni<sup>2+</sup>, lead ion-Pb<sup>2+</sup>, zinc ion-Zn<sup>2+</sup>) (Abbah et al., 2008; Chen et al., 2007; DeRamos et al., 1997; Knight et al., 2002; Mierisch et al., 2003; Sun & Tan, 2013; Tigli & Gumusderelioglu, 2009; Wang et al., 2003; Wong, 2004; Wong et al., 2001), trivalent cations (lanthanum ion-La<sup>3+</sup>, praseodymium ion-Pr<sup>3+</sup>, neodymium ion-Nd<sup>3+</sup>, europium ion-Eu<sup>3+</sup>, terbium ion-Tb<sup>3+</sup>) (DeRamos et al., 1997), or multiple cations (Co<sup>2+</sup> and Ca<sup>2+</sup>) (Focaroli et al., 2016) but neither magnesium ion-Mg<sup>2+</sup> nor monovalent cations (Chen et al., 2007; DeRamos et al., 1997; Goh et al., 2012). During crosslinking, divalent metal ions exhibit a preference for GG blocks and an increase in the extent of binding when increasing ionic radius, while trivalent metal ions display a preference for GG blocks and an increase in the extent of binding for both GG and MM blocks when increasing the charge density (DeRamos et al., 1997). The contrast in the modes of interaction of divalent and trivalent cations with alginic acid may be related to differences in coordination number and/or to hydration remaining in the inner sphere of ions (DeRamos et al., 1997).

The physicochemical and bioscaffold properties of alginate have been reported to depend on the M/G ratio (Hunt & Grover, 2010; Park et al., 2009) and on the concentration of the alginate and gelling solutions (Ca<sup>2+</sup>) (Paige & Vacanti, 1995). First, M/G ratios differ according to the source of raw material used in alginate manufacture (Hunt & Grover, 2010; Park et al., 2009), with high M/G ratio alginates primarily derived from *Macrocystis pyrifera* (Loredo et al., 1996)/*Durvillea potarum* (Dornish et al., 2001) and low M/G ratio alginates from *Laminaria hyperboreana* (Loredo et al., 1996). M/G ratios have also an impact on the biological activities of the chondrocytes at incorporation, including cell adhesion, colonization, migration, nutrition diffusion, and proliferation (Wang et al., 2003). Low M/G ratio alginates retain greater tensile strength (Hunt & Grover, 2010; Wang et al., 2003), offering a substrate against which traction can be exerted and therefore aid cell adhesion, colonization, and subsequent migration (Wang et al., 2003). Additionally, the

diffusion of large molecules is impeded by alginate, an effect that is less evident for alginates with low M/G ratio (Enobakhare et al., 2006). In this regard, low M/G ratio alginates allow for optimal cell proliferation (Heiligenstein et al., 2011a). The mechanical properties which include dynamic modulus, peak strain, and peak stress is improved when using low M/G ratio alginates while high M/G ratio alginates yield weaker and more elastic hydrogels (Andrade et al., 2011; Loredo et al., 1996; Wong et al., 2001). Second, alginate concentrations of 0.5-4% (weight/volume, w/v) and  $\text{Ca}^{2+}$  concentrations of 15-144 mM have been reported to be suitable for cartilage regeneration (Jang et al., 2014; Paige et al., 1996). A hydrogel with optimal handling characteristics can be obtained with alginate at 1-1.5% (w/v) and  $\text{Ca}^{2+}$  at 30-50 mM (Paige & Vacanti, 1995). Most research was developed with alginate at 1.2% (w/v) and  $\text{Ca}^{2+}$  at 102 mM (Chuang et al., 2012; Cohen et al., 2003; Guo et al., 1989; Hwang et al., 2007; Jin et al., 2007; Madry et al., 2003b, 2005; Marijnissen et al., 2002; Samuel et al., 2018; Stockwell, 1978; Varshney et al., 2010). The adhesion, colonization, and migration of embedded cells are enhanced when increasing the concentration of alginate (Enobakhare et al., 2006; Ren et al., 2012) or of  $\text{Ca}^{2+}$  (Jang et al., 2014; Khan & Ahmad, 2013), while the diffusion of large molecules becomes gradually impeded (Enobakhare et al., 2006; Wang et al., 2008). The effects of the alginate and  $\text{Ca}^{2+}$  concentrations occur in a dose-dependent manner (Ren et al., 2012; Zhang et al., 2020). Of note, the stiffness (Enobakhare et al., 2006) and compressive modulus (Ren et al., 2012) increase with the alginate concentration and the compressive while the shear moduli increase with the  $\text{Ca}^{2+}$  concentration (Jang et al., 2014). At low  $\text{Ca}^{2+}$  concentrations, temporary hydrogels can be obtained as highly viscose solutions while stable gelation may result from permanent associations of crosslinking structures at high  $\text{Ca}^{2+}$  levels (Khan & Ahmad, 2013). Specially,  $\text{Ca}^{2+}$  concentrations of 36-, 72-, and 144-mM using alginate at 2% has no effect on hydrogel degradation (Jang et al., 2014).

### 3.3.3. Alginate hydrogel dissolution

Alginate hydrogels dissolve upon loss of polyvalent cations, releasing high and low molecular weight alginate strands (Bouhadir et al., 2001) via spontaneous or induced dissolution. Spontaneous dissolution occurs upon substitution of crosslinking polyvalent by monovalent ions such as  $\text{Na}^+$  (Smidsrød & Skjåk-Braek, 1990). Large differences are reported in dissolving times (Ishikawa et al., 1999; Matthew et al., 1995; Wu et al., 2002) possibly as a result of differences in experimental models, implant volumes, material forms, and external environment (Wang et al., 2003). Induced dissolution occurs by chelation of crosslinking polyvalent ions with dissolving buffer (Loredo et al., 1996; Petit et al., 1996; Shakibaei & De Souza, 1997; Wan et al., 2008) including ethylenediaminetetraacetic acid (EDTA) (50 mM) (De Ceuninck et al., 2004; Wan et al., 2008),

citrate (55 mM sodium citrate in 0.15 M NaCl) (Jonitz et al., 2011; Wan et al., 2008), and phosphate solution (Grandolfo et al., 1993; Shakibaei & De Souza, 1997). Typically, 50 mM EDTA is more cytotoxic than 55 mM citrate and 55 mM citrate is more cytotoxic than phosphate-buffered saline (PBS) when dissolved for the same period of time (Cohen et al., 2011). One of the major advantages of alginate is that the hydrogel where cells entrapped can be dissolved by chelation (Hauselmann et al., 1992, 1994).

#### 3.3.4. Alginate hydrogel features

Alginate hydrogels can be prepared in a microscopically homogeneous manner (Aydelotte et al., 1998) with a compression modulus from 1 to 1,000 kilopascal (kPa) (Drury et al., 2004) and a shear modulus from 0.02 to 40 kPa (Drury et al., 2004). Such hydrogels exhibit pH-responsive properties, with higher swelling ratios when increasing pH values due to chain expansion from the presence of ionic carboxylate groups on the backbone (Sun & Tan, 2013).

#### 3.3.5. Alginate hydrogels for gene therapy applications

Alginate has gained significant attention in the field of tissue engineering due to its physiochemical and mechanical features that allow this material to form hydrogels (Lee & Mooney, 2012). The ability of alginate to mimic the native extracellular matrix also provides a unique opportunity to generate adapted scaffolds for the regeneration of cartilage tissue (Liu et al., 2022). The incorporation of rAAV vectors within alginate hydrogels and their release from such hydrogels, based on the concept of alginate-based cell delivery and implantation for articular cartilage regeneration (Heiligenstein et al., 2011a, 2011b; Kaul et al., 2006; Madry et al., 2003b, 2005), is a feasible and attractive method that has been explored by our institute using rAAV vectors carrying a reporter gene (*lacZ* coding for  $\beta$ -galactosidase) to genetically modify reparative human mesenchymal stromal cells in a spatiotemporal, controlled delivery manner (Diaz-Rodriguez et al., 2015). Yet, there is no data indicating that this innovative, alginate hydrogel-guided rAAV vector delivery system (1) can be applied to human osteoarthritic articular chondrocytes as another source of cells relevant of articular cartilage regeneration and (2) can deliver therapeutic genes such as *sox9* and TGF- $\beta$  in either human osteoarthritic articular chondrocytes or human mesenchymal stromal cells as an effective tool to durably trigger the reparative activities of these targets for improved cartilage (chondro-)regeneration. The focus of this thesis was therefore to investigate this novel strategy to offer convenient, future therapeutic options for the treatment of articular cartilage lesions.

## 4. HYPOTHESES

The goal of this thesis was therefore to evaluate - for the first time to our best knowledge- the potential of alginate hydrogels to incorporate and deliver therapeutic rAAV vectors as highly innovative systems to stimulate the reparative activities of human osteoarthritic articular chondrocytes and human mesenchymal stromal cells via administration of highly potential genes coding for the SOX9 and TGF- $\beta$  factors as future sources of improved therapeutic cells for the purpose of articular cartilage regeneration.

To implement this strategy, the following hypotheses were tested:

- 1. Alginate-based hydrogels are capable of efficiently and durably incorporating and delivering rAAV vectors as a means to genetically modify human osteoarthritic articular chondrocytes.***
- 2. Alginate-based hydrogels are capable of efficiently and durably incorporating and delivering therapeutic (sox9, TGF- $\beta$ ) rAAV vectors to both reparative human osteoarthritic articular chondrocytes and human mesenchymal stromal cells in order to stimulate their reparative activities for the purpose of improved articular cartilage regeneration.***

## 5. MATERIALS

### 5.1. Biological materials

#### 5.1.1. Tissues and cells

**Table 8.** Tissues and cells used in the studies

Tissues and cells	Origin or Manufacturers
HEK-293 cells	Gene Therapy Center of University of Pittsburgh (PA, USA)
human bone marrow aspirates	Department of Orthopaedic Surgery, Saarland University Hospital, (Homburg, Germany)
human femoral condyles	Department of Orthopaedic Surgery, Saarland University Hospital, (Homburg, Germany)

Abbreviation: HEK: human embryonic kidney.

#### 5.1.2. Bacteria and viruses

**Table 9.** Bacteria and viruses used in the studies

Bacteria and viruses	Specifications	Manufacturers
Ad5 helper virus (sheared)	N/A	Gene Therapy Center of University of North Carolina (NC, USA)
<i>E. coli</i>	One Shot TOP10	Invitrogen (Karlsruhe, Germany)

Abbreviations: Ad: adenovirus; *E. coli*: *Escherichia coli*; N/A: not available.

#### 5.1.3. Biomolecules

**Table 10.** Nucleic acids used in the studies

Category	Nucleic acids	Specifications	Manufacturers
DNA	DNA	D1501, 50 mg	Sigma (Taufkirchen, Germany)
	hsox9 cDNA	with FLAG tag, 1.7 kbp	Institute for Human Genetics and Anthropology of Albert-Ludwig University (Freiburg, Germany)
	hTGF- $\beta$ cDNA	pORF9-hTGF $\beta$ 1, 1.2 kbp	Invivogen (Toulouse, France)
	<i>lacZ</i> cDNA	N/A	Division of Infectious Disease of Harvard Medical School (MA, USA)
	RFP cDNA	N/A	Division of Infectious Disease of Harvard Medical School (MA, USA)
plasmids	AAV-2 plasmid	from pSSV9, with CMV-IE	Gene Therapy Center of University of North Carolina (NC, USA)
	Ad8 helper plasmid	from pSSV9, with <i>rep</i> and <i>cap</i>	Gene Therapy Center of University of North Carolina (NC, USA)
primers	ACAN For	NDPRXMJ, GAGATGGAGGGTGAGGTC	Invitrogen (Karlsruhe, Germany)
	ACAN Rev	NDRWR7G, ACGCTGCCTCGGGCTTC	Invitrogen (Karlsruhe, Germany)
	COL10A1 For	NDT2KTE, CCCTCTTGTTAGTGCCAACC	Invitrogen (Karlsruhe, Germany)
	COL10A1 Rev	NDU7FDC, AGATTCCAGTCCTTGGGTCA	Invitrogen (Karlsruhe, Germany)

Category	Nucleic acids	Specifications	Manufacturers
	COL1A1 For	ND2XJJP, ACGTCCTGGTGAAGTTGGTC	Invitrogen (Karlsruhe, Germany)
	COL1A1 Rev	ND33D4M, ACCAGGGAAGCCTCTCTCTC	Invitrogen (Karlsruhe, Germany)
	COL2A1 For	NDMGAGP, GGACTTTTCTCCCCTCTCT	Invitrogen (Karlsruhe, Germany)
	COL2A1 Rev	NDNK32M, GACCCGAAGGTCTTACAGGA	Invitrogen (Karlsruhe, Germany)
	GAPDH For	NDYMWEV, GAAGGTGAAGGTCGGAGTC	Invitrogen (Karlsruhe, Germany)
	GAPDH Rev	NDZTPYT, GAAGATGGTGATGGGATTTTC	Invitrogen (Karlsruhe, Germany)
	hsox9 For	NDH6MCV, ACACACAGCTCACTCGACCTTG	Invitrogen (Karlsruhe, Germany)
	hsox9 Rev	NDKCFWT, GGGAAATTCTGGTTGGTCCTCT	Invitrogen (Karlsruhe, Germany)
	hTGF- $\beta$ For	NDFVX4J, TACCATGCCAACTTCTGTCTGGGA	Invitrogen (Karlsruhe, Germany)
	hTGF- $\beta$ Rev	NDGZTPG, ATGTTGGACAACCTGCTCCACCTTG	Invitrogen (Karlsruhe, Germany)

Abbreviations: AAV: adeno-associated virus; ACAN: aggrecan; Ad: adenovirus; *cap*: capsid (open reading frame, i.e. gene); cDNA: complementary deoxyribonucleic acid; CMV-IE: cytomegalovirus-immediate early; COL10A1: type-X collagen (gene); COL1A1: type-I collagen (gene); COL2A1: type-II collagen (gene); DNA: deoxyribonucleic acid; For: forward; GAPDH: glyceraldehyde-3-phosphate dehydrogenase; hsox9: human sex-determining region Y-type high mobility group box 9; hTGF- $\beta$ : human transforming growth factor beta; kbp: kilobase pair; *lacZ*:  $\beta$ -galactosidase; mg: milligram; N/A: not available; ORF: open reading frames; *rep*: replication (open reading frame, i.e. gene); Rev: reverse; RFP: red fluorescent protein.

**Table 11.** Proteins used in the studies

Category	Proteins	Specifications	Manufacturers
agents	BSA	A7284, 50 ml	Sigma (Taufkirchen, Germany)
	glutamine	G7513, 20 ml	Sigma (Taufkirchen, Germany)
	recombinant FGF-2	100-18b, 5 $\mu$ g	Peptotech (Cranbury, USA)
antibodies	anti-SOX9 (C-20)	sc-17341, goat	Santa Cruz (Dallas, USA)
	anti-TGF- $\beta$ 1 (V)	sc-146, rabbit	Santa Cruz (Dallas, USA)
	anti-type-I collagen	ab90395, mouse	Abcam (Berlin, Germany)
	anti-type-II collagen	II-II6B3, mouse	DSHB (Lowa City, USA)
	anti-type-X collagen	C7974, mouse	Sigma (Taufkirchen, Germany)
	biotinylated anti-goat IgG (H+L)	VC-BA-9500, horse	Biozol (Eching, Germany)
	biotinylated anti-mouse IgG (H+L)	VC-BA-9200, goat	Biozol (Eching, Germany)
	biotinylated anti-rabbit IgG (H+L)	VC-BA-1000, goat	Biozol (Eching, Germany)
	enzymes	collagenase (CLS)	C1-22, 232 U/mg, 1 g
papain		P3125, 2x, 100 mg	Sigma (Taufkirchen, Germany)
RNase-free DNase		M6101, 1 U/ $\mu$ l, 1 ml	Promega (Madison, USA)
trypsin EDTA		T4174, 10x, 100 ml	Sigma (Taufkirchen, Germany)

Abbreviations: BSA: bovine serum albumin; DNase: deoxyribonuclease; EDTA: ethylenediaminetetraacetic acid; FGF-2: basic fibroblast growth factor; g: gram; IgG: immunoglobulin G; mg: milligram; ml: milliliter; RNase: ribonuclease; SOX9: sex-determining region Y-type high mobility group box 9; TGF- $\beta$ : transforming growth factor beta;  $\mu$ g: microgram;  $\mu$ l: microliter.

**Table 12.** Saccharides used in the studies

Saccharides	Specifications	Manufacturers
agarose	15510-019, 100 g	Fisher (Schwerte, Germany)
chondroitin sulfate	27043, 10 g	Sigma (Taufkirchen, Germany)
D (+)-sucrose	10239610, 1 kg	Fisher (Schwerte, Germany)

Abbreviations: g: gram; kg: kilogram.

**Table 13.** Commercial media used in the studies

Mixtures	Specifications	Manufacturers
DMEM	41965039, 500 ml	Gibco (Schwerte, Germany)
FBS	10270-106, 500 ml	Gibco (Schwerte, Germany)
LB	12795027, 500 g	Invitrogen (Schwerte, Germany)
Opti-MEM	31985-047, 500 ml	Gibco (Schwerte, Germany)
SOC-Medium	S1797, 5 ml	Sigma (Taufkirchen, Germany)

Abbreviations: DMEM: Dulbecco's Modified Eagle Medium; FBS: fetal bovine serum; g: gram; LB: lysogeny broth; ml: milliliter; Opti-MEM: improved Minimal Essential Medium; SOC-Medium: super optimal medium with catabolic repressor medium.

## 5.2. Chemicals

### 5.2.1. Solid reagents

**Table 14.** Solid reagents used in the studies

Solid reagents	Specifications	Manufacturers
alcian blue 8GX	A5268, 100 g	Sigma (Taufkirchen, Germany)
alginate	GRINDSTED AlgPH155	Danisco (Brabrand, Denmark)
ampicillin	A9518, 5 g	Sigma (Taufkirchen, Germany)
CaCl <sub>2</sub> -2H <sub>2</sub> O	C5080, 500 g	Sigma (Taufkirchen, Germany)
chloroquine	C6628, 25 g	Sigma (Taufkirchen, Germany)
D-cysteine HCl monohydrate	C8005, 1 g	Sigma (Taufkirchen, Germany)
DMMB	20335.01, 1 g	Serva (Heidelberg, Germany)
eosin	7089.1, 50 g	Carl Roth (Karlsruhe, Germany)
fast green	211922, 5 g	MP (Illkirch, France)
guanidine hydrochloride	G3272, 25 g	Sigma (Taufkirchen, Germany)
HEPES	B24701555, 100 g	Fisher (Schwerte, Germany)
Hoechst 33258	B2883, 25 mg	Sigma (Taufkirchen, Germany)
Na <sub>2</sub> HPO <sub>4</sub> -7H <sub>2</sub> O	S9390, 500 g	Sigma (Taufkirchen, Germany)
NaCl	S7653, 1 kg	Sigma (Taufkirchen, Germany)
NaOH	S8045, 500 g	Sigma (Taufkirchen, Germany)
toluidine blue	89640, 25 g	Sigma (Taufkirchen, Germany)

Abbreviations: CaCl<sub>2</sub>-2H<sub>2</sub>O: calcium chloride-dihydrate; DMMB: dimethylmethylene blue; g: gram; HCl: hydrochloric acid; HEPES: 4-(2-hydroxyethyl)-1-piperazineethanesulfonic acid; kg: kilogram; mg: milligram; Na<sub>2</sub>HPO<sub>4</sub>-7H<sub>2</sub>O: di-sodium hydrogen phosphate heptahydrate; NaCl: sodium chloride; NaOH: sodium hydroxide.

### 5.2.2. Liquid reagents

**Table 15.** Liquid reagents used in the studies

Liquid reagents	Specifications	Manufacturers
acetic acid (glacial)	A6283, 100 ml	Sigma (Taufkirchen, Germany)
alizarin red	TMS-008-C, 50 ml	EMD Millipore (Darmstadt, Germany)
distilled water	11518886, 500 ml	Gibco (Schwerte, Germany)
distilled water	W4502, 1 l	Sigma (Taufkirchen, Germany)
EDTA	15575-038, 100 ml	Gibco (Schwerte, Germany)
ethanol	10644795, Mol Biology Grade, 500 ml	Fisher (Schwerte, Germany)
ethanol	K928.3, >99.7%, 2.5 l	Carl Roth (Karlsruhe, Germany)
formaldehyde	PZN 02653025, 4%, 1 l	Otto Fischar (Saarbrücken, Germany)
formic acid	10457830, 90%, 500 ml	Fisher (Schwerte, Germany)
glycerol	G5516, 100 ml	Sigma (Taufkirchen, Germany)
H <sub>2</sub> O <sub>2</sub>	30%, 100 ml	UKS (Homburg, Germany)
HCl	84415, 37%, 100 ml	Sigma (Taufkirchen, Germany)
hematoxylin A nach weigert	X906.1, 500 ml	Carl Roth (Karlsruhe, Germany)
hematoxylin B nach weigert	X907.1, 500 ml	Carl Roth (Karlsruhe, Germany)
hematoxylin nach harris	X903.1, 500 ml	Carl Roth (Karlsruhe, Germany)
isopropanol	10215331, 1 l	Acros Organics (Schwerte, Germany)
NaOH	S2770, 1N, 100 ml	Sigma (Taufkirchen, Germany)
PBS	D8537, 1x, 500 ml	Sigma (Taufkirchen, Germany)
PCR-grade water	T143.5, 20 ml	Carl Roth (Karlsruhe, Germany)
penicillin-streptomycin	P4333, 104 U/ml-104 µg/ml, 100 ml	Sigma (Taufkirchen, Germany)
red blood cell lysing buffer	R7757, 100 ml	Sigma (Taufkirchen, Germany)
safranin O	CN01.1, 500 ml	Carl Roth (Karlsruhe, Germany)
TAE buffer	15558-042, 1 l	Gibco (Schwerte, Germany)
Tris-HCl	15568-025, 1 l	Gibco (Schwerte, Germany)
triton X100	3051.3, 250 ml	Carl Roth (Karlsruhe, Germany)
trypan blue	T8154, 0.4%, 20 ml	Sigma (Taufkirchen, Germany)

Abbreviations: EDTA: ethylenediaminetetraacetic acid; H<sub>2</sub>O<sub>2</sub>: hydrogen peroxide; HCl: hydrochloric acid; l: liter; ml: milliliter; NaOH: sodium hydroxide; PBS: phosphate-buffered saline; PCR: polymerase chain reaction; TAE: Tris-acetate-EDTA; µg: microgram.

### 5.2.3. Analysis kits

**Table 16.** Analysis kits used in the studies

Analysis kits and constituents	Specifications	Manufacturers
1 <sup>st</sup> Strand cDNA Synthesis kit for RT-PCR (AMV)	11483188001	Roche (Mannheim, Germany)
RT-PCR 10x Reaction Buffer	N/A	
RT-PCR AMV Reverse Transcriptase	N/A	
RT-PCR Control RNA	N/A	
RT-PCR Deoxynucleotide Mix	N/A	
RT-PCR MgCl <sub>2</sub>	N/A	
RT-PCR primer pair	N/A	
RT-PCR RNase Inhibitor	N/A	
RT-PCR Water	N/A	

<b>Analysis kits and constituents</b>	<b>Specifications</b>	<b>Manufacturers</b>
$\beta$ -gal Staining kit	11828673001	Roche (Mannheim, Germany)
Iron buffer	11828673001	
X-Gal solution	11828673001	
AAV2 Titration ELISA	PRATV	Progen (Heidelberg, Germany)
ELISA ASSB 20x	K16-02	
ELISA Biotin Concentrate	K14-34	
ELISA KC	K10-31	
ELISA STOP	K18-02	
ELISA Strep-HRP 20x	K14-35	
ELISA TMB	K60-02+	
ABC-HRP kit	PK-4000	Vector Laboratories (Eching, Germany)
ABC Reagent A	30015	
ABC Reagent B	30016	
BCA Protein assay	23225	Fisher (Rockford, USA)
BCA BSA	23209	
BCA Reagent A	23228	
BCA Reagent B	1859078	
Brilliant III Ultra-Fast SYBR Green QPCR Master Mix	600882	Agilent (Waldbronn, Germany)
Master Mix	600882-51	
Cell Proliferation Reagent WST-1	05015944001	Roche (Mannheim, Germany)
WST-1	11644807001	
DAB Substrate kit	SK4100	Vector Laboratories (Eching, Germany)
DAB buffer	30040	
DAB H <sub>2</sub> O <sub>2</sub>	30041	
DAB stain	30039	
ELISA Human TGF- $\beta$ 1 Immunoassay kit	DB100B	R&D (Wiesbaden, Deutschland)
ELISA Calibrator Diluent RD5-53 Concentrate	895587	
ELISA Color Reagent A	895000	
ELISA Color Reagent B	895001	
ELISA Diluent RD1-21	895215	
ELISA Stop Solution	895174	
ELISA TGF- $\beta$ 1 Conjugate	893003	
ELISA TGF- $\beta$ 1 Microplate	891124	
ELISA TGF- $\beta$ 1 Standard	891126	
ELISA Wash Buffer Concentrate	895003	
Plasmid DNA Purification kit	PureYield	Promega (Madison, USA)
Cell Lysis Solution	A7125	
Cell Resuspension Solution	A7115	
Column Wash Solution	A252B	
Endotoxin Removal Solution	A251B	
Neutralization Solution	A1485	
Nuclease-Free Water	P119C	
PureYield Binding Column	A245A	
PureYield Clearing Column	A246A	

Analysis kits and constituents	Specifications	Manufacturers
RNeasy Protect Mini kit	74104	QIAGEN (Hilden, Germany)
RNeasy Collection Tubes	0890321/148021457	
RNeasy Mini Spin Column	160045920	
RNeasy RLT Lysis Buffer	163048274	
RNeasy RNase-Free Water	163043375	
RNeasy RPE Wash Buffer	166044704	
RNeasy RW1 Wash Buffer	0169027829	

Abbreviations: AAV: adeno-associated virus; ABC: avidin-biotin complex; BCA: bicinchoninic acid; BSA: bovine serum albumin; cDNA: complementary DNA; DAB: diaminobenzidine; DNA: deoxyribonucleic acid; ELISA: enzyme-linked immunosorbent assay; H<sub>2</sub>O<sub>2</sub>: hydrogen peroxide; HRP: horseradish peroxidase; MgCl<sub>2</sub>: magnesium chloride; QPCR: quantitative polymerase chain reaction; RNase: ribonuclease; RT-PCR: reverse transcription polymerase chain reaction; TGF-β: transforming growth factor beta; WST-1: water-soluble tetrazolium salt-1; X-Gal: 5-bromo-4-chloro-3-indolyl-β-D-galactopyranoside; β-gal: β-galactosidase.

### 5.3. Laboratory formulations

#### 5.3.1. Media

**Table 17.** Reconstituted media used in the studies

Media	Ingredients
bacteria culture medium	99.9% (v/v) LB 0.1% (v/v) 100 mg/ml ampicillin
cell culture medium	1% (v/v) Pen/Strep 10% (v/v) FBS 89% (v/v) DMEM
post-transfection medium	1% (v/v) 100X glutamine 15% (v/v) FBS 84% (v/v) DMEM
transfection medium	10% (v/v) FBS 120 μM chloroquine stock 90% (v/v) Opti-MEM

Abbreviations: DMEM: Dulbecco's Modified Eagle Medium; FBS: fetal bovine serum; LB: lysogeny broth; mg: milligram; ml: milliliter; Opti-MEM: improved Minimal Essential Medium; Pen/Strep: penicillin/streptomycin; v/v: volume/volume; μM: micromolar.

#### 5.3.2. Buffers

**Table 18.** Buffers used in the studies

Buffers	Ingredients
HBS 2x	1.5 mM Na <sub>2</sub> HPO <sub>4</sub> ·7H <sub>2</sub> O 280 mM NaCl 50 mM HEPES
PBE	0.01 M EDTA 0.1 M Na <sub>2</sub> HPO <sub>4</sub> ·7H <sub>2</sub> O

Buffers	Ingredients
TE 0.1x	1 mM EDTA 10 mM Tris/HCl
TEN 1x	1 mM EDTA 10 mM Tris/HCl 100 mM NaCl

Abbreviations: EDTA: ethylenediaminetetraacetic acid; HBS: HEPES-buffered saline; HCl: hydrochloric acid; HEPES: 4-(2-hydroxyethyl)-1-piperazineethanesulfonic acid; M: molar; mM: millimolar; Na<sub>2</sub>HPO<sub>4</sub>·7H<sub>2</sub>O: di-sodium hydrogen phosphate heptahydrate; NaCl: sodium chloride; PBE: PBS-EDTA; PBS: phosphate-buffered saline; TE: Tris-EDTA; TEN: Tris-EDTA-NaCl.

### 5.3.3. Solutions

**Table 19.** Solutions used in the studies

Solutions	Ingredients
β-gal staining working solution	5% (v/v) X-Gal solution 95% (v/v) Iron buffer
ABC working solution	10 ml PBS 2 drops Reagent A 2 drops Reagent B
alcian blue working solution	1% (w/v) alcian blue 8GX 1 N HCl
alizarin red differentiation solution	0.01 % (v/v) 37% HCl 99.99% (v/v) 95% ethanol
BCA working solution	2% (v/v) Reagent B 98% (v/v) Reagent A
DAB working solution	2 drops buffer 2 drops H <sub>2</sub> O <sub>2</sub> 4 drops DAB 5 ml distilled water
digestion solution	98% (v/v) DMEM 0.2% (w/v) collagenase 2% (v/v) Pen/Strep
DMMB sample solution	50% (v/v) DMMB solution A 50% (v/v) cell lysate
DMMB solution A	10 mM D-cysteine HCl monohydrate PBE
DMMB solution B	53 M chondroitin sulfate DMMB solution A
DMMB solution C	0.2% (v/v) DMMB solution B 99.8% (v/v) DMMB solution A
DMMB working solution	0.3% (v/v) 90% formic acid 0.5% (v/v) 95% ethanol 2.56% (v/v) 1 M NaOH 16 mg dimethylmethylene blue-chloride

Solutions	Ingredients
eosin solution	0.5% (w/v) eosin distilled water
fast green solution	0.02% (w/v) fast green distilled water
hematoxylin solution	50% (v/v) hematoxylin A nach weigert 50% (v/v) hematoxylin B nach weigert
Hoechst sample solution	20% (v/v) cell lysate 80%(v/v) TEN buffer
Hoechst standard solution	10 mM DNA PBE
Hoechst working solution	2 mM Hoechst TEN buffer
lysis solution	125 mM papain PBE
polymerase chain reaction system (50 µl)	150 nM primers 4% (v/v) cDNA 50% (v/v) Master Mix 46% distilled water
pre-infection solution	0.75% (v/v) 3-10 MOI Ad5 helper virus 99.25% (v/v) DMEM
reverse transcription system (20 µl)	4% (v/v) reverse transcriptase 5% (v/v) RNase inhibitor 10% (v/v) 10x reaction buffer 10% (v/v) dNTPs 10% (v/v) primer 20% (v/v) MgCl <sub>2</sub> 41% (v/v) RNA
transfection solution	18 mM target plasmid 6 mM Ad8 helper plasmid 45% (v/v) TE buffer 5% (v/v) 2.5 M CaCl <sub>2</sub> 50% (v/v) HBS
toluidine blue solution	1% (w/v) fast green distilled water

Abbreviations: ABC: avidin-biotin complex; Ad: adenovirus; BCA: bicinchoninic acid; CaCl<sub>2</sub>: calcium chloride; cDNA: complementary DNA; DAB: diaminobenzidine; DMEM: Dulbecco's Modified Eagle Medium; DMMB: dimethylmethylene blue; DNA: deoxyribonucleic acid; dNTPs: deoxynucleotide triphosphates; EDTA: ethylenediaminetetraacetic acid; H<sub>2</sub>O<sub>2</sub>: hydrogen peroxide; HBS: HEPES-buffered saline; HCl: hydrochloric acid; HEPES: 4-(2-hydroxyethyl)-1-piperazineethanesulfonic acid; M: molar; mg: milligram; MgCl<sub>2</sub>: magnesium chloride; ml: milliliter; mM: millimolar; MOI: multiplicity of infection; N: newton; NaCl: sodium chloride; NaOH: sodium hydroxide; nM: nanomolar; PBE: PBS-EDTA; PBS: phosphate-buffered saline; Pen/Strep: penicillin/streptomycin; RNA: ribonucleic acid; RNase: ribonuclease; TE: Tris-EDTA; TEN: Tris-EDTA-NaCl; v/v: volume/volume; w/v: weight/volume; X-Gal: 5-bromo-4-chloro-3-indolyl-β-D-galactopyranoside; β-gal: β-galactosidase; µl: microliter.

## 5.4. Laboratory supplies

### 5.4.1. Consumables

**Table 20.** Consumables used in the studies

Consumables	Specifications	Manufacturers
8x tube strips (QPCR)	401428	Agilent (Waldbronn, Germany)
96-well Mikrottestplatten F-Profil (BCA)	9293.1	Carl Roth (Karlsruhe, Germany)
96-well plates (QPCR)	401333	Agilent (Waldbronn, Germany)
Bunsen burner	Labogaz 206	Campingaz (Wallis and Futuna, France)
cell culture inserts	Millicell PICM01250, 0.4 µm	Merck (County Cork, Ireland)
cell scrapers	83.1832	SARSTEDT (Nümbrecht, Germany)
cell strainers	10321264, 100 µm	Fisher (Schwerte, Germany)
Cellstar flask	658170, T75	Greiner Bio-One (Frickenhausen, Germany)
centrifugation tubes	188271, 15 ml	Greiner Bio-One (Frickenhausen, Germany)
centrifugation tubes	227261, 50 ml	Greiner Bio-One (Frickenhausen, Germany)
centrifugation tubes	AB0620, 0.2 ml	Fisher (Schwerte, Germany)
Cutfix stainless scalpel	5518075	Aesculap (Tuttlingen, Germany)
Erlenmeyer flask	FB33142, 1 l	Fisher (Schwerte, Germany)
forceps	N/A	UKS (Homburg, Germany)
glass bottom	9653620, 100 ml	Fisher (Schwerte, Germany)
glass bottom	9653640, 500 ml	Fisher (Schwerte, Germany)
hydrogel spatula	N/A	UKS (Homburg, Germany)
multiwell plates	3598, 96 well	Corning (Durham, USA)
multiwell plates	657160, 6 well	Greiner Bio-One (Frickenhausen, Germany)
multiwell plates	662160, 24 well	Greiner Bio-One (Frickenhausen, Germany)
multiwell plates	677180, 48 well	Greiner Bio-One (Frickenhausen, Germany)
needles	21 G	B BRAUN (Melsungen, Germany)
OptiPlate-96 black (Hoechst-Assay)	6005270	Perkin Elmer (Hamburg, Germany)
parafilm	PM-996	Carl Roth (Karlsruhe, Germany)
Petri dishes	83.3902.300, 10 cm	SARSTEDT (Nümbrecht, Germany)
PP tubes	10451043, 1.5 ml	Eppendorf (Hamburg, Germany)
PP tubes	187261, 14 ml	Greiner Bio-One (Frickenhausen, Germany)
PS tubes	191160, 14 ml	Greiner Bio-One (Frickenhausen, Germany)
safe-lock tubes	0030121.589, 1.5 ml	Eppendorf (Hamburg, Germany)
stripette serological pipets	734-1739 (4489), 25 ml	Corning (Durham, USA)
stripette serological pipets	86.1254.001, 10 ml	SARSTEDT (Nümbrecht, Germany)
syringe filters	KH54.1, 0,22 µm	Carl Roth (Karlsruhe, Germany)
syringes	Inject 4606108V, 10 ml	B BRAUN (Melsungen, Germany)
syringes	Inject 9166017V, 1 ml	B BRAUN (Melsungen, Germany)
tips	741045, 100-1,000 µl	Greiner Bio-One (Frickenhausen, Germany)
tips	741065, 10-200 µl	Greiner Bio-One (Frickenhausen, Germany)
tips	9260.1, 0.5-10 µl	Carl Roth (Karlsruhe, Germany)
weighing paper	1-7217, 10x13 cm	neoLab (Heidelberg, Deutschland)

Abbreviations: BCA: bicinechonic acid; cm: centimeter; G (needle): gauge; l: liter; N/A: not available; ml: milliliter; PP: polypropylene; PS: polystyrene; QPCR: quantitative polymerase chain reaction;  $\mu$ l: microliter;  $\mu$ m: micrometer.

## 5.4.2. Equipment

**Table 21.** Equipment used in the studies

Equipment	Specifications	Manufacturers
analytical balance	ABT [100-5NM]	Kern (Balingen, Germany)
autoclave	AMA-240	Astell (Sidcup, England)
biosafety cabinet	BioWizard Silver Line	KOJAIR (Mantta-Vilppula, Finland)
centrifuge	5804 R	Eppendorf (Hamburg, Germany)
combination shaker	K15/500	Noctua (Vienna, Austria)
eluator vacuum elution device	A1071	Promega (Madison, USA)
freezer	BL-V-720	Kirsch (Willstätt-Sand, Germany)
freezer	GSS32421/02	Bosch (Gerlingen, Germany)
freezer	PLATINUM 550H	Angelantoni (Massa, Italy)
hemocytometer	0640110	Marienfeld (Lauda-Konigshofen, Germany)
incubator	CB150	BINDER (Tuttlingen, Germany)
incubator chamber	IH50	Noctua (Vienna, Austria)
light microscope	BX45	OLYMPUS (Hamburg, Germany)
fluorescent microscope (inverted)	CK41	OLYMPUS (Hamburg, Germany)
metal bath	CTM	HTA-BioTec (Bovenden, Germany)
microliter centrifuge	Z216MK	Hermle LaborTechnik (Wehingen, Germany)
microplate reader	GENios A-5082	TECAN (Grödig, Austria)
digital camera	DP22	OLYMPUS (Hamburg, Germany)
mini cooler	89511-794	VWR (Darmstadt, Germany)
mixer	Junior 3000	Frobel Labortechnik (Lindau, Germany)
multiplex quantitative PCR system	Mx3000P <sup>®</sup> QPCR operator system	Agilent (Waldbronn, Germany)
PCR Thermal Cycler	5332	Eppendorf (Hamburg, Germany)
pipettes	Eppendorf research [0.5-10 $\mu$ l]	Eppendorf (Hamburg, Germany)
pipettes	Eppendorf research [10-100 $\mu$ l]	Eppendorf (Hamburg, Germany)
pipettes	Eppendorf research [100-1,000 $\mu$ l]	Eppendorf (Hamburg, Germany)
pipettes	Eppendorf research [20-200 $\mu$ l]	Eppendorf (Hamburg, Germany)
pipetus	9907200	Hirschmann Laborgeräte (Eberstadt, Germany)
power supply	U-RFL-T	OLYMPUS (Hamburg, Germany)
Prism high speed centrifuge	C2500	Labnet (Mexico)
pumps	2522Z-02	WELCH (Denver, USA)
safety cabinet	2-453-GAHD	Kottermann (hanigsen, Germany)
spectrophotometer	6131 02238	Eppendorf (Hamburg, Germany)
universal laboratory centrifuge	Z300	Hermle LaborTechnik (Wehingen, Germany)
vortex	V-1 plus	bioSan (Riga, Latvia)
water bath	WTB	Memmert (Schwabach, Germany)

Abbreviations: PCR: polymerase chain reaction; QPCR: quantitative polymerase chain reaction;  $\mu$ l: microliter.

### 5.4.3. Software

**Table 22.** Software used in the studies

<b>Software</b>	<b>Specifications</b>	<b>Manufacturers</b>
Affinity Photo	V2	Serif (Nottingham, UK)
BioRender	online	BioRender (Toronto, Canada)
Camera software	cellSens Standard 1.18	OLYMPUS (Hamburg, Germany)
MxPro QPCR software	Mx3000P	Stratagene California (La Jolla, USA)
Office 2021	16-74	Microsoft (Washington, USA)
Prism	9.5.1	GraphPad Software (Boston, USA)
ImageJ	1.53t	National Institutes Health (Maryland, USA)

Abbreviation: QPCR: quantitative polymerase chain reaction.

## 6. METHODS

### 6.1. Study design

#### 6.1.1. Ethical approvals

Prior to being included in the study, all patients (age 58-78 years, with patient number = 12) were given comprehensive information and subsequently gave their informed consent in written form.

All procedures of the study were in strict conformity with the guidelines of the Declaration of Helsinki. The research protocol received prior approval from the Saarland Ethics Committee with the Ethics Application Approval Registration Number: Ha67/12.

#### 6.1.2. Experimental design

The research was designed to improve cartilage (chondro-)regeneration by incorporation of therapeutic rAAV vectors upon alginate gelation with  $\text{Ca}^{2+}$  and rAAV vector delivery for the gradual transduction of human osteoarthritic articular chondrocytes and of human mesenchymal stromal cells (**Figure 4**).

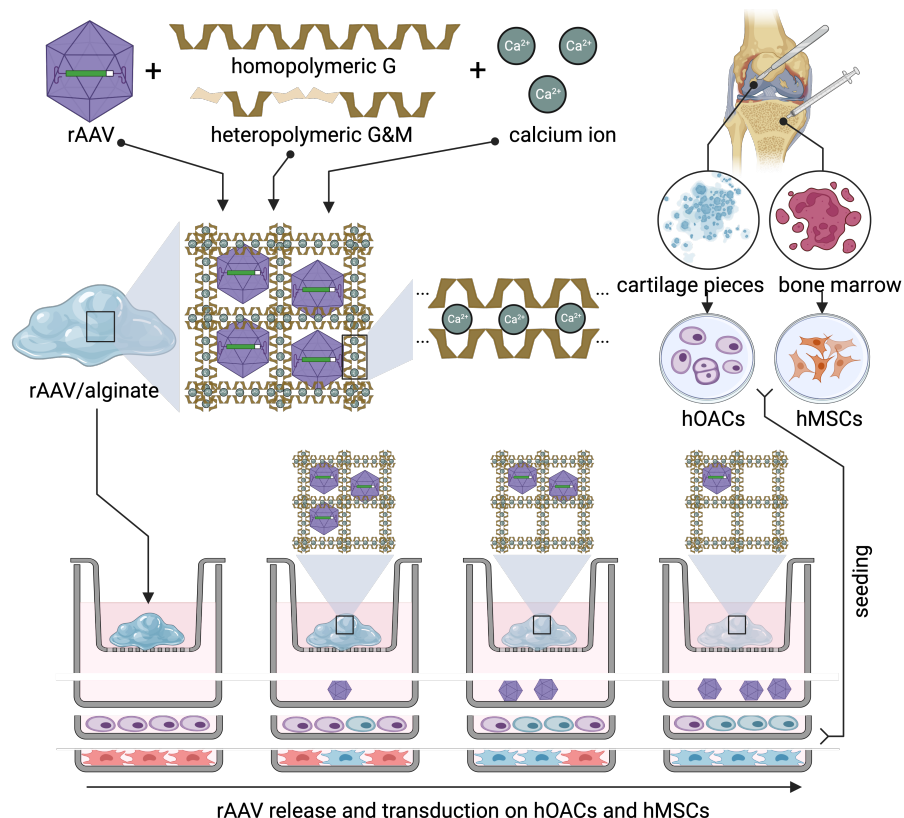


**Figure 4.** Experimental design of the study. The scheme shows the manipulation and application of rAAV/alginate hydrogel systems to transduce hOACs and hMSCs. Abbreviations: G: 1,4-linked  $\alpha$ -L-guluronic acid; hMSCs: human mesenchymal stromal cells; hOACs: human osteoarthritic articular chondrocytes; M: 1,4-linked  $\beta$ -D-mannuronic acid; rAAV: recombinant adeno-associated virus (created with BioRender).

The evaluations in human osteoarthritic articular chondrocytes and human mesenchymal stromal cells were planned to monitor the conditions of effective rAAV vector release, the kinetics of rAAV vector release, and the therapeutic effects of the rAAV vectors released from the alginate hydrogels by an analysis of transgene expression, of the effects on the biological and chondrogenic activities, and on the osteogenic, hypertrophic, and mineralization activities (**Figure 5**).

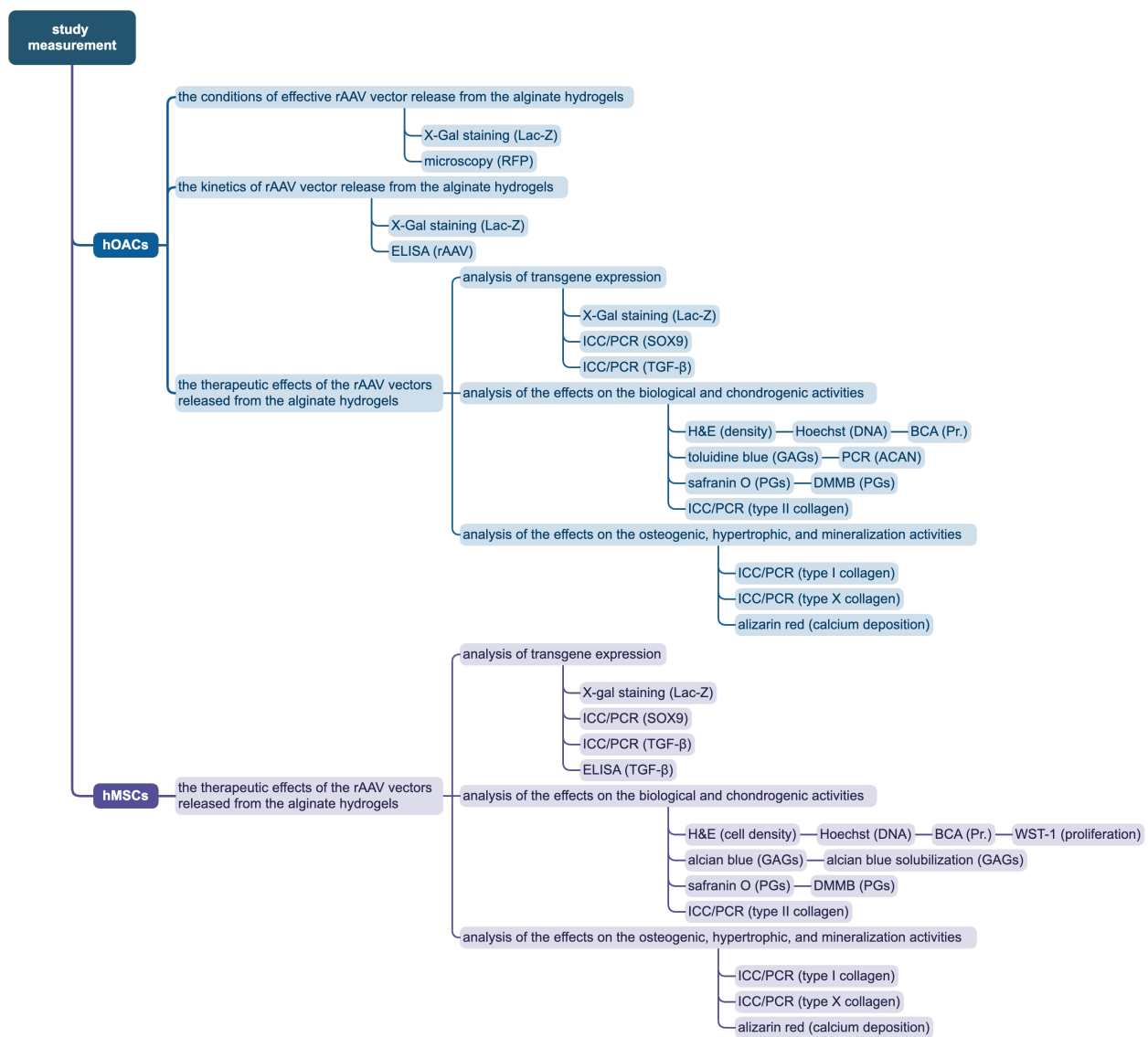


**Figure 5.** Experimental evaluations were performed in the study. The scheme shows the procedures employed to monitor the conditions of effective rAAV vector release, the kinetics of rAAV vector release, and the therapeutic effects of the rAAV vectors released from the alginate hydrogels by an analysis of transgene expression, of the effects on the biological and chondrogenic activities, and on the osteogenic, hypertrophic, and mineralization activities. Abbreviations: ACAN: aggrecan; BCA: bichoninic acid; DMMB: dimethylmethylene blue; DNA: deoxyribonucleic acid; ELISA: enzyme-linked immunosorbent assay; GAGs: glycosaminoglycans; H&E: hematoxylin and eosin; hMSCs: human mesenchymal stromal cells; hOACs: human osteoarthritic articular chondrocytes; ICC: immunocytochemistry; *lacZ*:  $\beta$ -galactosidase; PCR: polymerase chain reaction. PGs: proteoglycans; Pr.: protein; rAAV: recombinant adeno-associated virus; RFP: red fluorescent protein; SOX9: sex-determining region Y-type high mobility group box 9; TGF- $\beta$ : transforming growth factor beta; X-Gal: 5-bromo-4-chloro-3-indolyl- $\beta$ -D-galactopyranoside (created with Affinity Photo).

### 6.1.3. Research groups

The following groups were assigned to the experiments performed in this project:

- no vector/alginate,
- rAAV-*lacZ* ( $\beta$ -galactosidase reporter gene)/alginate,
- rAAV-RFP (red fluorescent protein reporter gene)/alginate,
- rAAV-FLAG-hsox9/alginate,
- rAAV-hTGF- $\beta$ /alginate,
- free rAAV-*lacZ*, and
- free rAAV-RFP

depending on the objectives of the research and on the cell targets (**Table 23**).

**Table 23.** Research groups

Research objectives	Targets	Groups
rAAV vector release conditions	• hOACs	<ul style="list-style-type: none"> <li>• no vector/alginate</li> <li>• rAAV-<i>lacZ</i>/alginate</li> <li>• free rAAV-<i>lacZ</i></li> </ul>
	• hOACs	<ul style="list-style-type: none"> <li>• no vector/alginate</li> <li>• rAAV-RFP/alginate</li> <li>• free rAAV-RFP</li> </ul>
rAAV vector release kinetics	• hOACs	<ul style="list-style-type: none"> <li>• no vector/alginate</li> <li>• rAAV-<i>lacZ</i>/alginate</li> <li>• free rAAV-<i>lacZ</i></li> </ul>
therapeutic effects of released rAAV vectors	• hOACs	<ul style="list-style-type: none"> <li>• rAAV-<i>lacZ</i>/alginate</li> <li>• rAAV-FLAG-hsox9/alginate</li> <li>• rAAV-hTGF-<math>\beta</math>/alginate</li> </ul>
	• hMSCs	<ul style="list-style-type: none"> <li>• rAAV-<i>lacZ</i>/alginate</li> <li>• rAAV-FLAG-hsox9/alginate</li> <li>• rAAV-hTGF-<math>\beta</math>/alginate</li> </ul>

Abbreviations: FLAG: FLAG tag; hMSCs: human mesenchymal stromal cells; hOACs: human osteoarthritic articular chondrocytes; hsox9: human sex-determining region Y-type high mobility group box 9; hTGF- $\beta$ : human transforming growth factor beta; *lacZ*:  $\beta$ -galactosidase; rAAV: recombinant adeno-associated virus; RFP: red fluorescent protein.

## 6.2. Cell culture preparation

### 6.2.1. Primary human osteoarthritic articular chondrocytes (hOACs) cultures

Human osteoarthritic articular chondrocytes were isolated and cultured according to a previously validated and well-established protocol, the efficacy of which has been confirmed in prior studies (Cucchiari et al., 2007, 2009; Daniels et al., 2019; Rey-Rico et al., 2017, 2018; Tao et al., 2016b; Venkatesan et al., 2013) (**Figure 4**). In this goal, sterile articular cartilage was collected from the distal parts of femoral condyles (osteochondral slices, 1- to 3-centimeter (cm) in diameter) obtained from hematologically healthy patients (age 58-66 years, with patient number = 5) who underwent total knee arthroplasty using a scalpel in order to produce small tissue pieces. These small cartilage pieces were next dissected into smaller fragments and stored in Dulbecco's Modified Eagle Medium (DMEM). In parallel, a digestion solution was prepared comprising DMEM, 0.2% collagenase, and 1% penicillin/streptomycin (Pen/Strep) that was sterilized using a 0.2 micrometer ( $\mu\text{m}$ ) filter. Next, DMEM was removed from the cartilage pieces and replaced with this prepared digestion solution for an overnight incubation at 37 Celsius ( $^{\circ}\text{C}$ ) under 5% carbon dioxide ( $\text{CO}_2$ ). The next day, the digested cartilage pieces were pipetted up and down to separate and detach the intrinsic cells from the tissue. A 100- $\mu\text{m}$  cell strainer was placed on top of a 50-milliliter (-ml) Falcon tube. The cell suspension was pipetted onto the cell strainer. The strainer was then washed with 10 ml of serum-free DMEM. The flow-through was centrifuged for 5 minutes at 1,500 revolutions per minute (rpm) to pellet the cells. The supernatant was discarded and the cell pellet was resuspended in cell culture medium (DMEM, 10% FBS, 1% Pen/Strep). The cell suspension was transferred in a T75 flask and incubated at 37 $^{\circ}\text{C}$  under 5%  $\text{CO}_2$ .

### 6.2.2. Primary human mesenchymal stromal cells (hMSCs) cultures

Human mesenchymal stromal cells were isolated and cultured according to a previously validated and well-established protocol, the efficacy of which has been confirmed in prior studies (Cucchiari et al., 2013; Frisch et al., 2014; Meng et al., 2020; Morscheid et al., 2019a; Rey-Rico et al., 2015b; Tao et al., 2016a; Venkatesan et al., 2012, 2018a) (**Figure 4**). In this goal, sterile bone marrow aspirates (approximately 15 ml,  $0.4\text{-}1.2 \times 10^9$  cells/ml) were collected from the distal parts of femoral condyles in hematologically healthy patients (age 74-78 years, with patient number = 7) who underwent total knee arthroplasty. Each bone marrow aspirate was transferred in a 50-ml centrifugation tube and washed with serum-free DMEM in a total volume of 50 ml. The tube was centrifuged at 1,500 rpm for 5 minutes at room temperature (RT) and the supernatant

was carefully removed using a wide-mouth pipette. Subsequently, 5 ml of serum-free DMEM and 5 ml of red blood cell Lysing buffer were added and followed by thorough mixing. The tube was then filled with serum-free DMEM to a total volume of 30 ml and centrifuged at 1,500 rpm for 5 minutes at RT. The supernatant was discarded and the pellet resuspended in 15-20 ml of cell culture medium. The cell suspension was then transferred in a T75 cell culture flask and incubated at 37°C under 5% CO<sub>2</sub> for 24 hours. The next day, the flask was gently shaken to detach the non-adherent cells in the supernatant. The cell suspension was then transferred to a new T75 cell culture flask and incubated at 37°C under 5% CO<sub>2</sub>. The flask where adherent human mesenchymal stromal cells already started to expand was further cultivated with 15-20 ml of cell culture medium at 37°C under 5% CO<sub>2</sub>. The cell culture medium was then supplemented with FGF-2 (1 nanogram (ng)/ml), ensuring cell proliferation without impacting the differentiation potential of human mesenchymal stromal cells (Cucchiaroni et al., 2011).

### 6.2.3. Cell passaging and cell counting

Human osteoarthritic articular chondrocytes and human mesenchymal stromal cells were passaged at a 1:3 ratio when reaching 75-85% confluency according to the following procedure. First, the cell culture medium was removed from the T75 cell culture flasks and the cells were washed with 10-15 ml of PBS. After removal of the PBS, the cell monolayer was evenly covered with 5 ml of trypsin. Following an incubation for 15 minutes at 37°C under 5% CO<sub>2</sub>, 10 ml of cell culture medium was added to stop the trypsinization on the already detached cells. Repeated pipetting and rinsing of the culture surface led to a complete detachment of the cells from the bottom of the cell culture flasks. Subsequently, the entire cell suspension was transferred to a 50-ml centrifugation tube, filled up to 20 ml with serum-free DMEM, and centrifuged at 1,500 rpm for 5 minutes at RT. The supernatant was removed and the cell pellet was resuspended in cell culture medium. Based on subculture ratio, the respective volume of the cell suspension was transferred to new T75 cell culture flasks that were then incubated at 37°C under 5% CO<sub>2</sub>. For this study, both human osteoarthritic articular chondrocytes and human mesenchymal stromal cells were used at low passages ( $\leq 2$ ). Cell counting was performed in the in-cell suspensions using vital staining of the cells with trypan blue and employing a hemocytometer. For the preparation of the trypan blue/cell solution, 10 microliters ( $\mu$ l) of trypan blue and 10  $\mu$ l of cell suspension were transferred to a 1.5-ml polypropylene (PP) tube. Each of the two independent counting grids of a hemocytometer was loaded with 10  $\mu$ l of the trypan blue/cell solution and the cells were counted using a light microscope (BX45). Taking into account the dilution factor, cell counting was carried out in duplicate and a mean value was calculated.

### 6.3. Production of rAAV vectors

rAAV vectors were derived from genomic clones of the adeno-associated virus serotype 2 (AAV-2) of the pSSV9 strain (a derivative of the pEMBL8 plasmid) and produced using a helper-dependent system requiring (i) AAV-based plasmids each containing independent genes of interest (transgenes), (ii) the adenovirus 8 (Ad8) helper plasmid, and (iii) the adenovirus 5 (Ad5) helper virus (Cucchiari et al., 2011; Dente et al., 1983; Samulski et al., 1987, 1989; Venkatesan et al., 2012) (**Figure 6**).

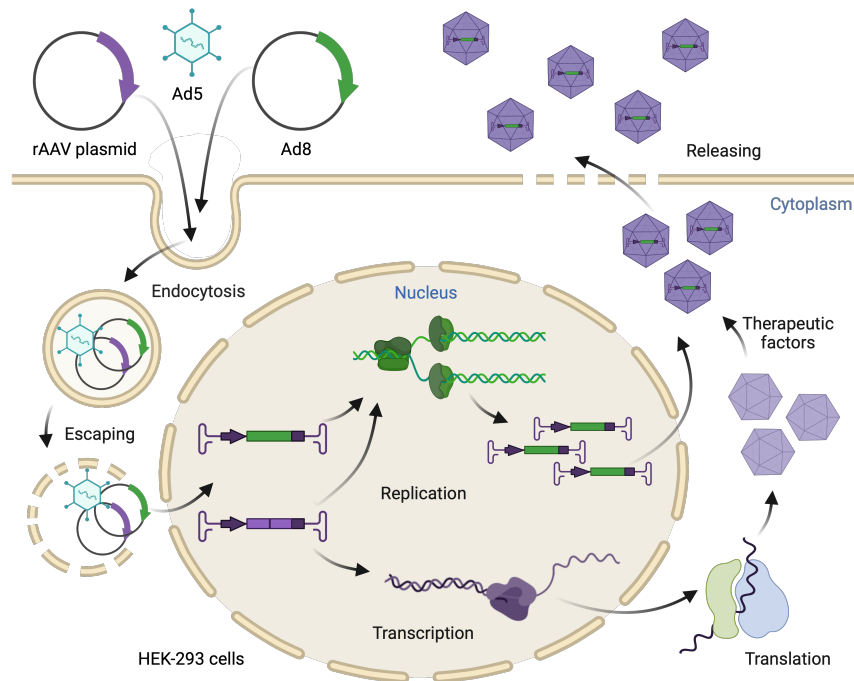


**Figure 6.** rAAV vector production in HEK-293 cells. The scheme shows the steps of replication and transcription in the cell nucleus and the steps of translation and final assembly in the cytoplasm. Abbreviations: Ad5: adenovirus 5 helper virus; Ad8: adenovirus 8 helper plasmid; HEK: human embryonic kidney; rAAV: recombinant adeno-associated virus (created with BioRender).

#### 6.3.1. AAV-derived plasmids used in the study

The multiple cloning site (MCS) of the pSSV9 plasmid enabled the cloning of various transgenes in the form of a complementary DNA (cDNA) (Yue & Dongsheng, 2002). The RFP, FLAG-hsox9, and hTGF- $\beta$  cDNA sequences were cloned in AAV-2-derived plasmids by Prof. Dr. rer. nat. Cucchiari (ép. Madry) from the Center of Experimental Orthopaedics of the Saarland University (Cucchiari et al., 2003, 2007, 2018; Frisch et al., 2014) and the *lacZ* cDNA sequence was cloned in the same AAV-2-derived plasmid by Dr. Du from the Division of Infectious Disease at Harvard

Medical School (Du et al., 1996). All constructs were generously made available for the current study.

### 6.3.2. Plasmid transformation and enrichment

The competent *Escherichia coli* (*E. coli*) bacteria were employed to propagate the candidate plasmids including the AAV-2 genomic plasmids and the Ad8 helper plasmid (Orth et al., 2008). The transformation of the plasmids carrying the FLAG-hsox9, hTGF- $\beta$ , *lacZ*, and RFP cDNA sequences in *E. coli* was carried out using the heat shock method according to the following established standard protocol (Hanahan, 1983).

First, 100  $\mu$ l of commercially available bacteria suspension and 100 ng of each plasmid independently (FLAG-hsox9, hTGF- $\beta$ , *lacZ*, and RFP) were added to separate reaction vessels. The process was followed by cooling for 30 minutes on ice, then by a heat shock for 1 minute in a water bath at 40°C, and again cooling on ice for 2 minutes. Maximum transformation efficiency was achieved by adding 900  $\mu$ l of super optimal medium with catabolic repressor medium (SOC-Medium) for a subsequent incubation for 90 minutes at 30°C on a shaker at 250 rpm. Once the incubation ended, 10  $\mu$ l of the bacteria-plasmid suspension was applied to ampicillin-containing agar plates, incubated for 24 hours at 30°C, and finally stored as a glycerol stock at -20°C. The enrichment of the bacteria took place in the form of an overnight pre-culture and a subsequent overnight bacterial culture according to the following established standard protocol (Cucchiaroni et al., 2003, 2007). The process initiated with the introduction of 5  $\mu$ l of bacteria with 5 ml of bacteria culture medium (lysogeny broth - LB, 0.1% ampicillin) into a polystyrene (PS) tube. The mixture was then placed in a shaker at 150 rpm set to operate overnight at 30°C. The following day, 5 ml of the overnight bacteria supernatant was transferred to an Erlenmeyer flask containing 300 ml of bacteria culture medium. This resulting solution was then placed on a shaker at 125 rpm set to incubate overnight at 30°C. The entirety of the procedure was executed with close proximity to the Bunsen burner.

### 6.3.3. Plasmid isolation and quantification

For plasmid isolation using the Plasmid DNA Purification kit, *E. coli* bacteria were centrifuged at 5,000 relative centrifugal force (rcf) for 10 minutes at RT. The resultant pellet from 150 ml of the bacteria supernatant was resuspended in 6 ml of Cell Resuspension Solution via careful pipetting to ensure uniformity. The process was followed by the addition of 6 ml of Cell Lysis Solution and by inverting 3-5 times the tube for thorough mixing, and by a subsequent incubation period of 3

minutes at RT. Next, 10 ml of Neutralization Solution was added and mixed by inverting the tube 5-10 times. The lysate was then subjected to centrifugation at 15,000 rcf for 15 minutes at RT. Meanwhile, a column stack was assembled using a blue PureYield Clearing Column atop a white PureYield Binding Column. The supernatant was carefully transferred into the column stack and vacuum was applied until all the liquid fully passed through both columns. The vacuum was slowly released, leaving only the binding column on the manifold after removing the blue clearing column. The binding column received 5 ml of Endotoxin Removal Wash with vacuum pulling the solution through the column. Subsequently, 20 ml of Column Wash Solution was applied to the binding column and the vacuum was reapplied. The membrane was then dried by applying vacuum for 30-60 seconds. The binding column was removed from the vacuum manifold and tapped on a paper towel to eliminate any excess ethanol. A 1.5-ml PP tube was positioned at the base of the Eluator Vacuum Elution Device. Upon assembling the Eluator Vacuum Elution Device, the DNA binding column was inserted and fully seated on the collar. This assembly was then placed on a vacuum manifold. Finally, 400  $\mu$ l of Nuclease-Free Water were added to the DNA binding membrane within the binding column, followed by an incubation period of 1 minute. Maximum vacuum was then applied for 1 minute and the PP tube was removed prior to the further analyses.

For plasmid quantification including plasmid concentration and purity, a photometric determination was performed using a 1:100 dilution of the plasmid with polymerase chain reaction (PCR)-grade water. For this purpose, absorptions at 260 nm ( $OD^{260\text{ nm}}$ ) and at 280 nm ( $OD^{280\text{ nm}}$ ) were measured. The measurements included a blank value (500  $\mu$ l of PCR-grade water) and individual samples (5  $\mu$ l of sample + 495  $\mu$ l of PCR-grade water). The plasmid concentrations in  $\mu$ g/ml were determined based on the following assumption: 1-unit optical density (OD)  $\triangleq$  50  $\mu$ g/ml (for double-stranded plasmid DNA). The absorbance measurements at 260 nm ( $OD^{260\text{ nm}}$ ) were used to calculate the plasmid concentrations in  $\mu$ g/ml. The purity of the plasmid DNA was assessed based on the following assumption:  $OD^{260\text{ nm}}/OD^{280\text{ nm}} = 1.8\text{-}2.0$  (for pure DNA samples). This ratio is commonly used to evaluate the purity of nucleic acids where a value between 1.8 and 2.0 indicates relatively pure DNA without significant contamination from proteins or other impurities.

#### 6.3.4. Packaging of rAAV vectors

For the packaging (production) of rAAV vectors, the previously isolated rAAV plasmids (FLAG-hsox9, hTGF- $\beta$ , *lacZ*, and RFP) were introduced in human embryonic kidney (HEK)-293 cells, a human kidney cell line with adenoviral genes E1a and E1b expression (Madry et al., 2003a), according to the following established standard protocol (Cucchiaroni et al., 2011). Initially, 1.8 x

10<sup>6</sup> HEK-293 cells were transferred with 10 ml of DMEM into a Petri dish (100 mm) and subsequently incubated for 48 hours at 37°C under 5% CO<sub>2</sub>. For the further procedures on the third day, the cells were employed if reaching 60-70% confluency. A pre-infection solution containing the Ad5 helper virus used to generate ITRs during the production of rAAV vector was prepared and allocated in Petri dishes at 4 ml per dish which were then incubated for 90 minutes at 37°C under 5% CO<sub>2</sub> (Madry et al., 2003a). In the meantime, a transfection solution (18 mM target plasmid, 6 mM Ad8 helper plasmid, 45% Tris-EDTA - TE - buffer, 5% 2.5 M calcium chloride - CaCl<sub>2</sub>, 50% 4-(2-hydroxyethyl)-1-piperazineethanesulfonic acid - HEPES-buffered saline - HBS) was prepared in a PP tube and incubated for 30 minutes at RT. Meanwhile, the transfection medium (Opti-MEM, 10% FBS, 120 µM chloroquine stock) was prepared. After incubation of the pre-infection system, the medium was removed and 5 ml of transfection medium were added to each Petri dish. Next, 1 ml of transfection solution was added dropwise per Petri dish and incubated for 24 hours at 37°C under 5% CO<sub>2</sub>. On the fourth day, a post-transfection medium (DMEM, 15% FBS, 1% 100X glutamine) was prepared and then transferred in the Petri dishes. The medium from the incubated Petri dishes was removed and 6 ml of post-transfection medium were added per Petri dish and incubated for 24 hours at 37°C under 5% CO<sub>2</sub>. On the fifth day, the medium was removed and 6 ml of 10% sucrose were added to each Petri dish. Subsequently, the adherent cells were detached from the bottom of the Petri dishes using a cell scraper and transferred into a 15-ml tube and centrifuged for 15 minutes at 200 rcf at RT. The entire supernatant of the centrifugation tube was then discarded and remaining residues were pipetted off. The cell aggregate was then resuspended in 10% sucrose (200 µl/centrifugation tube) and the cell suspension was transferred into 1.5-ml sterile PP tube and stored at -20°C. On the sixth day, 3 freeze-thaw cycles were performed. The frozen cell suspensions were incubated in a water bath at 37°C for 5 minutes, mixed in a vortex shaker for 1.5 minutes, and stored at -80°C for 25 minutes per cycle. The process was followed by an incubation for 5 minutes in a water bath at 37°C, by mixing in a vortex shaker for 2 minutes and by centrifugation at 500 rcf for 10 minutes at 4°C. The supernatants were transferred into a new 1.5-ml sterile PP tube, incubated for 45 minutes in water bath at 52°C, and centrifuged for 10 minutes at 12,000 rcf at 4°C. The supernatants were transferred into a new 1.5-ml sterile PP tube and 3 µl of RNase-free DNase (1 U/µl) were added to each supernatant and incubated for 60 minutes at 37°C under 5% CO<sub>2</sub>. The vectors were used directly for transduction or alternatively stored at -20°C. This method has been highly reproducible to generate rAAV vector preparations at titers averaging 10<sup>10</sup> transgene copies/ml (around 1/500 functional viral particles) (Amini et al., 2023; Cucchiariini et al., 2007).

## 6.4. Production and manipulation of rAAV/alginate hydrogel systems

### 6.4.1. Preparation of alginate hydrogels

First, a hydrogel spatula was sterilized with 70% ethanol. Subsequently, 0.03-gram (g) alginate (PH155) was introduced in a 50-ml centrifugation tube containing 1 ml of PBS, resulting in a 3% solution. This mixture was rapidly homogenized, initially through spinning the Falcon tube to disperse the alginate. Next, a series of vortexing and centrifugation steps were employed to guarantee the full dissolution of the alginate. Simultaneously, a CaCl<sub>2</sub> solution was prepared by adding 0.757 g of CaCl<sub>2</sub> to 50 ml of deionized water, resulting in a 103 millimolar (mM) solution. Both the CaCl<sub>2</sub> solution and PBS were then carefully transferred to a 6-well plate, distributing 8-10 ml of each solution across two individual wells. The formation of this setup provided the ideal conditions for the ensuing experimental stages.

### 6.4.2. Incorporation of rAAV vectors in alginate hydrogels

1.5-ml PP tubes received 270 µl of rAAV vectors followed by incorporation of different volumes of 3% alginate as described in **Table 24** to reach final, specific alginate concentrations depending on the experimental requirements of the further analyses. The prepared rAAV/alginate mixtures were then loaded in a 1-ml syringe with a 21-G needle and carefully dropped into the CaCl<sub>2</sub> solution to permit the incorporation of the rAAV vectors within the alginate hydrogel. Following hydrogel formation using different gelation times depending on the specific experimental requirements of the further analyses, a gentle wash was performed by transferring the hydrogel in a PBS solution for an approximate duration of one second via a sterilized hydrogel spatula. The hydrogels were then placed in a 24-well plate insert, ensuring that each insert accommodated cell culture medium with a volume range of 3-500 µl.

**Table 24.** Preparation of the rAAV/alginate hydrogel systems

rAAV (µl)	Alginate (3%, µl)	Final alginate concentration
270.0	308.0	1.6%
270.0	100.0	0.8%
270.0	41.5	0.4%
270.0	19.3	0.2%

Abbreviations: rAAV: recombinant adeno-associated virus; µl: microliter.

### 6.4.3. Transduction of the cell targets with the rAAV/alginate hydrogel systems

Human osteoarthritic articular chondrocytes and human mesenchymal stromal cells were resuspended and seeded on cell culture plates in monolayer cultures at determined cell seeding amounts depending on the specific experimental requirements of the further analyses using cell culture medium and kept at 37°C under 5% CO<sub>2</sub> (**Table 25**). When the cells reached 70-80% confluency, a 24-hour serum starvation phase was initiated to synchronize the cell cycle and further cellular responses.

**Table 25.** Preparation of the target cells for transduction

Culture scale	Seeding conditions	Transduction amount (70-80% confluency)
96-well plates	5 x 10 <sup>3</sup> cells/well	1 x 10 <sup>4</sup> cells/well
48-well plates	1 x 10 <sup>4</sup> cells/well	2 x 10 <sup>4</sup> cells/well
24-well plates	2 x 10 <sup>4</sup> cells/well	3 x 10 <sup>4</sup> cells/well (applied primarily)
6-well plates	8 x 10 <sup>4</sup> cells/well	12 x 10 <sup>4</sup> cells/well

Human osteoarthritic articular chondrocytes and human mesenchymal stromal cells were then treated by direct application of the rAAV/alginate hydrogel systems at precise multiplicities of infection (MOI = ratio of rAAV functional viral particles to the cell numbers, knowing that rAAV vector preparations averaged 10<sup>10</sup> transgene copies/ml, with around 1/500 functional viral particles) depending on the specific experimental requirements of the further analyses using cell culture medium at 37°C under 5% CO<sub>2</sub> (**Table 26**). The cell culture medium was replaced every two days over a total period of 21 days prior to processing the cell cultures for the further analyses (Frisch et al., 2014; Rey-Rico et al., 2016b; Venkatesan et al., 2012).

**Table 26.** Transduction conditions using the rAAV/alginate hydrogel systems

Research Targets	Groups	rAAV (µl)	MOI
hOACs	• no vector/alginate	0	0
	• rAAV- <i>lacZ</i> /alginate	120/60	80/40
	• free rAAV- <i>lacZ</i>	120/60	80/40
hOACs	• no vector/alginate	0	0
	• rAAV-RFP/alginate	120/60	80/40
	• free rAAV-RFP	120/60	80/40
hOACs	• no vector/alginate	0	0
	• rAAV- <i>lacZ</i> /alginate	120	80
	• free rAAV- <i>lacZ</i>	120	80
hOACs	• rAAV- <i>lacZ</i> /alginate	120	80
	• rAAV-FLAG- <i>hsox9</i> /alginate	120	80
	• rAAV-hTGF-β/alginate	120	80
hMSCs	• rAAV- <i>lacZ</i> /alginate	120	80
	• rAAV-FLAG- <i>hsox9</i> /alginate	120	80
	• rAAV-hTGF-β/alginate	120	80

Abbreviations: FLAG: FLAG tag; hsox9: human sex-determining region Y-type high mobility group box 9; hTGF- $\beta$ : human transforming growth factor beta; *lacZ*:  $\beta$ -galactosidase; MOI: multiplicity of infection; rAAV: recombinant adeno-associated virus; RFP: red fluorescent protein;  $\mu$ l: microliter.

## **6.5. Cell culture processing**

### **6.5.1. Cell culture fixation**

The cell cultures were washed with PBS and a 4% formaldehyde solution was then added to the samples for 1 hour at RT. The solution was then carefully removed and the cells were washed twice with PBS to remove any residual formaldehyde. The cell cultures were stored at 4°C prior to performing the further analyses.

### **6.5.2. Cell culture lysis**

The cell cultures were trypsinized and centrifuged at 3,000 rpm for 10 minutes at RT. The supernatant was carefully removed and a lysis solution (125 microgram ( $\mu$ g) papain/ml in PBE, i.e., PBS-EDTA at 0.01 M) was added to the cell pellet (1 ml per  $10^6$  counted cells). After vortexing for 3 minutes, the mixture was placed in a water bath under 400 rpm for 2 hours at 60°C to facilitate lysis. The cell lysates were stored at -20°C prior to performing the further analyses.

## **6.6. Evaluation of rAAV vector release from the alginate hydrogel systems**

The quantitative estimation of the rAAV vector release from the alginate hydrogel systems was carried out using a specific AAV2 Titration ELISA (Cucchiarini et al., 2011) based on an antigen-antibody reaction as part of a specific immunological reaction (Aydin, 2015). In this assay, a genetically engineered antibody directed against an AAV capsid antigen was bound to a microtiter plate. Upon addition of the rAAV-containing test sample culture supernatants, the AAV antigen contained therein specifically may bind to this anti-AAV capsid antibody and may be revealed by the application of a specific secondary antibody coupled to an enzyme that may react by the addition of a chromogenic substrate to form a colored reaction product photometrically measurable and directly proportional to the amount of bound AAV antigen according to a provided calibration curve.

The following steps were taken to determine the concentrations of rAAV vector release in test sample culture supernatants according to the manufacturer's recommendations. The assay

buffer, ASSB 1x, was prepared by diluting 20x ASSB (1:20) with distilled water. The kit control was reconstituted in 500 µl of ASSB 1x and serial dilutions were prepared with ASSB 1x. For the Biotin 1x solution, the Biotin Concentrate was reconstituted in 750 µl of ASSB 1x immediately before use and subsequently diluted (1:20) with ASSB 1x. Likewise, Strep-HRP 1x was prepared by diluting Strep-HRP20x (1:20) with ASSB 1x immediately before use. For the kit control series, dilutions were carried out ranging from undiluted to a dilution (1:64) with the following concentrations: 2.2E+09 (undiluted), 1.1E+09, 5.5E+08, 2.8E+08, 1.4E+08, 6.9E+07, 3.4E+07, and 0 (labeled as KC1 to KC7, and KC0). The reconstitution was performed with 250 µl of each concentration plus 250 µl of 1x ASSB (Assay Buffer Solution). The assay was then performed as follows: KC, KC0, and supernatant dilutions were added to wells at 100 µl per well and incubated for 1 hour at 37°C. The wells were washed three times with 200 µl of ASSB 1x followed by the addition of 100 µl of Biotin 1x per well and incubation for 1 hour at 37°C. Three other washes were then performed with 200 µl of ASSB 1x followed by the addition of 100 µl of Strep-HRP 1x per well and by an incubation for 1 hour at 37°C. After three washes with 200 µl of ASSB 1x, 100 µl of TMB was added per well and incubated for 15 minutes at RT. The reaction was stopped by adding 100 µl of STOP solution at RT per well. The plate was read at the wavelengths of 450 nm and 650 nm within 30 minutes. Values in the test sample culture supernatants were calculated with regard to the calibration curve.

## **6.7. Detection of transgene expression**

### **6.7.1. X-Gal staining**

The principle of the assay is to determine whether cells transduced with the rAAV-*lacZ* vector overexpress the carried *E. coli* β-galactosidase (β-gal) reporter gene (Cucchiarini et al., 2003; Madry et al., 2003a). A colored reaction is produced in cells expressing β-gal when adding X-Gal (5-bromo-4-chloro-3-indolyl-β-D-galactopyranoside), a substrate of this enzyme that becomes hydrolyzed to 5-bromo-4-chloro-3-indoxyl oxidized as a insoluble indigo compound.

The cell cultures were fixed and washed twice in PBS as described in § 6.5.1. The β-gal Staining kit was brought to RT and the reagents were thawed in a water bath for 15 minutes at 37°C. The β-gal staining working solution was prepared mixing the X-Gal solution (5%, v/v) with the Iron buffer (95%, v/v) of the kit by vortexing during 1 minute and by inversion during eight minutes to ensure proper mixing. The solution was then filtered (0.2 µm) to remove undesirable crystals and added to cover the fixed cell cultures for a 6-hour incubation. Samples were examined under a light microscope (BX45) and documented by microphotography (digital camera DP22).

### 6.7.2. Live fluorescence

The principle of the assay is to determine whether cells transduced with the rAAV-RFP vector overexpress the carried red fluorescent protein (RFP) reporter gene (Cucchiari et al., 2003; Madry et al., 2003a).

The cell cultures were directly examined under a live fluorescent microscope (CK41) with using a 568 nm filter and documented by microphotography (digital camera DP22).

### 6.7.3. TGF- $\beta$ ELISA

The principle of the assay is to determine whether cells transduced with the rAAV-hTGF- $\beta$  vector overexpress the carried human TGF- $\beta$  candidate gene (Frisch et al., 2014, 2016a, 2016b, 2017; Morscheid et al., 2019a; Venkatesan et al., 2013).

The following steps were taken using the ELISA Human TGF- $\beta$ 1 Immunoassay kit according to the manufacturer's recommendations. The Calibrate Diluent RD5-53 was prepared by adding 20 ml of the Calibrate Diluent RD5-53 Concentrate to 60 ml of distilled water for a total volume of 80 ml. Then, the standards were prepared in PP tubes at concentrations ranging from 2,000 picogram (pg)/ml to 31.3 pg/ml through serial dilutions using the Calibrate Diluent RD5-53. The cell supernatants were then activated by centrifuging at high speed for 1 minute at RT, transferring 100  $\mu$ l of supernatant to a new 1.5-ml PP tube, mixing with 20  $\mu$ l of 1 N hydrochloric acid (HCl), incubating for 10 minutes at RT, and neutralizing with 20  $\mu$ l of 1.2 N sodium hydroxide (NaOH)/0.5 molar (M) 4-(2-hydroxyethyl)-1-piperazineethanesulfonic acid (HEPES). A washing buffer was prepared by combining 20 ml of Wash Buffer Concentrate with 480 ml of distilled water for a total of 500 ml and the substrate solution was prepared by mixing equal volumes of Color Reagents A and B, protecting them from light. Standards, control (C), and activated samples were then added to the wells of the kit (50  $\mu$ l each) and the plate was incubated for 2 hours at RT after adding 50  $\mu$ l of Diluent RD1-21 per well. Following this incubation, the plate was washed three times with 400  $\mu$ l of washing buffer and 100  $\mu$ l of TGF- $\beta$ 1 Conjugate was added to each well, followed by an incubation of 2 hours at RT. The plate was washed again as described above and 100  $\mu$ l of substrate solution were added to each well. The plate was incubated for 30 minutes at RT, protected from light. Finally, 100  $\mu$ l of Stop Solution were added to each well and the plate was gently tapped to mix. The absorbances were measured in a microplate reader (GENios A-5082) using a wavelength at 450 nm. The TGF- $\beta$  concentrations in the samples were calculated relative to the calibration curve (TGF- $\beta$  standards).

#### 6.7.4. SOX9 and TGF- $\beta$ immunodetection

The principle of the assay is to determine whether cells transduced with either the rAAV-FLAG-hsox9 or the rAAV-hTGF- $\beta$  vectors overexpress the carried sox9 or TGF- $\beta$  candidate genes based on an antigen-antibody interaction within the framework of a defined immunological response employing the biotin-avidin method (Bratthauer, 2010; Brentjens et al., 2013; Rey-Rico et al., 2016b; Venkatesan et al., 2012).

The cell cultures were fixed and washed twice in PBS as described in § 6.5.1. followed by a step of cell permeabilization using 0.1% triton X-100 solution (4  $\mu$ l in 4 ml of PBS) for a 10-minute incubation period. The cell cultures were washed once with PBS and then treated for 20 minutes with 0.3% hydrogen peroxide solution (40  $\mu$ l of 30% hydrogen peroxide (H<sub>2</sub>O<sub>2</sub>) in 4 ml of distilled water) to quench endogenous peroxidase activity. The cell cultures were then blocked for 30 minutes with 0.5% bovine serum albumin (BSA; 20  $\mu$ l in 4 ml of PBS) to minimize nonspecific binding followed by an overnight incubation at 4°C with each respective (SOX9 or TGF- $\beta$ ) primary antibody prepared in 0.5% BSA (anti-SOX9 antibody: 1:60; anti-TGF- $\beta$  antibody: 1:50). One day later, the cell cultures were gently washed with PBS and each respective secondary biotinylated antibody prepared in PBS (1:200) was applied for 1 hour at RT. During this incubation, the horseradish peroxidase (HRP)-linked avidin-biotin complex (ABC) that reacts with the biotinylated secondary antibodies was prepared, followed by a 30-minute stabilization at RT. The cell cultures were then treated with ABC-HRP for 30 minutes at RT. During this incubation, the 3,3'-diaminobenzidine (DAB) chromogen, a substrate of HRP that produces a brown precipitate insoluble in alcohol, was prepared 5 minutes before further addition to the reaction. The cell cultures were then treated with DAB for no more than seven minutes until a brown coloration was achieved, followed by a final wash with PBS. The samples were examined under a light microscope (BX45) and documented by microphotography (digital camera DP22).

### 6.8. Biochemical analyses

#### 6.8.1. Hoechst 33258 assay

The principle of the assay is to quantitatively estimate the DNA contents in the cell cultures based on the detection of the dibenzimidazole fluorescent dye Hoechst 33258 that intercalates in DNA molecules (Cucchiaroni et al., 2011; Venkatesan et al., 2012).

A Hoechst working solution was prepared from a stock solution (1 milligram (mg)/ml) diluted 1:500 in Tris-EDTA-NaCl (TEN) buffer to give a final concentration of 2  $\mu$ g/ml. A DNA

standard solution was prepared from a stock solution (1 mg/ml) diluted 1:100 in PBE to give a final concentration of 10 µg/ml. The DNA standards were prepared in a series of dilutions using TEN buffer, yielding final DNA concentrations of 0, 25, 50, 75, 100, and 200 ng in 100 µl total volume. For the assay, 20 µl of cell lysates were prepared as described in § 6.5.2. or of the standards were combined with 80 µl of TEN buffer and added to the wells of a flat black 96-well plate (GRE96fb). Next, 100 µl of the Hoechst working solution was added to each well and mixed by pipetting up and down. This step involved a time-dependent reaction. The fluorescent signals were then measured from the top in a microplate reader (GENios A-5082) using excitation and emission wavelengths at 360 nm (365 nm optimal) and 465 nm (458 nm optimal), respectively. The DNA contents in the samples were calculated relative to the calibration curve (DNA standards).

### 6.8.2. Dimethylmethylene blue (DMMB) assay

The principle of the assay is to quantitatively estimate the extracellular PG contents in the cell cultures by binding to the DMMB dye (Cucchiarini et al., 2011; Rey-Rico et al., 2016b; Venkatesan et al., 2012).

A DMMB working solution was prepared using 16 mg DMMB prepared in 0.3% (v/v) 90% formic acid, 0.5% (v/v) 95% ethanol, and 2.56% (v/v) 1 M NaOH. Three working solutions were then sequentially prepared, including solution A (10 mM D-cysteine HCl monohydrate in PBE), solution B (53 M chondroitin sulfate in solution A), and solution C (99.8% v/v solution A with 0.2% v/v solution B). To establish PG (chondroitin sulfate) standards, various volumes of solutions C and A were combined to generate six discrete concentrations (100% to 0%), each with a total volume of 40 µl (100% by 40 µl of solution C and 0 µl of solution A; 80% by 32 µl of solution C and 8 µl of solution A; 60% by 24 µl of solution C and 16 µl of solution A; 40% by 16 µl of solution C and 24 µl of solution A; 20% by 8 µl of solution C and 32 µl of solution A; and 0% by 0 µl of solution C and 40 µl of solution A). For the assay, 40 µl of cell lysates were prepared as described in § 6.5.2. or of the standards were added to the wells of a white 96-well plate (GRE96ft) and combined with 250 µl of the DMMB working solution by pipetting up and down. The absorbances were then measured in a microplate reader (GENios A-5082) using a wavelength at 595 nm. The PG contents in the samples were calculated relative to the calibration curve (PG standards).

### 6.8.3. WST-1 assay

The principle of the assay is to quantitatively estimate the indices of cell proliferation in the cell cultures based on the use of a water-soluble tetrazolium salt (WST), a water-soluble dye that gives

a particular absorption spectrum of the formed formazan (Amini et al., 2023; Cai et al., 2023; Venkatesan et al., 2020b).

The medium of the cell cultures was first replaced with 100  $\mu$ l of fresh DMEM per well that was then combined with 10  $\mu$ l of Cell Proliferation Reagent WST-1 and the plate was then incubated for 30 minutes to 4 hours at 37°C. Prior to the time-dependent (optimization) measurements, the plate was shaken for 1 minute at RT. The absorbances were then measured in a microplate reader (GENios A-5082) using a wavelength range of 420 nm-480 nm. The indices of cell proliferation in the samples were directly used as optical density (OD) values.

#### 6.8.4. Alcian blue assay

The principle of the analysis is to quantitatively estimate extracellular acidic polysaccharides in the cell cultures based on a staining with alcian blue, a polyvalent basic dye (Meng et al., 2020; Rey-Rico et al., 2018; Urich et al., 2020).

An alcian blue working solution was prepared using 57.318 g alcian blue prepared in 100 ml of distilled water (or 11.4 g in 20 ml for smaller volumes). A 6 M guanidine-HCl solution was also prepared in parallel. The cell cultures were fixed and washed twice in PBS as described in § 6.5.1. and 500  $\mu$ l of alcian blue working solution were then added to the cell cultures for 15 minutes at 37°C. The samples were examined under a light microscope (BX45) and documented by microphotography (digital camera DP22). The cell cultures were next treated with 500  $\mu$ l of 6 M guanidine-HCl solution for 30 minutes at 37°C. The absorbances were then measured in a microplate reader (GENios A-5082) using a wavelength at 595 nm. The polysaccharides contents in the samples were calculated relative to 6 M guanidine-HCl (blank).

#### 6.8.5. Bicinchoninic acid (BCA) assay

The principle of the assay is to quantitatively estimate the total protein contents in the cell cultures based on the reduction of  $\text{Cu}^{2+}$  to  $\text{Cu}^{+}$  through complex formation with proteins in an alkaline environment, the concentration of total proteins being directly proportional to the amounts of reduced copper (Huang et al., 2010). This assay allows to quantitatively standardize all other biochemical parameters described above.

A working solution was prepared by mixing 50 parts of BCA Reagent A with 1 part of BCA Reagent B. A series of bovine serum albumin (BSA) standards was prepared using a stock solution at 2 mg/ml as follows: Solution A at 2,000  $\mu$ g/ml was prepared by adding 75  $\mu$ l of BSA stock solution; Solution B at 1,500  $\mu$ g/ml was made with 31.3  $\mu$ l of distilled water and 93.8  $\mu$ l of BSA

stock solution; Solution C was made at 1,000 µg/ml using equal parts of water and of BSA stock solution; subsequent solutions D through H were serially diluted to concentrations of 750, 500, 250, 125, and 25 µg/ml, respectively. Solution I containing only distilled water was used as blank (0 µg/ml). For the assay, 25 µl of cell lysates were prepared as described in § 6.5.2. or of the standards were added to the wells of a white 96-well plate (GRE96ft) and combined with 200 µl of the working solution by pipetting up and down and the plate was then shaken for 30 seconds and incubated for 30 minutes at 37°C. After incubation, the plate was allowed to equilibrate for 5 minutes at RT. The absorbances were then measured in a microplate reader (GENios A-5082) using a wavelength at 562 nm. The total protein contents in the samples were calculated relative to the calibration curve (total protein standards).

## **6.9. Histological analyses**

### **6.9.1. Hematoxylin-eosin (H&E) staining**

The principle of the analysis is to evaluate the cell densities in the cell cultures based on a staining with hematoxylin, an oxidation-derived natural dye that forms positively-charged complexes with aluminum ions, thus staining basophilic structures in blue under acidic conditions (Chan, 2014) and with eosin, a synthetic dye that counterstains azophilic structures in red (Chan, 2014).

A hematoxylin solution was prepared by mixing an equimolar combination of hematoxylin A and hematoxylin B solutions nach Weigert. A 0.5% eosin solution was prepared by direct dilution in distilled water. The cell cultures were fixed and washed twice in PBS as described in § 6.5.1. and 500 µl of hematoxylin solution was added to the cell cultures for 10 minutes at RT, followed by a washing with distilled water. A 1% HCl solution was next briefly added and removed, followed by the application of warm water for 4 minutes at RT. The cell cultures were again treated by addition of 500 µl of hematoxylin solution for 6 minutes at RT and then rinsed with distilled water. The cell cultures were finally treated by addition of 500 µl of eosin solution for 5 minutes at RT and then rinsed with distilled water. The samples were examined under a light microscope (BX45) and documented by microphotography (digital camera DP22).

### **6.9.2. Toluidine blue staining**

The principle of the analysis is to evaluate the deposition of glycosaminoglycans in the cell cultures based on a staining with toluidine blue, a basic thiazine dye that binds specifically to negatively charged glycosaminoglycans, allowing for their detection through a blue coloration (Bergholt et

al., 2019; Cucchiarini et al., 2011; Venkatesan et al., 2012).

A 1% toluidine blue solution was prepared in distilled water. The cell cultures were fixed and washed twice in PBS as described in § 6.5.1. and 500 µl of toluidine blue solution were added to the cell cultures for 15 minutes at RT, followed by a washing with distilled water. The samples were examined under a light microscope (BX45) and documented by microphotography (digital camera DP22).

### 6.9.3. Safranin O staining

The principle of the analysis is to evaluate the deposition of proteoglycans in the cell cultures based on a staining with safranin O, an azo dye with an affinity for negatively charged proteoglycans, allowing for their detection through a red coloration (Brittberg, 2010).

A hematoxylin solution was prepared as described in § 6.9.1. A safranin O solution was prepared by direct dilution in distilled water. A fast green (0.02%) solution was prepared for counterstaining by dissolving 0.2 g of fast green in 1 l of distilled water. A acetic acid (glacial) (1%) solution was prepared by mixing 1 ml of acid acetic glacial with 100 ml of distilled water. The cell cultures were fixed and washed twice in PBS as described in § 6.5.1. and 500 µl of hematoxylin solution was added to the cell cultures for 10 minutes at RT, followed by a washing with distilled water. The cell cultures were then treated by addition of 500 µl of fast green solution for 5 minutes at RT, followed by a brief treatment with 500 µl of acetic acid (glacial) solution and by addition of 500 µl of safranin O solution for 5 minutes at RT. The samples were examined under a light microscope (BX45) and documented by microphotography (digital camera DP22).

### 6.9.4. Alizarin red staining

The principle of the analysis is to evaluate the deposition of calcium phosphate in the cell cultures based on a staining with alizarin red, a calcium-binding dye with an affinity for calcium deposits, allowing for their detection through a bright red coloration (Cucchiarini et al., 2011; Venkatesan et al., 2012).

An alizarin red solution was commercially prepared and an alizarin red differentiation solution was prepared by mixture of 37% HCl and 95% ethanol. The cell cultures were fixed and washed twice in PBS as described in § 6.5.1. and 500 µl of alizarin red solution was added to the cell cultures for 4 minutes at RT, followed by a washing with distilled water. The cell cultures were then treated by addition of 500 µl of alizarin red differentiation solution for 30 seconds at RT, followed by a washing with distilled water. The samples were examined under a light microscope

(BX45) and documented by microphotography (digital camera DP22).

## **6.10. Immunocytochemical analysis**

The principle of the analysis is to evaluate the deposition of collagens (type-I, -II, and -X collagen) in the cell cultures based on an antigen-antibody interaction within the framework of a defined immunological response employing the biotin-avidin method mostly as described in § 6.7.4. (Bratthauer, 2010; Brentjens et al., 2013; Rey-Rico et al., 2016b; Venkatesan et al., 2012).

The cell cultures were fixed and washed twice in PBS as described in § 6.5.1. followed by a step of cell permeabilization using 0.1% triton X-100 solution (4 µl in 4 ml of PBS) for a 10-minute incubation period. The cell cultures were washed once with PBS and then treated for 20 minutes with 0.3% hydrogen peroxide solution (40 µl of 30% hydrogen peroxide (H<sub>2</sub>O<sub>2</sub>) in 4 ml of distilled water) to quench endogenous peroxidase activity. The cell cultures were then blocked for 30 minutes with 0.5% bovine serum albumin (BSA; 20 µl in 4 ml of PBS) to minimize nonspecific binding followed by an overnight incubation at 4°C with each respective (type-I, -II, or -X collagen) primary antibody prepared in 0.5% BSA (anti-type-I collagen antibody: 1:200; anti-type-II collagen antibody: undiluted; anti-type-X collagen antibody: 1:200). One day later, the cell cultures were gently washed with PBS and each respective secondary biotinylated antibody prepared in PBS (1:200) was applied for 1 hour at RT. During this incubation, the horseradish peroxidase (HRP)-linked avidin-biotin complex (ABC) that reacts with the biotinylated secondary antibodies was prepared, followed by a 30-minute stabilization at RT. The cell cultures were then treated with ABC-HRP for 30 minutes at RT. During this incubation, the 3,3'-diaminobenzidine (DAB) chromogen, a substrate of HRP that produces a brown precipitate insoluble in alcohol, was prepared 5 minutes before further addition to the reaction. The cell cultures were then treated with DAB for no more than seven minutes until a brown coloration was achieved, followed by a final wash with PBS. The samples were examined under a light microscope (BX45) and documented by microphotography (digital camera DP22).

## **6.11. Histomorphometrically analysis**

The principle of the analysis is to quantitatively estimate the results of the biochemical, histological, and immunocytochemical analyses performed in the cell cultures in § 6.8.4., § 6.9., and § 6.10. (Venkatesan et al., 2012).

The cell densities on H&E-stained cell cultures were measured as the ratio of the cell numbers per area of the site evaluated at four randomized sites using CellSens, ImageJ, and

Affinity Photo (Venkatesan et al., 2012). The average optical density (AOD) on alcian blue-, toluidine blue-, safranin O-, and alizarin red-stained and on SOX9/TGF- $\beta$ /anti-type-I/-II/-X collagen immunocytochemically-stained cell cultures was measured as the ratio of the staining intensity to the whole area of the site evaluated at four randomized sites using CellSens, ImageJ, and Affinity Photo (Venkatesan et al., 2012). The intensities of alcian blue, safranin O, and alizarin red staining and those of SOX9/TGF- $\beta$ /anti-type-I/-II/-X collagen immunocytochemical staining were scored for uniformity and density using a modified Bern score grading system (0 = no staining; 1 = heterogeneous/weak staining; 2 = homogeneous/moderate staining; 3 = homogeneous/intense staining; 4 = very intense staining) (Venkatesan et al., 2012). Scoring was blindly performed by two individuals (including the candidate here) regarding the conditions (Venkatesan et al., 2012).

## **6.12. Real-time reverse transcription polymerase chain reaction (RT-PCR)**

The principle of the analysis is to quantitatively estimate the expression profiles of specific genes (*sox9*, TGF- $\beta$ , aggrecan - ACAN, type-I collagen - COL1A1, type-II collagen - COL2A1, type-X collagen - COL10A1) in the cell cultures relative to the glyceraldehyde-3-phosphate dehydrogenase (GAPDH) used as a housekeeping, internal control gene (Venkatesan et al., 2012, 2022).

For total cellular ribonucleic acid (RNA) isolation, the cell cultures ( $\sim 10^7$  cells) were collected and the cell culture medium was first entirely removed, followed by addition of 350  $\mu$ l of RLT Lysis Buffer from the RNeasy Protect Mini kit was added by pipetting up and down for 2 minutes at RT. The cell lysates (around 350  $\mu$ l) were then subjected to centrifugation at 13,000 rpm for 3 minutes at RT. Next, 1.5-ml Collection Tubes were first labeled and Mini Spin Columns were set up in 2-ml Collection Tubes. The supernatants were then cautiously removed by pipetting them in the 1.5-ml Collection Tubes. An equal volume of 70% ethanol (350  $\mu$ l) was then introduced and mixed by pipetting. The samples were then transferred to Mini Spin Columns, centrifuged at 13,000 rpm for 30 seconds at RT, with the flow-through being subsequently discarded. The Mini Spin Columns were then treated with 350  $\mu$ l of RW1 Wash Buffer followed by centrifugation at 13,000 rpm for 30 seconds at RT, with the flow-through being subsequently discarded. This step was repeated using 250  $\mu$ l of RPE Wash Buffer. Finally, the Mini Spin Columns were placed in new 2-ml Collection Tubes and centrifuged to dry the membrane. The Mini Spin Columns were then placed in 1.5-ml PP tubes, treated with 40  $\mu$ l of RNase-Free Water and centrifuged at 13,000 rpm for 30 seconds at RT for RNA elution.

For reverse transcription, 8.2  $\mu$ l of the obtained RNA eluate were processed for cDNA synthesis using the 1<sup>st</sup> Strand cDNA Synthesis kit for RT-PCR (AMV) by mixing with 2  $\mu$ l of 10x

Reaction Buffer, 4  $\mu$ l of magnesium chloride ( $\text{MgCl}_2$ ), 2  $\mu$ l of Deoxynucleotide Mix, a pair of primers specific of the gene of interest (150 nM each primer), 1  $\mu$ l of RNase inhibitor, and 0.8  $\mu$ l of Reverse Transcriptase. and the final mixture volume of 20  $\mu$ l was used for the PCR Thermal Cycler.

For RT-PCR, 2  $\mu$ l of the obtained cDNA product were amplified by mixing with 25  $\mu$ l of Brilliant III Ultra-Fast SYBR Green QPCR Master Mix, 150 nM primers, and PCR-grade water to reach a final volume of 50  $\mu$ l. The procedure was performed using a Mx3000P<sup>®</sup> QPCR operator system as follows: [10 minutes at 95°C], amplification by 40 cycles [denaturation for 30 seconds at 95°C, annealing for 1 minute at 55°C, extension for 30 seconds at 72°C], denaturation [1 minute at 95°C], and final incubation [30 seconds at 55°C]. The threshold cycle (Ct) value for each gene of interest was measured for each amplified sample using the MxPro QPCR software and values were normalized to GAPDH expression using the  $2^{-\Delta\Delta\text{Ct}}$  method. This method is a robust quantitative approach in real-time PCR experiments for the analysis of gene expression levels. By normalizing the Ct values against a reference gene to calculate a  $\Delta\text{Ct}$ , and comparing it to a control sample to derive a  $\Delta\Delta\text{Ct}$ , the  $2^{-\Delta\Delta\text{Ct}}$  method enables the translation of  $\Delta\Delta\text{Ct}$  values into a fold change in gene expression.

### **6.13. Statistical analysis**

Data were given as mean and standard deviation (SD) or median and interquartile range for each separate experiment. All conditions were performed in triplicate in three independent experiments per patient, using all patients in all experiments. The Shapiro-Wilk normality test and the F test or the Brown-Forsythe test were employed to check for normal distribution and equal variance. The Wilcoxon test, the Mann-Whitney test, and the Kruskal-Wallis test were employed for nonparametric analysis and the Dunn's test for multiple comparisons. The one sample t-test, the unpaired t-test, Ordinary one-way ANOVA, and the Welch test were employed for parametric analysis and the Dunnett's/Dunnett's T3 tests for multiple comparisons. *P* values/adjusted *P* values were reported with  $P \leq 0.05$  considered statistically significant. Scatter plot diagrams consistently displayed individual data points (dots). Depending on the data distribution, either the mean value (middle line) and 95% confidence interval (dotted line) or the median (middle line) and 95% confidence interval (dotted line) were presented. Box plot diagrams always showed the interquartile range (upper and lower borders of the boxes), the minimum and maximum (whiskers), the mean value (+), the median (middle line), and the individual data points (dots). All measurements were performed with Prism.

## 7. RESULTS

### 7.1. Ability of alginate-based hydrogels to deliver rAAV vectors in human osteoarthritic articular chondrocytes

This evaluation aimed at testing the first hypothesis:

***"Alginate-based hydrogels are capable of efficiently and durably incorporating and delivering rAAV vectors as a means to genetically modify human osteoarthritic articular chondrocytes".***

#### 7.1.1. Optimization of rAAV delivery in human osteoarthritic articular chondrocytes via alginate hydrogels

Human osteoarthritic articular chondrocytes were first employed to systematically test various experimental conditions of rAAV-*lacZ* and rAAV-RFP delivery over time (21 days) via alginate hydrogels in order to optimize the parameters of preparation of the system, including the concentration and gelation properties of the alginate, the doses of rAAV vector, and the features of the targets cells themselves (**Figure 7A**). Expression of *lacZ* was monitored by X-Gal staining (**Figure 7B**) and that of RFP by detection of live fluorescence (**Figure 7D**), with a histomorphometrically analysis of the corresponding average optical densities (AOD) over an extended period of 21 days (**Figures 7C, 7E**).

First, the rAAV vector dose-dependent effect was noted, with a detectable augmentation of the expression of *lacZ* (**Figures 7B, 7C**) and of RFP (**Figures 7D, 7E**) when increasing the MOI from 40 to 80 of either vector type relative to the no vector or free vector conditions. Second, decreasing the alginate concentration allowed to enhance the expression levels of *lacZ* (**Figures 7B, 7C**) and of RFP (**Figures 7D, 7E**). Third, a time of 1 minute appeared as the optimal gelation time to prepare the alginate hydrogel (**Figures 7B-7E**). Based on these findings, the conditions of rAAV-associated MOI of 80, an alginate concentration of 0.2%, and a gelation time of 1 minute for the alginate hydrogel were selected as optimal conditions to prepare the systems.

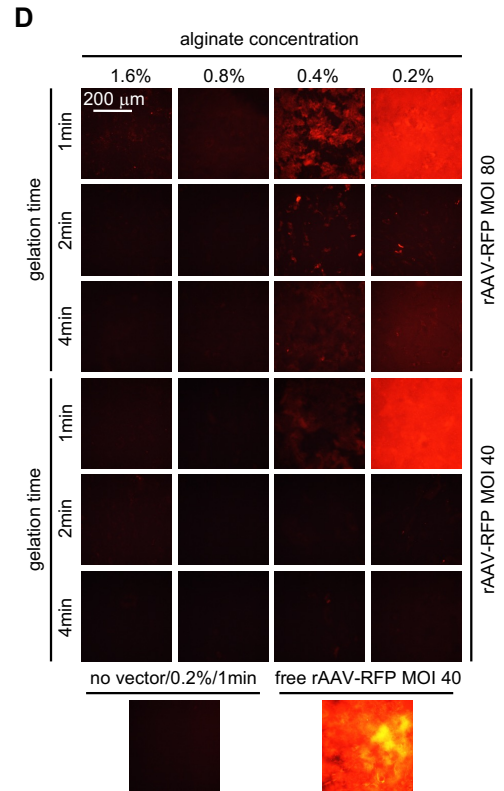
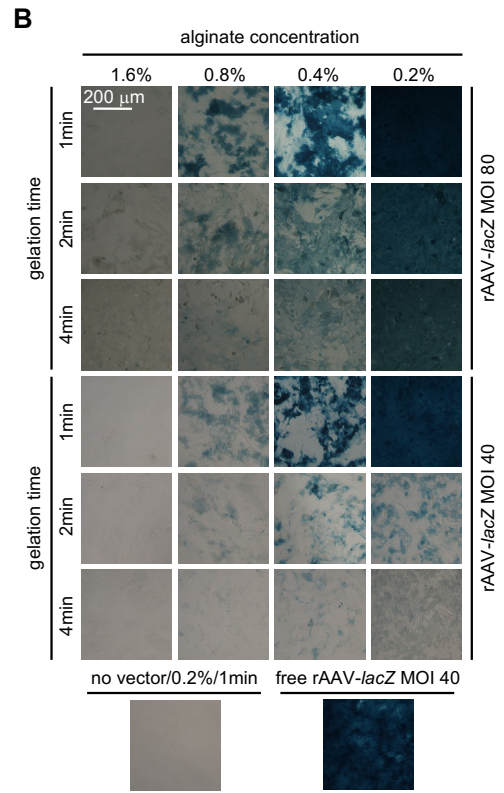
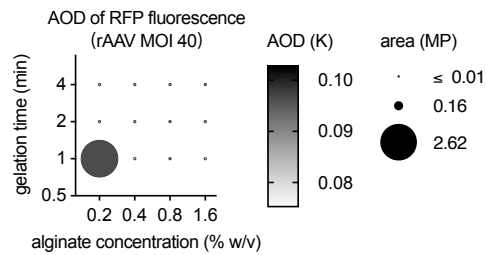
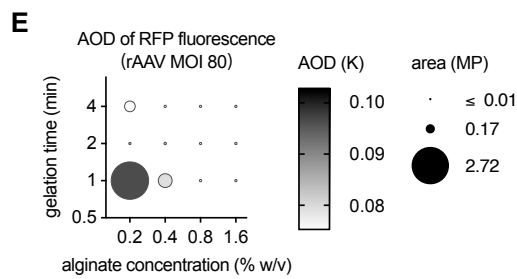
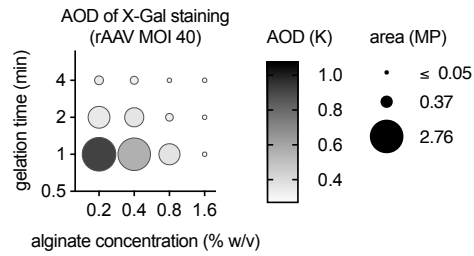
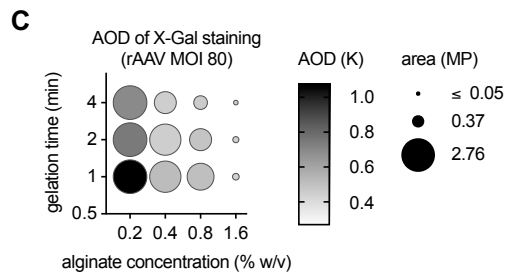
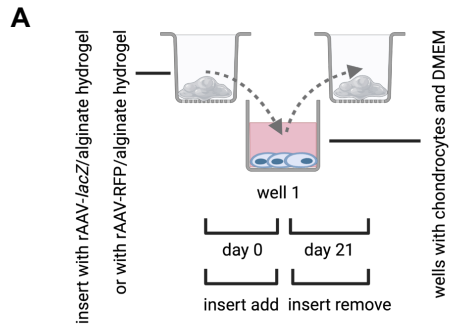


**Figure 7.** Optimization of rAAV delivery in human osteoarthritic articular chondrocytes via alginate hydrogels. **(A)** Experimental design of the application of the rAAV (*lacZ* or RFP)/alginate hydrogel systems to hOACs over time. **(B)** X-Gal staining when delivering rAAV-*lacZ* relative to the no vector or free vector conditions after 21 days, using various MOIs, alginate concentrations, and gelation times (magnification x 20; scale bars: 200  $\mu\text{m}$ ; all representative data) with **(C)** an estimation of the corresponding AOD. **(D)** Detection of live fluorescence when delivering rAAV-RFP relative to the no vector or free vector conditions after 21 days, using various MOIs, alginate concentrations, and gelation times (magnification x 20; scale bars: 200  $\mu\text{m}$ ; all representative data) with **(E)** an estimation of the corresponding AOD. Abbreviations: AOD: average optical density; DMEM: Dulbecco's Modified Eagle Medium; hOACs: human osteoarthritic articular chondrocytes; K: kilo; *lacZ*:  $\beta$ -galactosidase; min: minute; MOI: multiplicity of infection; MP: megapixel; rAAV: recombinant adeno-associated virus; RFP: red fluorescent protein; w/v: weight/volume; X-Gal: 5-bromo-4-chloro-3-indolyl- $\beta$ -D-galactopyranoside;  $\mu\text{m}$ : micrometer (created with BioRender, Affinity Photo, and Prism).

### 7.1.2. Kinetics of rAAV vector release from alginate hydrogels

Human osteoarthritic articular chondrocytes were then employed to monitor the kinetics of rAAV vector release from the alginate hydrogels over time (21 days) using the optimal conditions evidenced and reported in § 7.1.1. to prepare the system (**Figure 8A**). Here, the rAAV-*lacZ* vector was applied using thus an MOI of 80 in 0.2% alginate with a gelation time of 1 min. Similar conditions were used in the absence of human osteoarthritic articular chondrocytes as a control experiment (**Figure 8D**). Expression of *lacZ* was monitored by X-Gal staining (**Figure 8B**) with an histomorphometrically analysis of the corresponding AOD (**Figure 8C**) and the kinetics of rAAV vector release from the alginate hydrogels was determined by ELISA (**Figures 8E, 8F**) over an extended period of 21 days.

First, the effective, controlled release of rAAV-*lacZ* was indirectly evidenced by a detectable augmentation of the expression of *lacZ* in human osteoarthritic articular chondrocytes over time relative to the no vector or free vector conditions (**Figures 8B, 8C**). Second, the effective, controlled release of rAAV-*lacZ* was directly evidenced by a detectable augmentation of the amounts of vectors released from the systems in the absence of human osteoarthritic articular chondrocytes over time (**Figures 8E, 8F**).

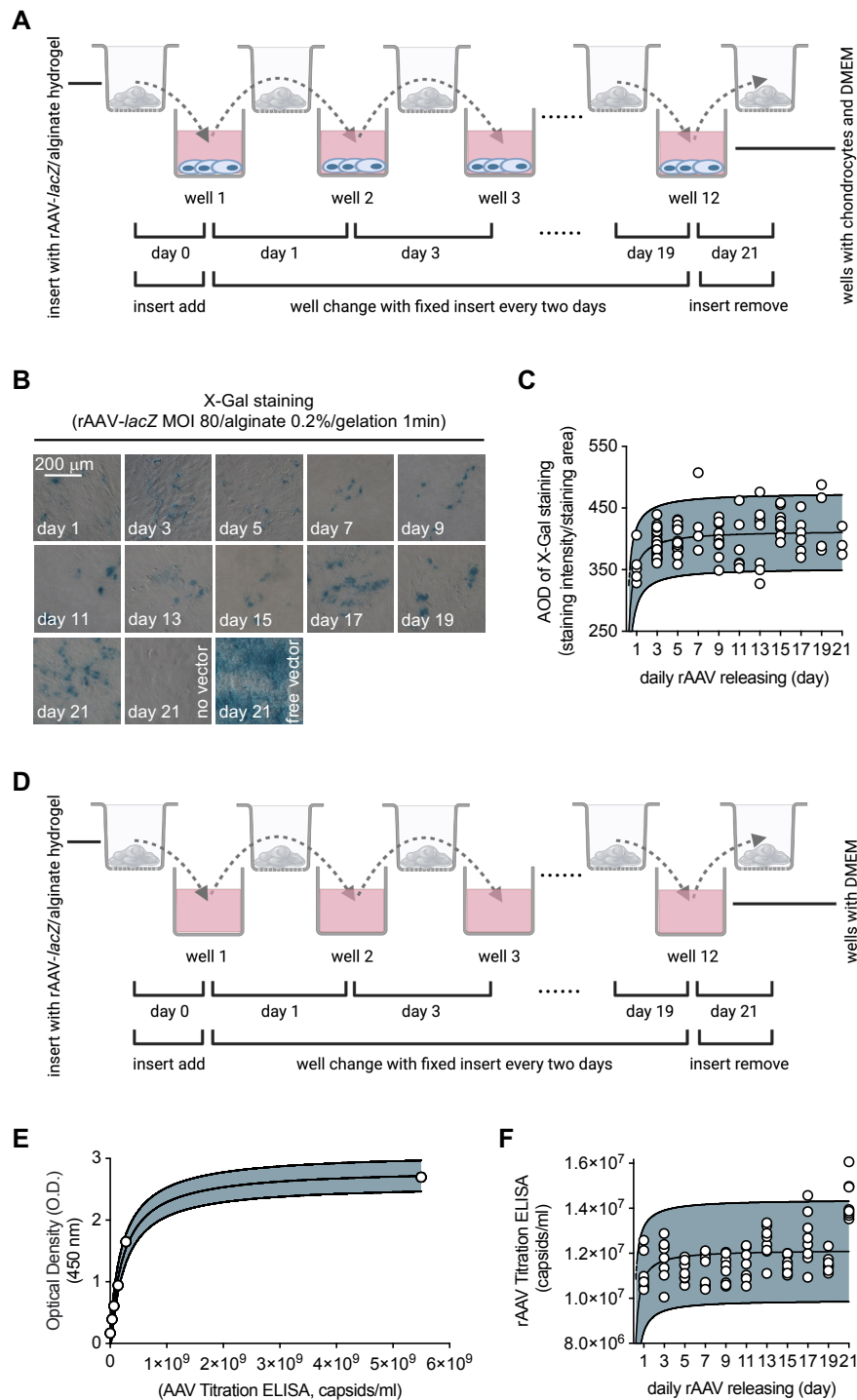


**Figure 8.** Kinetics of rAAV release from alginate hydrogels. **(A)** Experimental design of the application of the rAAV (*lacZ*)/alginate hydrogel systems in hOACs over time. **(B)** X-Gal staining when delivering rAAV-*lacZ* relative to the no vector or free vector conditions over time (magnification  $\times 20$ ; scale bars: 200  $\mu$ m; all representative data) with **(C)** an estimation of the corresponding AOD. **(D)** Experimental design of the application of the rAAV (*lacZ*)/alginate hydrogel systems in the absence of hOACs over time. **(E)** AAV Titration ELISA (unprocessed data) with **(F)** kinetics of data analysis. Abbreviations: AAV: adeno-associated virus; AOD: average optical density; DMEM: Dulbecco's Modified Eagle Medium; ELISA: enzyme-linked immunosorbent assay; hOACs: human osteoarthritic articular chondrocytes; *lacZ*:  $\beta$ -galactosidase; min: minute; ml: milliliter; MOI: multiplicity of infection; nm: nanometer; OD: optical density; rAAV: recombinant adeno-associated virus; X-Gal: 5-bromo-4-chloro-3-indolyl- $\beta$ -D-galactopyranoside;  $\mu$ m: micrometer (created with BioRender, Affinity Photo, and Prism).

## 7.2. Ability of alginate-based hydrogels to deliver therapeutic rAAV vectors in human osteoarthritic articular chondrocytes and in human mesenchymal stromal cells

This evaluation aimed at testing the second hypothesis:

***"Alginate-based hydrogels are capable of efficiently and durably incorporating and delivering therapeutic (sox9, TGF- $\beta$ ) rAAV vectors to both reparative human osteoarthritic articular chondrocytes and human mesenchymal stromal cells in order to stimulate their reparative activities for the purpose of improved articular cartilage regeneration".***

### 7.2.1. Transgene expression

#### 7.2.1.1. Transgene expression in human osteoarthritic articular chondrocytes

Human osteoarthritic articular chondrocytes were first employed to examine the ability of the optimally prepared rAAV/alginate hydrogel systems (§ 7.1.1.) to deliver the various therapeutic (sox9, TGF- $\beta$ ) candidate genes in order to test their lack of endogenous  $\beta$ -gal-like activities (**Figures 9A-9C**) and their potential to overexpress their respective gene products (SOX9, TGF- $\beta$ ) over time (21 days) (**Figures 9D-9N**). Expression of *lacZ* was monitored by X-Gal staining (**Figure 9A**) with a histomorphometrically analysis of the corresponding AOD (**Figure 9B**) and scores using a modified Bern grading system (**Figure 9C**) over an extended period of 21 days. Expression of sox9 and TGF- $\beta$  was monitored by immunocytochemical detection (**Figures 9D and 9H**, respectively) with a histomorphometrically analysis of the corresponding AOD (**Figures 9E and 9I**, respectively) and scores using a modified Bern grading system (**Figures 9F and 9J**, respectively), with a real-time RT-PCR analysis (**Figures 9G and 9K**, respectively), and an ELISA (**Figures 9L-9N**) over an extended period of 21 days.

First, the lack of endogenous  $\beta$ -gal-like activities mediated by the rAAV-FLAG-hsox9/alginate and rAAV-hTGF- $\beta$ /alginate hydrogel systems in human osteoarthritic articular chondrocytes over time was confirmed by the absence of X-Gal staining using these systems in contrast to the rAAV-*lacZ*/alginate hydrogel system (2- and 2.3-fold difference in the AOD *versus* the rAAV-FLAG-hsox9/alginate and rAAV-hTGF- $\beta$ /alginate hydrogel systems, respectively,  $P \leq 0.0001$ ; always 4-fold difference in the scores *versus* the rAAV-FLAG-hsox9/alginate and rAAV-hTGF- $\beta$ /alginate hydrogel systems, respectively,  $P \leq 0.0001$ ) (**Figures 9A-9C**). Second, the

effective expression of *sox9* mediated by the rAAV-FLAG-h*sox9*/alginate hydrogel system in human osteoarthritic articular chondrocytes over time was confirmed by the significant levels of SOX9 immunodetection using this system in contrast to the rAAV-*lacZ*/alginate and rAAV-hTGF- $\beta$ /alginate hydrogel systems (1.2- and 1.1-fold difference in the AOD *versus* the rAAV-*lacZ*/alginate and rAAV-hTGF- $\beta$ /alginate hydrogel systems, respectively,  $P \leq 0.004$ ; 4- and 2.7-fold difference in the scores *versus* the rAAV-*lacZ*/alginate and rAAV-hTGF- $\beta$ /alginate hydrogel systems, respectively,  $P \leq 0.0002$ ) (**Figures 9D-9F**). This observation was confirmed by the results of a real-time RT-PCR analysis (1.3- and 1.5-fold difference, respectively,  $P \leq 0.0002$ ) (**Figure 9G**). Third, the effective expression of TGF- $\beta$  mediated by the rAAV-hTGF- $\beta$ /alginate hydrogel system in human osteoarthritic articular chondrocytes over time was confirmed by the significant levels of TGF- $\beta$  immunodetection using this system in contrast to the rAAV-*lacZ*/alginate and rAAV-FLAG-h*sox9*/alginate hydrogel systems (always 1.4-fold difference in the AOD *versus* the rAAV-*lacZ*/alginate and rAAV-FLAG-h*sox9*/alginate hydrogel systems, respectively,  $P \leq 0.0001$ ; always 4-fold difference in the scores *versus* the rAAV-*lacZ*/alginate and rAAV-FLAG-h*sox9*/alginate hydrogel systems, respectively,  $P \leq 0.0022$ ) (**Figures 9H-9J**). This observation was confirmed by the results of a real-time RT-PCR analysis (2.6- and 2.3-fold difference, respectively,  $P \leq 0.031$ ) (**Figure 9K**) and by those of an ELISA (2-fold difference *versus* the rAAV-*lacZ*/alginate hydrogel system on day 21,  $P = 0.0032$ ) (**Figures 9L-9N**).

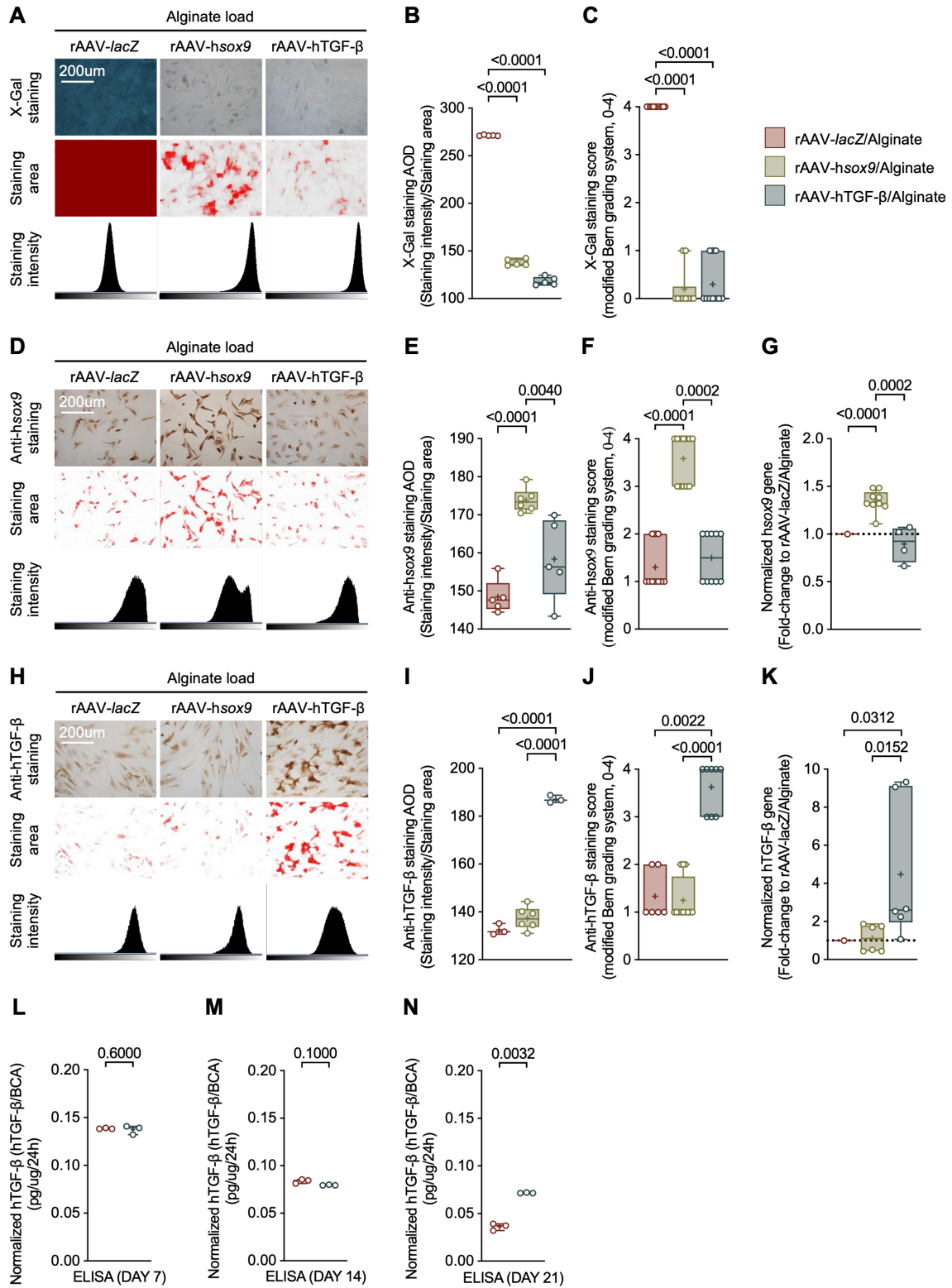


**Figure 9.** Targeted transgene overexpression from the rAAV/alginate hydrogel systems in human osteoarthritic articular chondrocytes. **(A)** X-Gal staining (magnification x 20; scale bars: 200  $\mu\text{m}$ ; all representative data) with **(B)** an estimation of the corresponding AOD ( $P$  values indicated) and **(C)** an estimation of the corresponding scores using a modified Bern grading system ( $P$  values indicated) after 21 days. **(D)** SOX9 immunodetection (magnification x 20; scale bars: 200  $\mu\text{m}$ ; all representative data) with **(E)** an estimation of the corresponding AOD ( $P$  values indicated), **(F)** an estimation of the corresponding scores using a modified Bern grading system ( $P$  values indicated), and **(G)** a real-time RT-PCR analysis ( $P$  values indicated) after 21 days. **(H)** TGF- $\beta$  immunodetection (magnification x 20; scale bars: 200  $\mu\text{m}$ ; all representative data) with **(I)** an estimation of the corresponding AOD ( $P$  values indicated), **(J)** an estimation of the corresponding scores using a modified Bern grading system ( $P$  values indicated), and **(K)** a real-time RT-PCR analysis ( $P$  values indicated) after 21 days, and **(L-N)** an estimation of the levels of TGF- $\beta$  production by ELISA on day 7 (**L**), day 14 (**M**), and day 21 (**N**). Abbreviations: AOD: average optical density; hsox9: human sex-determining region Y-type high mobility group box 9; hTGF- $\beta$ : human transforming growth factor beta; lacZ:  $\beta$ -galactosidase; rAAV: recombinant adeno-associated virus; sox9/SOX9: sex-determining region Y-type high mobility group box 9 (gene/protein); TGF- $\beta$ : transforming growth factor beta; X-Gal: 5-bromo-4-chloro-3-indolyl- $\beta$ -D-galactopyranoside;  $\mu\text{m}$ : micrometer (created with Affinity Photo and Prism).

### 7.2.1.2. Transgene expression in human mesenchymal stromal cells

Human mesenchymal stromal cells were first employed to examine the ability of the optimally prepared rAAV/alginate hydrogel systems (§ 7.1.1.) to deliver the various therapeutic (*sox9*, TGF- $\beta$ ) candidate genes in order to test their lack of endogenous  $\beta$ -gal-like activities (**Figures 10A-10C**) and their potential to overexpress their respective gene products (SOX9, TGF- $\beta$ ) over time (21 days) (**Figures 10D-10N**). Expression of *lacZ* was monitored by X-Gal staining (**Figure 10A**) with a histomorphometrically analysis of the corresponding AOD (**Figure 10B**) and scores using a modified Bern grading system (**Figure 10C**) over an extended period of 21 days. Expression of *sox9* and TGF- $\beta$  was monitored by immunocytochemical detection (**Figures 10D and 10H**, respectively) with a histomorphometrically analysis of the corresponding AOD (**Figures 10E and 10I**, respectively) and scores using a modified Bern grading system (**Figures 10F and 10J**), with a real-time RT-PCR analysis (**Figures 10G and 10K**, respectively), and an ELISA (**Figures 10L-10N**) over an extended period of 21 days.

First, the lack of endogenous  $\beta$ -gal-like activities mediated by the rAAV-FLAG-hsox9/alginate and rAAV-hTGF- $\beta$ /alginate hydrogel systems in human mesenchymal stromal cells over time was confirmed by the absence of X-Gal staining using these systems in contrast to the rAAV-lacZ/alginate hydrogel system (always 1.2-fold difference in the AOD *versus* the rAAV-FLAG-hsox9/alginate and rAAV-hTGF- $\beta$ /alginate hydrogel systems, respectively,  $P \leq 0.040$ ; always 8-fold difference in the scores *versus* the rAAV-FLAG-hsox9/alginate and rAAV-hTGF- $\beta$ /alginate hydrogel systems, respectively,  $P \leq 0.002$ ) (**Figures 10A-10C**). Second, the effective expression of *sox9* mediated by the rAAV-FLAG-hsox9/alginate hydrogel system in human mesenchymal stromal cells over time was confirmed by the significant levels of SOX9 immunodetection using this system in contrast to the rAAV-lacZ/alginate and rAAV-hTGF- $\beta$ /alginate hydrogel systems

(always 2.3-fold difference in the AOD *versus* the rAAV-*lacZ*/alginate and rAAV-hTGF- $\beta$ /alginate hydrogel systems, respectively,  $P \leq 0.0001$ ; always 1.5-fold difference in the scores *versus* the rAAV-*lacZ*/alginate and rAAV-hTGF- $\beta$ /alginate hydrogel systems, respectively,  $P \leq 0.0007$ ) (**Figures 10D-10F**). This observation was confirmed by the results of a real-time RT-PCR analysis (1.3- and 1.6-fold difference, respectively,  $P \leq 0.0497$ ) (**Figure 10G**). Third, the effective expression of TGF- $\beta$  mediated by the rAAV-hTGF- $\beta$ /alginate hydrogel system in human mesenchymal stromal cells over time was confirmed by the significant levels of TGF- $\beta$  immunodetection using this system in contrast to the rAAV-*lacZ*/alginate and rAAV-FLAG-hsox9/alginate hydrogel systems (1.7- and 2.1-fold difference in the AOD *versus* the rAAV-*lacZ*/alginate and rAAV-FLAG-hsox9/alginate hydrogel systems, respectively,  $P \leq 0.0001$ ; always 3-fold difference in the scores *versus* the rAAV-*lacZ*/alginate and rAAV-FLAG-hsox9/alginate hydrogel systems, respectively,  $P \leq 0.0004$ ) (**Figures 10H-10J**). This observation was confirmed by the results of a real-time RT-PCR analysis (always 1.3-fold difference, respectively,  $P \leq 0.0067$ ) (**Figure 10K**) and by those of an ELISA (2.2-, 1.9-, and 2.2-fold difference *versus* the rAAV-*lacZ*/alginate hydrogel system on days 7, 14, and 21, respectively,  $P \leq 0.0238$ ) (**Figures 10L-10N**).

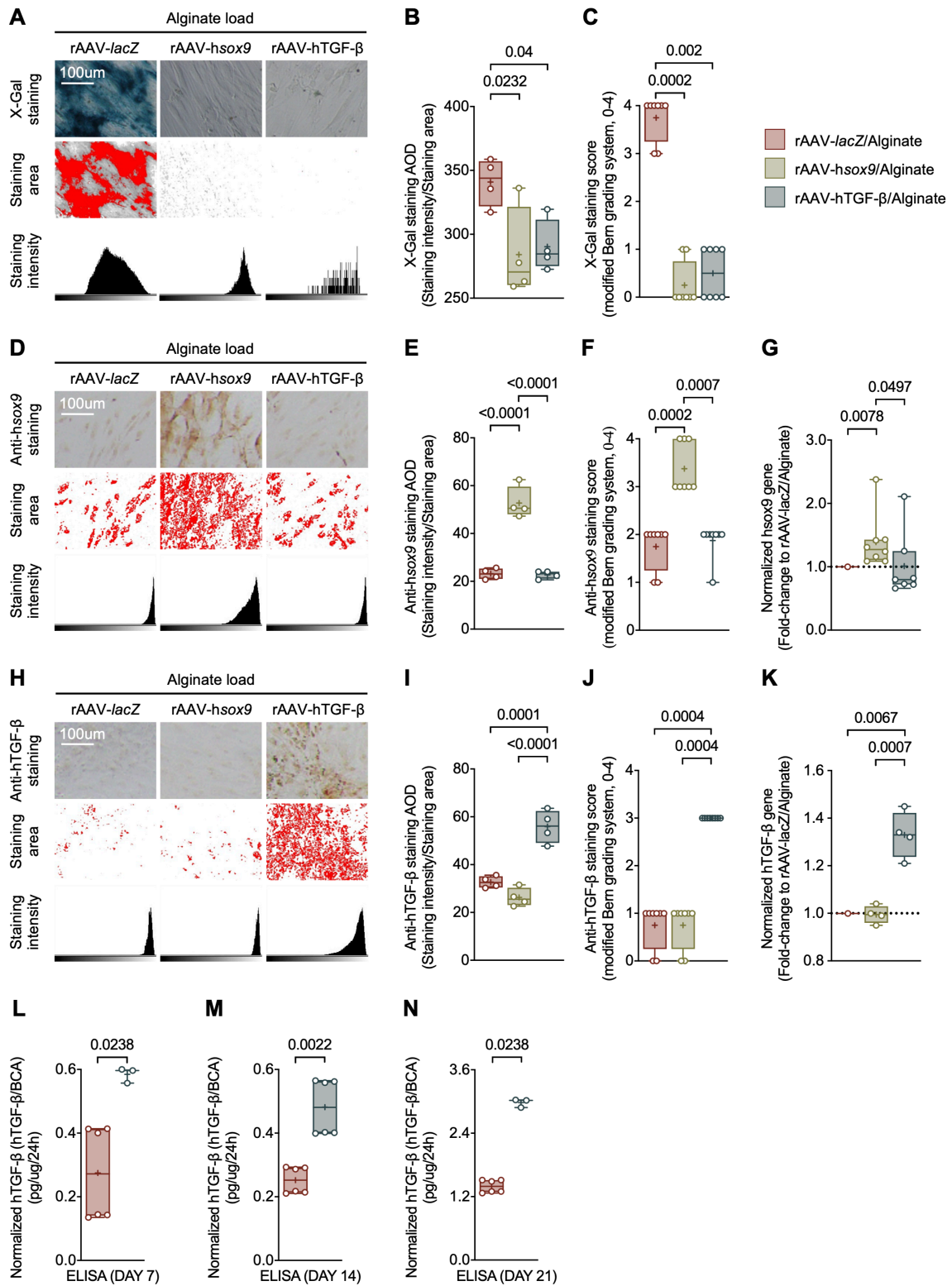


**Figure 10.** Targeted transgene overexpression from the rAAV/alginate hydrogel systems in human mesenchymal stromal cells. **(A)** X-Gal staining (magnification x 10; scale bars: 200  $\mu\text{m}$ ; all representative data) with **(B)** an estimation of the corresponding AOD ( $P$  values indicated) and **(C)** an estimation of the corresponding scores using a modified Bern grading system ( $P$  values indicated) after 21 days. **(D)** SOX9 immunodetection (magnification x 10; scale bars: 200  $\mu\text{m}$ ; all representative data) with **(E)** an estimation of the corresponding AOD ( $P$  values indicated), **(F)** an estimation of the corresponding scores using a modified Bern grading system ( $P$  values indicated), and **(G)** a real-time RT-PCR analysis ( $P$  values indicated) after 21 days. **(H)** TGF- $\beta$  immunodetection (magnification x 10; scale bars: 200  $\mu\text{m}$ ; all representative data) with **(I)** an estimation of the corresponding AOD ( $P$  values indicated), **(J)** an estimation of the corresponding scores using a modified Bern grading system ( $P$  values indicated), and **(K)** a real-time RT-PCR analysis ( $P$  values indicated) after 21 days, and **(L-N)** an estimation of the levels of TGF-  $\beta$  production by ELISA on day 7 (**L**), day 14 (**M**), and day 21 (**N**). Abbreviations: AOD: average optical density; BCA: bichononic acid; ELISA: enzyme-linked immunosorbent assay; h: hour; hsox9: human sex-determining region Y-type high mobility group box 9; hTGF- $\beta$ : human transforming growth factor beta; lacZ:  $\beta$ -galactosidase; pg: picogram; rAAV: recombinant adeno-associated virus; X-Gal: 5-bromo-4-chloro-3-indolyl- $\beta$ -D-galactopyranoside;  $\mu\text{g}$ : microgram;  $\mu\text{m}$ : micrometer (created with Affinity Photo and Prism).

## 7.2.2. Effects on the biological and chondroreparative activities

### 7.2.2.1. Effects on human osteoarthritic articular chondrocytes

Human osteoarthritic articular chondrocytes were then employed to examine the potential benefits of applying the optimally prepared candidate rAAV (*sox9*, TGF- $\beta$ )/alginate hydrogel systems (§ 7.1.1.) in order to test their ability to enhance the biological and chondroreparative activities of these cells over time (21 days) (**Figure 11**). The cell densities were monitored by H&E staining (**Figure 11A**) with a histomorphometrically analysis (**Figure 11B**) and the DNA contents were monitored using the Hoechst 33258 assay (**Figure 11C**) on day 21. The deposition of cartilage-specific glycosaminoglycans was monitored by toluidine blue staining (**Figure 11D**) with a histomorphometrically analysis of the corresponding AOD (**Figure 11E**) and scores using a modified Bern grading system (**Figure 11F**), with a real-time RT-PCR analysis (ACAN) (**Figure 11G**) on day 21. The deposition of cartilage-specific proteoglycans was monitored by safranin O staining (**Figure 11H**) with a histomorphometrically analysis of the corresponding AOD (**Figure 11I**) and scores using a modified Bern grading system (**Figure 11J**) and the PG contents were monitored by binding to the DMMB dye (**Figure 11K**) on day 21. The deposition of cartilage-specific type-II collagen was monitored by an immunocytochemical analysis (**Figure 11L**) with a histomorphometrically analysis of the corresponding AOD (**Figure 11M**) and scores using a modified Bern grading system (**Figure 11N**), with a real-time RT-PCR analysis (COL2A1) (**Figure 11O**) on day 21.

First, the cell densities (**Figures 11A and 11B**) and the DNA contents (**Figure 11C**) significantly increased in human osteoarthritic articular chondrocytes over time using the rAAV-FLAG-hsox9/alginate and rAAV-hTGF- $\beta$ /alginate hydrogel systems relative to the rAAV-

*lacZ*/alginate hydrogel system (cell densities: 1.3- and 1.8-fold difference by H&E staining, respectively,  $P \leq 0.0109$ ; DNA contents: 1.2- and 1.7-fold difference using the Hoechst 33258 assay, respectively,  $P \leq 0.0312$ ). Second, the deposition of glycosaminoglycans (**Figures 11D-11F**) and the expression of ACAN (**Figure 11G**) significantly increased in human osteoarthritic articular chondrocytes over time using the rAAV-FLAG-hsox9/alginate and rAAV-hTGF- $\beta$ /alginate hydrogel systems relative to the rAAV-*lacZ*/alginate hydrogel system (deposition of glycosaminoglycans: 1.2- and 1.1-fold difference and 3.5- and 2-fold difference in the AOD and scores of toluidine blue staining, respectively,  $P \leq 0.0059$  and  $P \leq 0.0013$ ; ACAN expression: 4.9- and 4.8-fold difference by real-time RT-PCR, respectively,  $P \leq 0.0009$ ). Third, the deposition of proteoglycans (**Figures 11H-11J**) and the PG contents (**Figure 11K**) significantly increased in human osteoarthritic articular chondrocytes over time using the rAAV-FLAG-hsox9/alginate and rAAV-hTGF- $\beta$ /alginate hydrogel systems relative to the rAAV-*lacZ*/alginate hydrogel system (deposition of proteoglycans: 1.2- and 1.1-fold difference and 3- and 2-fold difference in the AOD and scores of safranin O staining, respectively,  $P \leq 0.0001$  and  $P \leq 0.0014$ ; PG contents: always 1.1-fold difference using the DMMB dye,  $P \leq 0.0033$ ). Fourth, the deposition of type-II collagen (**Figures 11L-11N**) and the expression of COL2A1 (**Figure 11O**) significantly increased in human osteoarthritic articular chondrocytes over time using the rAAV-FLAG-hsox9/alginate and rAAV-hTGF- $\beta$ /alginate hydrogel systems relative to the rAAV-*lacZ*/alginate hydrogel system (deposition of type-II collagen: 1.2- and 1.3-fold difference and always 3-fold difference in the AOD and scores of type-II collagen immunostaining, respectively,  $P \leq 0.0001$  and  $P \leq 0.0003$ ; COL2A1 expression: 3.2- and 2.8-fold difference by real-time RT-PCR, respectively,  $P \leq 0.0005$ ).

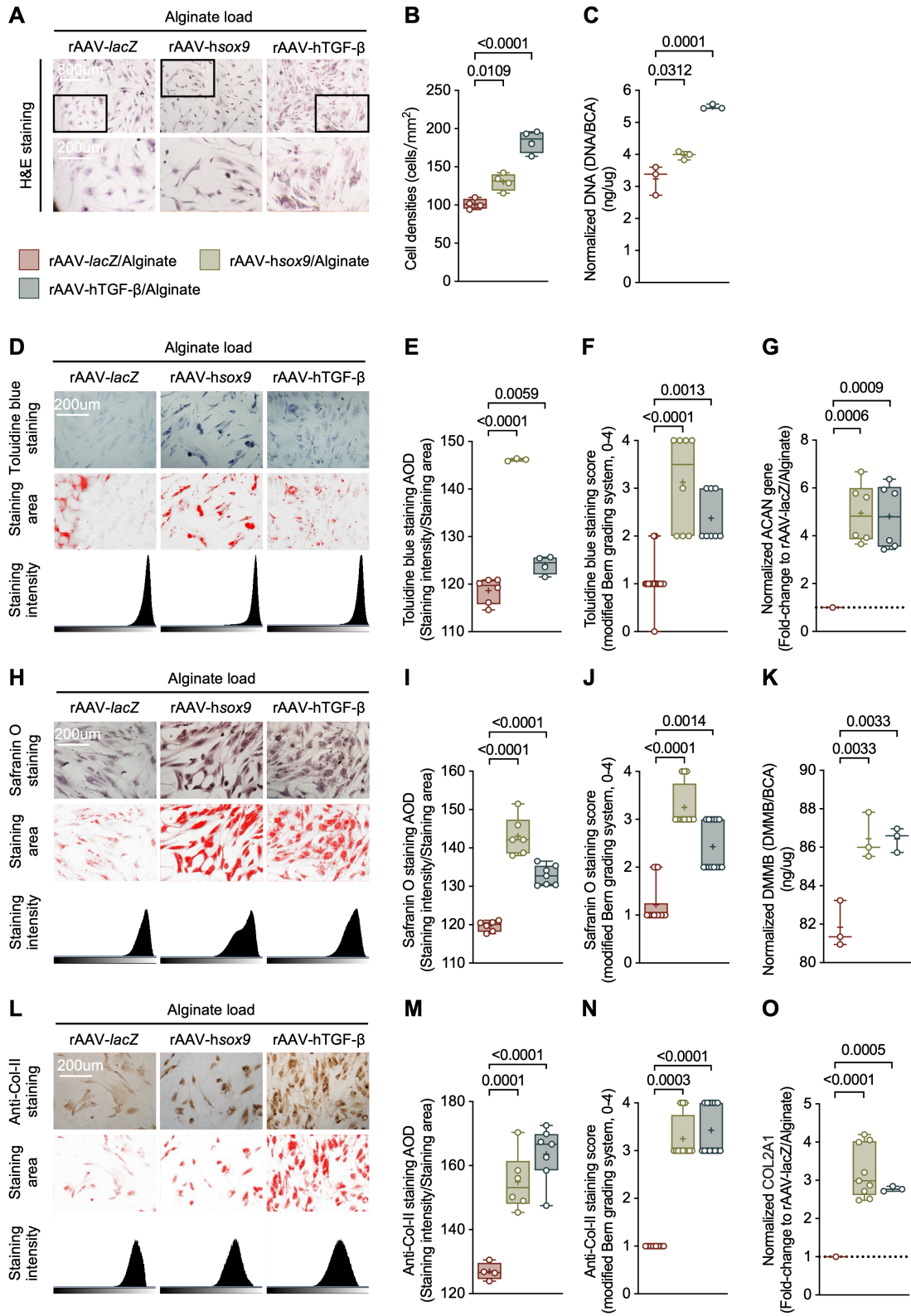


**Figure 11.** Effects of the rAAV/alginate hydrogel systems on the biological and chondrogenic activities in human osteoarthritic articular chondrocytes. **(A-C)** Evaluation of the cell proliferation indices by **(A)** H&E staining (magnification x 10; scale bars: 100 µm; all representative data) with **(B)** an estimation of the corresponding cell densities (*P* values indicated) and by **(C)** an estimation of the DNA contents using the Hoechst 33258 assay (*P* values indicated) after 21 days. **(D-G)** Evaluation of the deposition of glycosaminoglycans by **(D)** toluidine blue staining (magnification x 20; scale bars: 200 µm; all representative data) with **(E)** an estimation of the corresponding AOD (*P* values indicated), **(F)** an estimation of the corresponding scores using a modified Bern grading system (*P* values indicated), and **(G)** a real-time RT-PCR analysis for ACAN (*P* values indicated) after 21 days. **(H-K)** Evaluation of the deposition of proteoglycans by **(H)** safranin O staining (magnification x 20; scale bars: 200 µm; all representative data) with **(I)** an estimation of the corresponding AOD (*P* values indicated) and **(J)** an estimation of the corresponding scores using a modified Bern grading system (*P* values indicated) and by **(K)** an estimation of the PG contents by binding to the DMMB dye (*P* values indicated) after 21 days. **(L-O)** Evaluation of the deposition of type-II collagen by **(L)** immunodetection (magnification x 20; scale bars: 200 µm; all representative data) with **(M)** an estimation of the corresponding AOD (*P* values indicated), **(N)** an estimation of the corresponding scores using a modified Bern grading system (*P* values indicated), and **(O)** a real-time RT-PCR analysis for COL2A1 (*P* values indicated) after 21 days. Abbreviations: ACAN: aggrecan; AOD: average optical density; BCA: bicinchoninic acid; Col-II: type-II collagen; COL2A1: type-II collagen (gene); DMMB: dimethylmethylene blue; DNA: deoxyribonucleic acid; H&E: hematoxylin and eosin; hsox9: human sex-determining region Y-type high mobility group box 9; hTGF-β: human transforming growth factor beta; lacZ: β-galactosidase; mm: millimeter; ng: nanogram; rAAV: recombinant adeno-associated virus; µg: microgram; µm: micrometer (created with Affinity Photo and Prism).

#### 7.2.2.2. Effects on human mesenchymal stromal cells

Human mesenchymal stromal cells were then employed to examine the potential benefits of applying the optimally prepared candidate rAAV (*sox9*, TGF-β)/alginate hydrogel systems (§ 7.1.1.) in order to test their ability to enhance the biological and chondroreparative activities of these cells over time (21 days) (**Figure 12**). The cell densities were monitored by H&E staining (**Figure 12A**) with a histomorphometrically analysis (**Figure 12B**), the DNA contents were monitored using the Hoechst 33258 assay (**Figure 12C**), and the indices of cell proliferation were monitored using the WST-1 assay (**Figure 12D**) on day 21. The deposition of cartilage-specific glycosaminoglycans was monitored by alcian blue staining (**Figure 12E**) with a histomorphometrically analysis of the corresponding AOD (**Figure 12F**), of the corresponding scores using a modified Bern grading system (**Figure 12G**), and of the corresponding indices of alcian blue staining, with a real-time RT-PCR analysis (ACAN) (**Figure 12H**) on day 21. The deposition of cartilage-specific proteoglycans was monitored by safranin O staining (**Figure 12I**) with a histomorphometrically analysis of the corresponding AOD (**Figure 12J**) and scores using a modified Bern grading system (**Figure 12K**) and the PG contents were monitored by binding to the DMMB dye (**Figure 12L**) on day 21. The deposition of cartilage-specific type-II collagen was monitored by an immunocytochemical analysis (**Figure 12M**) with a histomorphometrically analysis of the corresponding AOD (**Figure 12N**) and scores using a modified Bern grading system (**Figure 12O**), with a real-time RT-PCR analysis (COL2A1) (**Figure 12P**) on day 21.

First, the cell densities (**Figures 12A and 12B**), the DNA contents (**Figure 12C**), and the

indices of cell proliferation (**Figure 12D**) significantly increased in human mesenchymal stromal cells over time using the rAAV-FLAG-hsox9/alginate and rAAV-hTGF- $\beta$ /alginate hydrogel systems relative to the rAAV-lacZ/alginate hydrogel system (cell densities: always 1.4-fold difference by H&E staining,  $P \leq 0.0001$ ; DNA contents: 1.4- and 1.6-fold difference using the Hoechst 33258 assay, respectively,  $P \leq 0.0149$ ; indices of cell proliferation: 2- and 2.9-fold difference using the WST-1 assay, respectively,  $P = 0.0184$  with the rAAV-hTGF- $\beta$ /alginate hydrogel system). Second, the deposition of glycosaminoglycans (**Figures 12E-12G**) and the expression of ACAN (**Figure 12H**) significantly increased in human mesenchymal stromal cells over time using the rAAV-FLAG-hsox9/alginate and rAAV-hTGF- $\beta$ /alginate hydrogel systems relative to the rAAV-lacZ/alginate hydrogel system (deposition of glycosaminoglycans: 1.2- and 1.4-fold difference, always 3-fold difference, and 1.3- and 1.8-fold difference in the AOD, scores, and indices of alcian blue staining, respectively,  $P \leq 0.0123$ , although statistical significance was not reached with the rAAV-FLAG-hsox9/alginate hydrogel system for the indices of alcian blue staining; ACAN expression: 1.5- and 2.6-fold difference by real-time RT-PCR, respectively,  $P \leq 0.0053$ ). Third, the deposition of proteoglycans (**Figures 12I-12K**) and the PG contents (**Figure 12L**) significantly increased in human mesenchymal stromal cells over time using the rAAV-FLAG-hsox9/alginate and rAAV-hTGF- $\beta$ /alginate hydrogel systems relative to the rAAV-lacZ/alginate hydrogel system (deposition of proteoglycans: 1.4- and 1.3-fold difference and always 2-fold difference in the AOD and scores of safranin O staining, respectively,  $P \leq 0.028$ ; PG contents: 1.3- and 1.8-fold difference using the DMMB dye, respectively,  $P \leq 0.0217$ ). Fourth, the deposition of type-II collagen (**Figures 12M-12O**) and the expression of COL2A1 (**Figure 12P**) generally significantly increased in human mesenchymal stromal cells over time using the rAAV-FLAG-hsox9/alginate and rAAV-hTGF- $\beta$ /alginate hydrogel systems relative to the rAAV-lacZ/alginate hydrogel system (deposition of type-II collagen: 1.9- and 1.6-fold difference and always 2-fold difference in the AOD and scores of type-II collagen immunostaining, respectively,  $P \leq 0.003$ ; COL2A1 expression: 1.3- and 1.2-fold difference by real-time RT-PCR, respectively,  $P \geq 0.1671$ ).

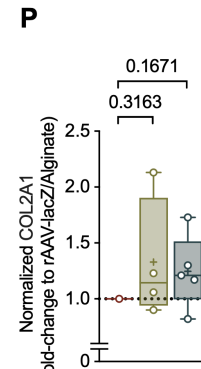
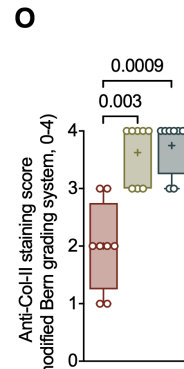
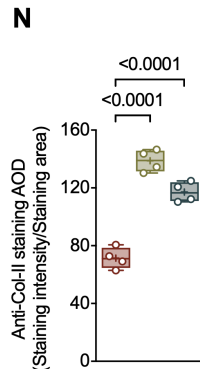
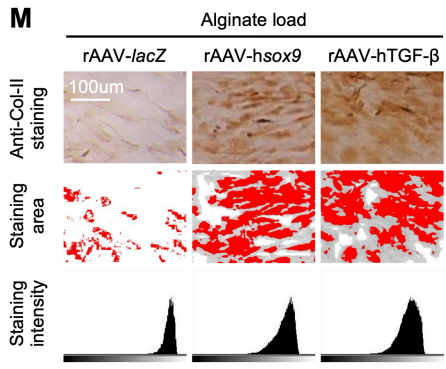
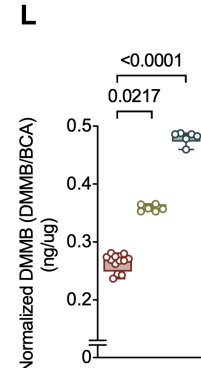
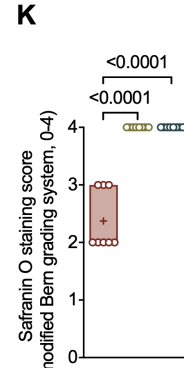
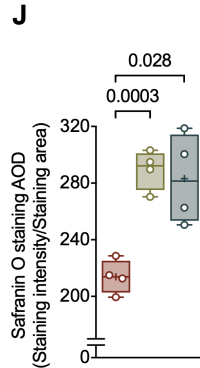
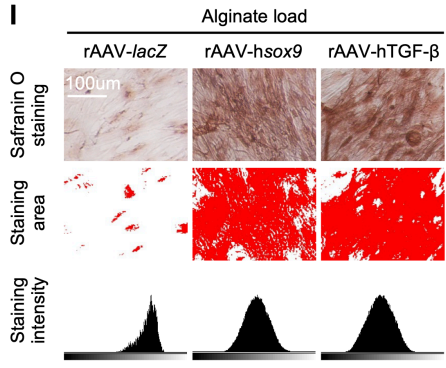
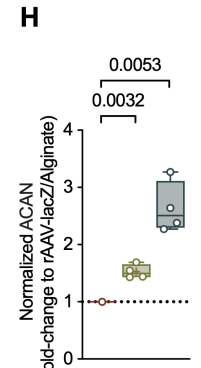
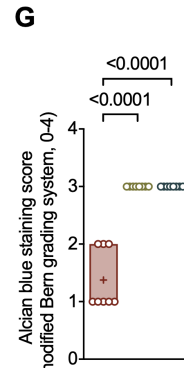
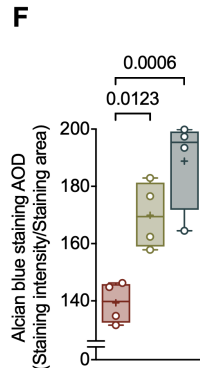
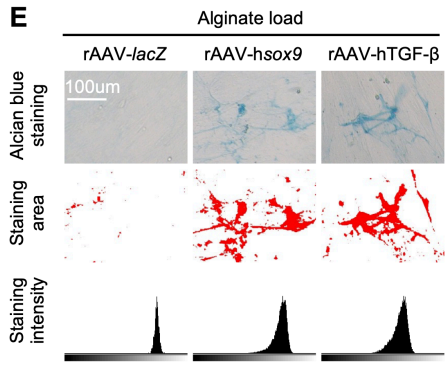
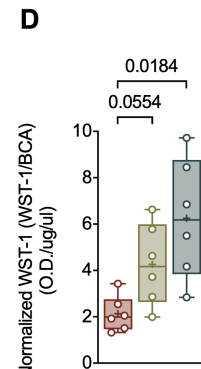
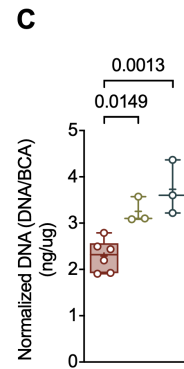
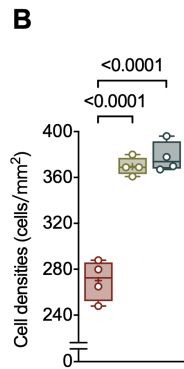
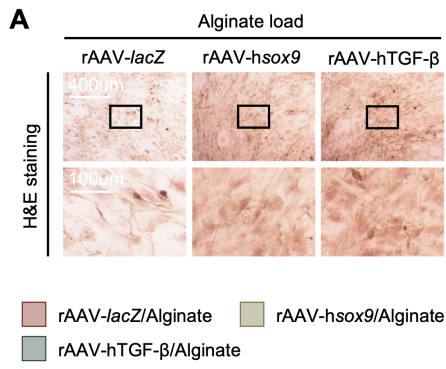


**Figure 12.** Effects of the rAAV/alginate hydrogel systems on the biological and chondrogenic activities in human mesenchymal stromal cells. **(A-D)** Evaluation of the cell proliferation indices by **(A)** H&E staining (magnification x 10; scale bars: 100  $\mu$ m; all representative data) with **(B)** an estimation of the corresponding cell densities (*P* values indicated), **(C)** an estimation of the DNA contents using the Hoechst 33258 assay (*P* values indicated), and **(D)** an estimation of the indices of cell proliferation using the WST-1 assay (*P* values indicated) after 21 days. **(E-H)** Evaluation of the deposition of glycosaminoglycans by **(E)** alcian blue staining (magnification x 10; scale bars: 100  $\mu$ m; all representative data) with **(F)** an estimation of the corresponding AOD (*P* values indicated), **(G)** an estimation of the corresponding scores using a modified Bern grading system (*P* values indicated), and **(H)** an estimation of the corresponding indices of alcian blue staining (*P* values indicated) after 21 days. **(I-L)** Evaluation of the deposition of proteoglycans by **(I)** safranin O staining (magnification x 10; scale bars: 100  $\mu$ m; all representative data) with **(J)** an estimation of the corresponding AOD (*P* values indicated) and **(K)** an estimation of the corresponding scores using a modified Bern grading system (*P* values indicated) and by **(L)** an estimation of the PG contents by binding to the DMMB dye (*P* values indicated) after 21 days. **(M-P)** Evaluation of the deposition of type-II collagen by **(M)** immunodetection (magnification x 10; scale bars: 100  $\mu$ m; all representative data) with **(N)** an estimation of the corresponding AOD (*P* values indicated), **(O)** an estimation of the corresponding scores using a modified Bern grading system (*P* values indicated), and **(P)** a real-time RT-PCR analysis for COL2A1 (*P* values indicated) after 21 days. Abbreviations: AOD: average optical density; BCA: bicinchoninic acid; Col-II: type-II collagen; COL2A1: type-II collagen (gene); DMMB: dimethylmethylene blue; DNA: deoxyribonucleic acid; H&E: hematoxylin and eosin; hsox9: human sex-determining region Y-type high mobility group box 9; hTGF- $\beta$ : human transforming growth factor beta; *lacZ*:  $\beta$ -galactosidase; mm: millimeter; ng: nanogram; OD: optical density; rAAV: recombinant adeno-associated virus; WST-1: water-soluble tetrazolium salt-1;  $\mu$ g: microgram;  $\mu$ l: microliter;  $\mu$ m: micrometer (created with Affinity Photo and Prism).

### 7.2.3. Effects on the osteogenic, hypertrophic, and mineralization activities

#### 7.2.3.1. Effects on human osteoarthritic articular chondrocytes

Human osteoarthritic articular chondrocytes were finally employed to examine the potential benefits of applying the optimally prepared candidate rAAV (*sox9*, TGF- $\beta$ )/alginate hydrogel systems (§ 7.1.1.) in order to test their ability to impact the osteogenic, hypertrophic, and mineralization activities of these cells over time (21 days) (**Figure 13**). The deposition of osteogenic type-I collagen was monitored by immunocytochemical detection (**Figure 13A**) with a histomorphometrically analysis of the corresponding AOD (**Figure 13B**) and scores using a modified Bern grading system (**Figure 13C**), with a real-time RT-PCR analysis (COL1A1) (**Figure 13D**) on day 21. The deposition of hypertrophic type-X collagen was monitored by immunocytochemical detection (**Figure 13E**) with a histomorphometrically analysis of the corresponding AOD (**Figure 13F**) and scores using a modified Bern grading system (**Figure 13G**), with a real-time RT-PCR analysis (COL10A1) (**Figure 13H**) on day 21. Mineralization was monitored by alizarin red staining (**Figure 13I**) with a histomorphometrically analysis of the corresponding AOD (**Figure 13J**) and scores using a modified Bern grading system (**Figure 13K**) on day 21.

First, the deposition of type-I collagen (**Figures 13A-13D**) significantly decreased in human osteoarthritic articular chondrocytes over time using the rAAV-FLAG-hsox9/alginate and

rAAV-hTGF- $\beta$ /alginate hydrogel systems relative to the rAAV-*lacZ*/alginate hydrogel system (deposition of type-I collagen: always 1.1-fold difference in the AOD and always 2-fold difference in the scores of type-I collagen immunostaining, respectively,  $P \leq 0.0006$  and  $P \leq 0.0001$ ; COL1A1 expression: 1.4- and 1.6-fold difference by real-time RT-PCR, respectively,  $P \leq 0.0001$ ). Second, the deposition of type-X collagen (**Figures 13E-13H**) generally significantly decreased in human osteoarthritic articular chondrocytes over time using the rAAV-FLAG-hsox9/alginate and rAAV-hTGF- $\beta$ /alginate hydrogel systems relative to the rAAV-*lacZ*/alginate hydrogel system (deposition of type-X collagen: no significant difference reached in the AOD and always 1.3-fold difference in the scores of type-X collagen immunostaining, respectively,  $P \leq 0.0221$  for the scores; COL10A1 expression: no significant difference reached by real-time RT-PCR). Third, mineralization (**Figures 13I-13K**) significantly increased in human osteoarthritic articular chondrocytes over time using the rAAV-FLAG-hsox9/alginate and rAAV-hTGF- $\beta$ /alginate hydrogel systems relative to the rAAV-*lacZ*/alginate hydrogel system (always 1.1-fold difference in the AOD and always 2-fold difference in the scores of alizarin red staining, respectively,  $P \leq 0.0079$  and  $P \leq 0.0005$ ).

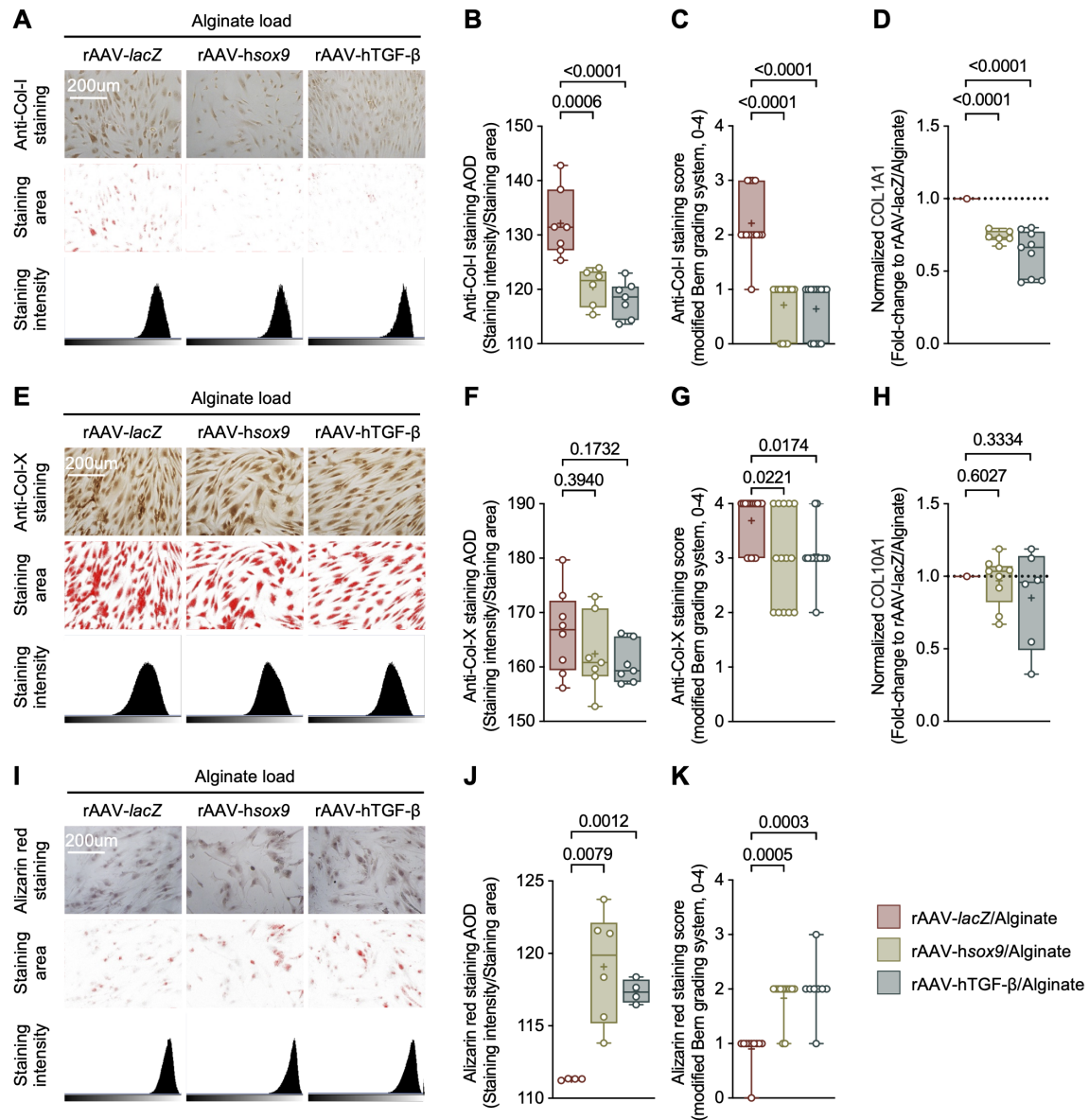


**Figure 13.** Effects of the rAAV/alginate hydrogel systems on the osteogenic, hypertrophic, and mineralization activities in human osteoarthritic articular chondrocytes. **(A-D)** Evaluation of the deposition of type-I collagen by **(A)** immunodetection (magnification x 20; scale bars: 200 µm; all representative data) with **(B)** an estimation of the corresponding AOD (*P* values indicated), **(C)** an estimation of the corresponding scores using a modified Bern grading system (*P* values indicated), and **(D)** a real-time RT-PCR analysis for COL1A1 (*P* values indicated) after 21 days. **(E-H)** Evaluation of the deposition type-X collagen by **(E)** immunodetection (magnification x 20; scale bars: 200 µm; all representative data) with **(F)** an estimation of the corresponding AOD (*P* values indicated), **(G)** an estimation of the corresponding scores using a modified Bern grading system (*P* values indicated), and **(H)** a real-time RT-PCR analysis for COL10A1 (*P* values indicated) after 21 days. **(I-K)** Evaluation of mineralization by **(I)** alizarin red staining (magnification x 20; scale bars: 200 µm; all representative data) with **(J)** an estimation of the corresponding AOD (*P* values indicated) and **(K)** an estimation of the corresponding scores using a modified Bern grading system (*P* values indicated) after 21 days. Abbreviations: AOD: average optical density; Col-I: type-I collagen; Col-X: type-X collagen; COL1A1: type-I collagen (gene); COL10A1: type-X collagen (gene); hsox9: human sex-determining region Y-type high mobility group box 9; hTGF-β: human transforming growth factor beta; lacZ: β-galactosidase; rAAV: recombinant adeno-associated virus; µm: micrometer (created with Affinity Photo and Prism).

### 7.2.3.2. Effects on human mesenchymal stromal cells

Human mesenchymal stromal cells were finally employed to examine the potential benefits of applying the optimally prepared candidate rAAV (*sox9*, TGF- $\beta$ )/alginate hydrogel systems (§ 7.1.1.) in order to test their ability to impact the osteogenic, hypertrophic, and mineralization activities of these cells over time (21 days) (**Figure 14**). The deposition of osteogenic type-I collagen was monitored by immunocytochemical detection (**Figure 14A**) with a histomorphometrically analysis of the corresponding AOD (**Figure 14B**) and scores using a modified Bern grading system (**Figure 14C**), with a real-time RT-PCR analysis (COL1A1) (**Figure 14D**) on day 21. The deposition of hypertrophic type-X collagen was monitored by immunocytochemical detection (**Figure 14E**) with a histomorphometrically analysis of the corresponding AOD (**Figure 14F**) and scores using a modified Bern grading system (**Figure 14G**), with a real-time RT-PCR analysis (COL10A1) (**Figure 14H**) on day 21. Mineralization was monitored by alizarin red staining (**Figure 14I**) with a histomorphometrically analysis of the corresponding AOD (**Figure 14J**) and scores using a modified Bern grading system (**Figure 14K**) on day 21.

First, the deposition of type-I collagen (**Figures 14A-14D**) significantly decreased in human mesenchymal stromal cells over time using the rAAV-FLAG-*hsox9*/alginate and rAAV-hTGF- $\beta$ /alginate hydrogel systems relative to the rAAV-*lacZ*/alginate hydrogel system (deposition of type-I collagen: 1.5- and 1.4-fold difference in the AOD and always 2-fold difference in the scores of type-I collagen immunostaining, respectively,  $P \leq 0.0042$ ; COL1A1 expression: 1.8- and 1.3-fold difference by real-time RT-PCR, respectively,  $P \leq 0.0022$ ). Second, the deposition of type-X collagen (**Figures 14E-14H**) significantly decreased in human mesenchymal stromal cells over time using the rAAV-FLAG-*hsox9*/alginate and rAAV-hTGF- $\beta$ /alginate hydrogel systems relative to the rAAV-*lacZ*/alginate hydrogel system (deposition of type-X collagen: always 1.3-fold difference in the AOD and always 1.5-fold difference in the scores of type-X collagen immunostaining, respectively,  $P \leq 0.0071$ ; COL10A1 expression: 1.5- and 1.6-fold difference by real-time RT-PCR, respectively,  $P \leq 0.0006$ ). Third, mineralization (**Figures 14I-14K**) significantly decreased in human mesenchymal stromal cells over time using the rAAV-FLAG-*hsox9*/alginate and rAAV-hTGF- $\beta$ /alginate hydrogel systems relative to the rAAV-*lacZ*/alginate hydrogel system (1.1- and 1.2-fold difference in the AOD and always 3-fold difference in the scores of alizarin red staining, respectively,  $P \leq 0.0111$ ).

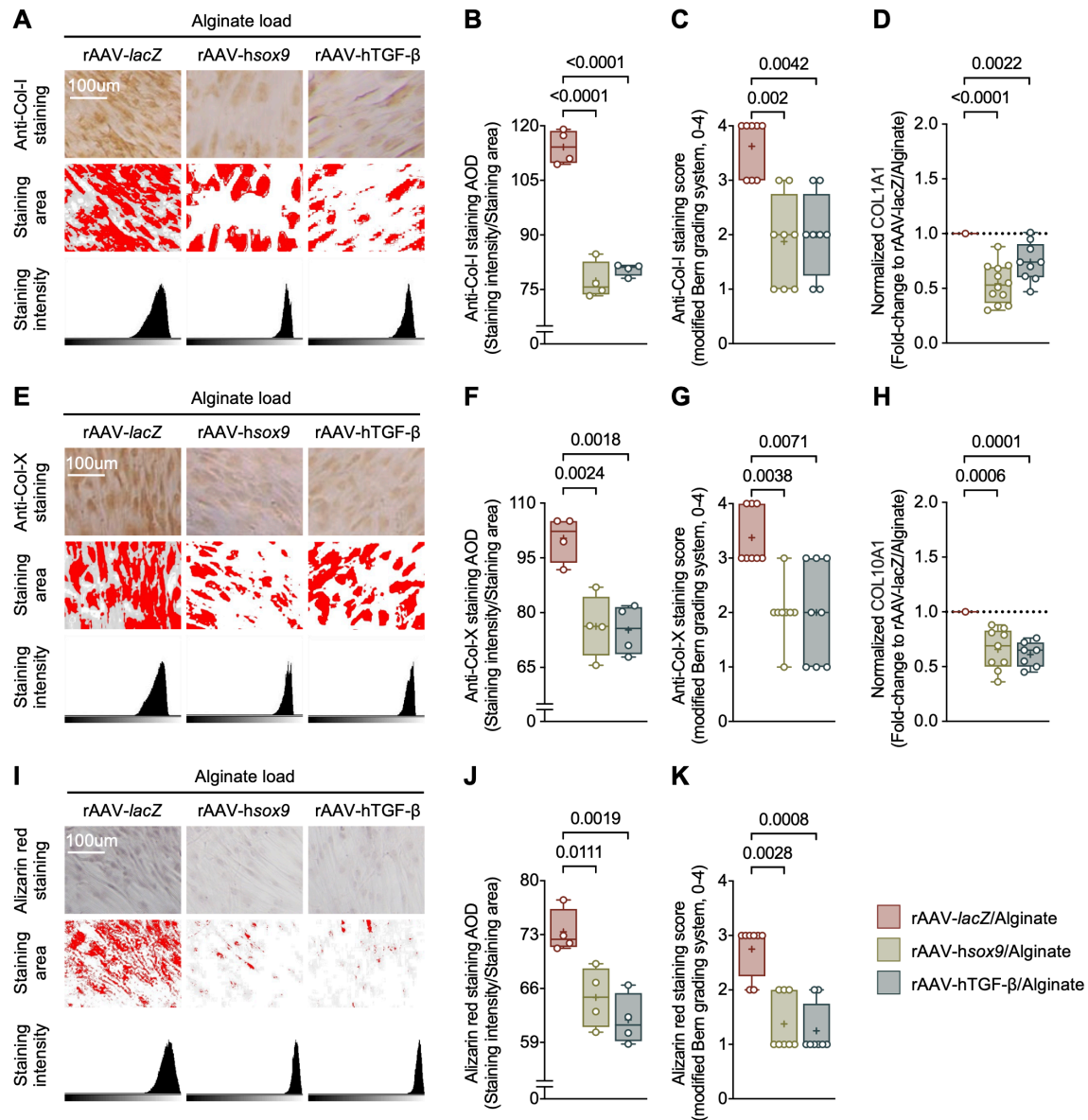


**Figure 14.** Effects of the rAAV/alginate hydrogel systems on the osteogenic, hypertrophic, and mineralization activities in human mesenchymal stromal cells. **(A-D)** Evaluation of the deposition of type-I collagen by **(A)** immunodetection (magnification x 10; scale bars: 100  $\mu$ m; all representative data) with **(B)** an estimation of the corresponding AOD (*P* values indicated), **(C)** an estimation of the corresponding scores using a modified Bern grading system (*P* values indicated), and **(D)** a real-time RT-PCR analysis for COL1A1 (*P* values indicated) after 21 days. **(E-H)** Evaluation of the deposition type-X collagen by **(E)** immunodetection (magnification x 10; scale bars: 100  $\mu$ m; all representative data) with **(F)** an estimation of the corresponding AOD (*P* values indicated), **(G)** an estimation of the corresponding scores using a modified Bern grading system (*P* values indicated), and **(H)** a real-time RT-PCR analysis for COL10A1 (*P* values indicated) after 21 days. **(I-K)** Evaluation of mineralization by **(I)** alizarin red staining (magnification x 10; scale bars: 100  $\mu$ m; all representative data) with **(J)** an estimation of the corresponding AOD (*P* values indicated) and **(K)** an estimation of the corresponding scores using a modified Bern grading system (*P* values indicated) after 21 days. Abbreviations: AOD: average optical density; Col-I: type-I collagen; Col-X: type-X collagen; COL1A1: type-I collagen (gene); COL10A1: type-X collagen (gene); hsox9: human sex-determining region Y-type high mobility group box 9; hTGF- $\beta$ : human transforming growth factor beta; lacZ:  $\beta$ -galactosidase; rAAV: recombinant adeno-associated virus;  $\mu$ m: micrometer (created with Affinity Photo and Prism).

## 8. DISCUSSION

Therapeutic rAAV vectors are potent gene transfer systems to treat traumatic articular cartilage defects and OA lesions (Cucchiariini & Madry, 2005, 2019; Madry & Cucchiariini, 2011, 2016; Madry et al., 2011). Their spatiotemporal efficacy is particularly notable in sites of cartilage injury when released from biocompatible scaffolds such as those derived from alginate (Diaz-Rodriguez et al., 2015; Liu et al., 2022; Maihofer et al., 2021). Growing evidence suggest that biomaterial-guided gene therapy enhances therapeutic outcomes relative to scaffold-free gene transfer methods (Cottard et al., 2004; Cucchiariini & Madry, 2019). Such an approach might also be superior to strategies relying on the sole administration of alginate without addition of therapeutic cues (genes) in translational setups (Liu et al., 2022). Recent studies also described the potential of alginate hydrogels to facilitate the effective and controlled release of rAAV vectors such as coding for the *lacZ* reporter gene in human mesenchymal stromal cells (Diaz-Rodriguez et al., 2015). Also, the feasibility of using rAAV/alginate hydrogel systems to deliver an IGF-I gene sequence was reported to partially address chondral defects in an inflammatory environment (Maihofer et al., 2021).

Based on these findings, the goal of the current work was to examine whether alginate hydrogels can formulate and deliver therapeutic rAAV vectors in a controlled release manner in human osteoarthritic articular chondrocytes and human mesenchymal stromal cells as a means to activate their cartilage-specific reparative activities upon transfer of the highly chondroreparative *sox9* and TGF- $\beta$  genes, for future convenient application of rAAV/alginate hydrogel systems as off-the-shelf systems (Zmora et al., 2002) to improve the processes of articular cartilage repair.

### 8.1. Ability of alginate-based hydrogels to deliver rAAV vectors in human osteoarthritic articular chondrocytes

The evaluations performed to address the first hypothesis ("*Alginate-based hydrogels are capable of efficiently and durably incorporating and delivering rAAV vectors as a means to genetically modify human osteoarthritic articular chondrocytes*") demonstrated that optimized rAAV delivery conditions (MOI of 80, alginate concentration of 0.2%, gelation time of 1 minute) allowed to support the successful, controlled release of rAAV (*lacZ*) from the alginate hydrogel in human osteoarthritic articular chondrocytes over time (21 days) (§ 7.1.1. and §7.1.2.).

Optimization of experimental working conditions was critical to reliably and reproducibly

achieve an effective release of rAAV gene vectors prior to monitor any potential therapeutic outcome, including for the goal of cartilage repair (Cucchiariini & Madry, 2019). Overall, the results revealed the pivotal roles played by the dose of vector, the concentration of alginate, and the time of gelation to modulate the release of rAAV from the alginate hydrogel. The vector dose is an indispensable determinant in the release dynamics (Nakai et al., 2005). The magnitude of this dosage is not merely a quantitative consideration but has profound implications for therapeutic outcomes. An insufficient amount of vector might render the therapeutic payload suboptimal, thereby potentially diminishing its intended efficacy. Conversely, an excessive dosage of vector poses the risk of inducing suboptimal responses that may lead to adverse cellular reactions. As highlighted, achieving the right balance is crucial to optimize therapeutic benefits while minimizing potential cellular perturbations like immunoreaction (Nakai et al., 2005). In the context of a controlled delivery strategy, the precise concentration of alginate hydrogel is an additional critical determinant of the release kinetics of the incorporated vectors. Alginate, a naturally occurring polymer, establishes a microenvironment conducive to nuanced modulation of these kinetics with crosslinking between calcium ionic and guluronic acid. Empirical observations suggest that an augmented alginate concentration tends to reduce vector release, leading to the limitation of intervention, whereas a reduced concentration may precipitate an accelerated release, thereby risking premature depletion of the therapeutic payload (Silva et al., 2006; Takka & Gurel, 2010). Regarding alginate gelation, a significant parameter of interest is generally the time of gelation characterized by the duration necessary for the alginate matrix to transition from a liquid to a semi-solid state. A protracted gelation period can lead to potential structural vulnerabilities within the matrix, potentially compromising the release of the vector (Takka & Gurel, 2010; Topuz et al., 2012). On the other hand, an expedited gelation process may not adequately establish an environment within which vectors may achieve a consistent and sustained release (Takka & Gurel, 2010; Topuz et al., 2012). This delicate balance emphasizes the need for a precise control and understanding of this parameter in biological applications.

Using such optimized conditions, the rAAV/alginate hydrogel system acted as a reservoir allowing for a sustained release of the vectors as noted in preliminary work (Diaz-Rodriguez et al., 2015; Maihofer et al., 2021). Evaluations of the every 2-day release profiles by X-Gal staining and ELISA revealed that the release of rAAV was consistent, with a rate of about 1.5% release/day upon control by the alginate hydrogel. Such tight release modalities are indispensable in therapeutic contexts where an extended presence of therapeutic agents is crucial, potentially obviating the need for recurrent administration. The current findings suggest that, when appropriately formulated, the alginate matrix stands as a potent instrument to modulate the dissemination of rAAV vectors. This study not only contributes to expand the body of the literature

in the field of gene therapy but also provides a foundational platform for future research in human regenerative medicine. Such endeavors are instrumental in refining the efficacy of these delivery mechanisms, with an ultimate aim to redeploy them into workable therapeutic translational applications.

## **8.2. Ability of alginate-based hydrogels to deliver therapeutic rAAV vectors in human osteoarthritic articular chondrocytes and in human mesenchymal stromal cells**

The evaluations performed to address the second hypothesis ("*Alginate-based hydrogels are capable of efficiently and durably incorporating and delivering therapeutic (sox9, TGF- $\beta$ ) rAAV vectors to both reparative human osteoarthritic articular chondrocytes and human mesenchymal stromal cells in order to stimulate their reparative activities for the purpose of improved articular cartilage regeneration*") demonstrated that the rAAV-FLAG-hsox9/alginate and rAAV-hTGF- $\beta$ /alginate hydrogel systems allowed to (i) respectively support the successful expression of sox9 and TGF- $\beta$  in human osteoarthritic articular chondrocytes and human mesenchymal stromal cells over time (21 days) relative to the control conditions (§ 7.2.1.1. and § 7.2.1.2.), (ii) increase the proliferative (cell densities, DNA contents) and cartilage-specific anabolic activities (expression and deposition of glycosaminoglycans, proteoglycans, type-II collagen) in human osteoarthritic articular chondrocytes and human mesenchymal stromal cells over time (21 days) relative to the control conditions (§ 7.2.2.1. and § 7.2.2.2.), and (iii) decrease undesirable anabolic activities (expression and deposition of type-I/-X collagen) in human osteoarthritic articular chondrocytes and human mesenchymal stromal cells over time (21 days) (§ 7.2.3.1. and § 7.2.3.2.) while also decreasing mineralization only in human mesenchymal stromal cells (with increases in human osteoarthritic articular chondrocytes) over time (21 days) relative to the control conditions (§ 7.2.3.2.).

### **8.2.1. Transgene expression**

Using optimized conditions of rAAV delivery from the alginate-based hydrogels, evidence was first provided that the rAAV-FLAG-hsox9/alginate and rAAV-hTGF- $\beta$ /alginate hydrogel systems did not trigger undesirable endogenous  $\beta$ -gal-like activities in both human osteoarthritic articular chondrocytes and human mesenchymal stromal cells. The results further revealed that the rAAV-*lacZ*/alginate hydrogel system successfully mediated marked and sustained levels of *lacZ*

expression in both human osteoarthritic articular chondrocytes and human mesenchymal stromal cells relative to control conditions, probably due to the effective controlled release of the vector from the hydrogel. This observation is consistent with preliminary observations (Diaz-Rodriguez et al., 2015) and extends previous findings in a scaffold-free gene transfer setup (Cucchiaroni et al., 2011) or using other scaffolds that are less biocompatible than alginate (carbon dots, self-assembling RAD-based peptide hydrogels, PEO-PPO-PEO-derived polymeric micelles) (Meng et al., 2020; Rey-Rico et al., 2015c, 2015d, 2016b). The data finally demonstrated that the rAAV-FLAG-hsox9/alginate and rAAV-hTGF- $\beta$ /alginate hydrogel systems successfully mediated marked and sustained levels of sox9 and TGF- $\beta$  expression, respectively, in both human osteoarthritic articular chondrocytes and human mesenchymal stromal cells relative to control conditions, probably due to the effective controlled release of the vector from the hydrogel. These observations extend previous findings in a scaffold-free gene transfer setup (Frisch et al., 2014; Tao et al., 2016a; Venkatesan et al., 2012, 2013) or using again other scaffolds that are less biocompatible than alginate (carbon dots, PEO-PPO-PEO-derived polymeric micelles) (Meng et al., 2020; Rey-Rico et al., 2017, 2018).

### 8.2.2. Effects on the biological and chondroreparative activities

Using optimized conditions of rAAV delivery from the alginate-based hydrogels, evidence was next provided that both the rAAV-FLAG-hsox9/alginate and rAAV-hTGF- $\beta$ /alginate hydrogel systems successfully and durably stimulated the biological and chondroreparative activities of human osteoarthritic articular chondrocytes and human mesenchymal stromal cells relative to control conditions, including the levels of cell proliferation and the deposition of specific extracellular matrix compounds (glycosaminoglycans, proteoglycans, type-II collagen), probably due to the effective and sustained levels of sox9 and TGF- $\beta$  expression via such systems. These observations are consistent with the properties of these two factors (Bi et al., 1999; Johnstone et al., 1998; Mackay et al., 1998) and extend previous findings in a scaffold-free gene transfer setup (Cucchiaroni et al., 2007; Daniels et al., 2019; Frisch et al., 2014, 2016a, 2016b, 2017; Tao et al., 2016a; Venkatesan et al., 2012, 2013) or using again other scaffolds that are less biocompatible than alginate (carbon dots, PEO-PPO-PEO-derived polymeric micelles) (Meng et al., 2020; Rey-Rico et al., 2017, 2018). Interestingly, the stimulating effects of the rAAV-FLAG-hsox9/alginate hydrogel system on cell proliferation stand in contrast to prior findings in a scaffold-free gene transfer setup of rAAV-FLAG-hsox9 (Cucchiaroni et al., 2007; Daniels et al., 2019; Venkatesan et al., 2012), possibly resulting from the tightly regulated vector release and expression afforded by the alginate-based hydrogel (Diaz-Rodriguez et al., 2015). Of further note, the rAAV-hTGF-

$\beta$ /alginate hydrogel system was overall more potent than the AAV-FLAG-hsox9/alginate hydrogel system in human mesenchymal stromal cells, as previously noted using other scaffolds (carbon dots) (Meng et al., 2020).

### 8.2.3. Effects on the osteogenic, hypertrophic, and mineralization activities

Using optimized conditions of rAAV delivery from the alginate-based hydrogels, evidence was finally provided that the rAAV-FLAG-hsox9/alginate and rAAV-hTGF- $\beta$ /alginate hydrogel systems successfully and durably reduced osteogenic, hypertrophic, and mineralization activities in human osteoarthritic articular chondrocytes and human mesenchymal stromal cells relative to control conditions, including the deposition of undesirable extracellular matrix compounds (type-I/-X collagen) and mineralization (human mesenchymal stromal cells), probably due to the effective and sustained levels of sox9 and TGF- $\beta$  expression via such systems. These observations are consistent with the properties of these two factors (Hattori et al., 2010b; Ma et al., 2003) and extend previous findings in a scaffold-free gene transfer setup (Daniels et al., 2019; Venkatesan et al., 2012, 2013) or using again other scaffolds that are less biocompatible than alginate (carbon dots, PEO-PPO-PEO-derived polymeric micelles) (Meng et al., 2020; Rey-Rico et al., 2017, 2018). Interestingly, the decreasing effects of the rAAV-hTGF- $\beta$ /alginate hydrogel system on such activities in human mesenchymal stromal cells and the increasing effects of the rAAV-FLAG-hsox9/alginate and rAAV-hTGF- $\beta$ /alginate hydrogel systems on mineralization in human osteoarthritic articular chondrocytes stand in contrast to prior findings in a scaffold-free gene transfer setup of rAAV-hTGF- $\beta$  (Frisch et al., 2014) or using again other scaffolds that are less biocompatible than alginate (PEO-PPO-PEO-derived polymeric micelles) (Rey-Rico et al., 2017, 2018), again possibly resulting from the tightly regulated vector release and expression afforded by the alginate-based hydrogel (Diaz-Rodriguez et al., 2015). Of further note, there was no difference in potency between the rAAV-FLAG-hsox9/alginate and the rAAV-hTGF- $\beta$ /alginate hydrogel systems.

### 8.3. Limitations and future directions

The present investigation aimed to assess the impact of the rAAV-FLAG-hsox9/alginate and rAAV-hTGF- $\beta$ /alginate hydrogel systems on the chondroregenerative capabilities of human osteoarthritic articular chondrocytes and human mesenchymal stromal cells *in vitro*, covering a well-established time frame of 21 days for the proper assessment of chondroregeneration and remodeling *in vitro* (Cucchiari et al., 2013; Johnstone et al., 1998; Venkatesan et al., 2013). To comprehensively

understand the long-term consequences of the rAAV-FLAG-hsox9/alginate and rAAV-hTGF- $\beta$ /alginate hydrogel systems, evaluations may be performed using extended observation periods, especially to further monitor the controlled release process and the degradation of the alginate hydrogel itself. Combined, simultaneous formulation of the two rAAV vectors (sox9 and TGF- $\beta$ ) within the hydrogels might be also envisaged to test whether concomitant expression of the two factors may improve the therapeutic outcomes (Cucchiariini et al., 2009; Morscheid et al., 2019a, 2019b; Tao et al., 2016a, 2016b, 2017). Finally, work in experimental cartilage lesions *in situ* (*ex vivo*) (Morscheid et al., 2019b; Rey-Rico et al., 2016b, 2017, 2018) and in relevant, translational animal models of (orthotopic) cartilage injury *in vivo* with a natural loading and inflamed environment (Cucchiariini et al., 2013, 2014b, 2018; Lange et al., 2021; Madry et al., 2020a; Maihofer et al., 2021; Rabie et al., 2023) will be particularly important to test the workability, efficacy, safety, and sustainability of the current therapeutic strategy prior to considering an application in patients in the future. Such essential work will need to include the evaluation of various vector(s) and hydrogel doses, the route of administration, the possible development of local and systemic immune and toxic reactions of the host, and the time-dependent efficacy of the therapy relative to strictly defined control conditions as performed here (reporter gene vectors, absence of vectors, scaffold-free vectors, etc.). Similar work may be also attempted in a different (osteogenic) microenvironment to examine possibly different outcomes like for the purpose of bone healing, and/or by co-delivering both gene vectors via alginate to expand the reparative outcomes in a durable manner.

#### **8.4. Clinical implications**

Biomaterial-guided delivery of chondroreparative gene sequences via gene transfer vectors to sites of articular cartilage injury is an attractive strategy to enhance cartilage repair by regulating the release of the therapeutic gene vectors in an improved spatiotemporal manner while preserving the gene transfer efficacy in a natural microenvironment (Cucchiariini & Madry, 2019). For clinical implications, the current rAAV/alginate hydrogel system may offer a new approach in targeted gene transfer using clinically adapted rAAV vectors (Rey-Rico & Cucchiariini, 2016a) designed for specific cell types to ensure an accurate delivery of therapeutic genes. The controlled release feature of this hydrogel system may allow for a longer availability of the therapeutic genes and of their products which may lead to improved and more lasting cartilage repair, reduce unwanted side effects, and provide a more precise treatment compared with scaffold-free gene transfer methods. While the primary use of the rAAV/alginate hydrogel system is for cartilage repair, its flexible design allows to envisage other applications which can be adapted to deliver various

therapeutic genes, opening up possibilities for broader medical applications. Furthermore, this hydrogel system aligns well with the concept of personalized medicine which can be tailored to fit individual genetic profiles and be adjusted to the specific needs of a patient. In conclusion, the rAAV/alginate hydrogel system offers a promising and flexible tool for cartilage repair and holds potential for broader medical applications.

## 9. CONCLUSIONS

In summary, the present study demonstrated the benefits of alginate-based hydrogel-guided controlled and overexpression of therapeutic rAAV-FLAG-hsox9 and rAAV-hTGF- $\beta$  vectors to significantly expand a source of improved (more potent) chondroreparative cells for the purpose of cartilage repair by counterbalancing the low metabolic activities of adult human osteoarthritic articular chondrocytes and human mesenchymal stromal cells. The current results advance the knowledge on the feasibility of biomaterial-guided gene therapy to enhance cartilage repair as a novel, minimally-invasive treatment for potential future clinical applications.

## 10. REFERENCES

- Abbah, S. A., Lu, W. W., Peng, S. L., Aladin, D. M., Li, Z. Y., Tam, W. K., Cheung, K. M., Luk, K. D., & Zhou, G. Q. (2008). Extracellular matrix stability of primary mammalian chondrocytes and intervertebral disc cells cultured in alginate-based microbead hydrogels. *Cell Transplant*, *17*(10-11), 1181-1192.
- Allay, J. A., Dennis, J. E., Haynesworth, S. E., Majumdar, M. K., Clapp, D. W., Shultz, L. D., Caplan, A. I., & Gerson, S. L. (1997). LacZ and interleukin-3 expression in vivo after retroviral transduction of marrow-derived human osteogenic mesenchymal progenitors. *Hum Gene Ther*, *8*(12), 1417-1427.
- Amini, M., Venkatesan, J. K., Nguyen, T. N., Liu, W., Leroux, A., Madry, H., Migonney, V., & Cucchiari, M. (2023). rAAV TGF-beta and FGF-2 overexpression via pNaSS-grafted PCL films stimulates the reparative activities of human ACL fibroblasts. *Int J Mol Sci*, *24*(13).
- Anderson, D. E., & Johnstone, B. (2017). Dynamic mechanical compression of chondrocytes for tissue engineering: a critical review. *Front Bioeng Biotechnol*, *5*, 76.
- Andrade, L. R., Arcanjo, K. D., Martins, H. S., dos Reis, J. S., Farina, M., Borojevic, R., & Duarte, M. E. (2011). Fine structure and molecular content of human chondrocytes encapsulated in alginate beads. *Cell Biol Int*, *35*(3), 293-297.
- Appaiahgari, M. B., & Vrati, S. (2015). Adenoviruses as gene/vaccine delivery vectors: promises and pitfalls. *Expert Opin Biol Ther*, *15*(3), 337-351.
- Argentaro, A., Sim, H., Kelly, S., Preiss, S., Clayton, A., Jans, D. A., & Harley, V. R. (2003). A SOX9 defect of calmodulin-dependent nuclear import in campomelic dysplasia/autosomal sex reversal. *J Biol Chem*, *278*(36), 33839-33847.
- Asari, A., Miyauchi, S., Kuriyama, S., Machida, A., Kohno, K., & Uchiyama, Y. (1994). Localization of hyaluronic acid in human articular cartilage. *J Histochem Cytochem*, *42*(4), 513-522.
- Asen, A. K., Goebel, L., Rey-Rico, A., Sohler, J., Zurakowski, D., Cucchiari, M., & Madry, H. (2018). Sustained spatiotemporal release of TGF-beta1 confers enhanced very early chondrogenic differentiation during osteochondral repair in specific topographic patterns. *FASEB J*, *32*(10), 5298-5311.
- Ashraf, S., Cha, B. H., Kim, J. S., Ahn, J., Han, I., Park, H., & Lee, S. H. (2016). Regulation of senescence associated signaling mechanisms in chondrocytes for cartilage tissue regeneration. *Osteoarthritis Cartilage*, *24*(2), 196-205.
- Athanasίου, K. A., Shah, A. R., Hernandez, R. J., & LeBaron, R. G. (2001). Basic science of articular cartilage repair. *Clin Sports Med*, *20*(2), 223-247.
- Aydelotte, M. B., Thonar, E. J., Mollenhauer, J., & Flechtenmacher, J. (1998). Culture of chondrocytes in alginate gel: variations in conditions of gelation influence the structure of the alginate gel, and the arrangement and morphology of proliferating chondrocytes. *In Vitro Cell Dev Biol Anim*, *34*(2), 123-130.
- Aydin, S. (2015). A short history, principles, and types of ELISA, and our laboratory experience with peptide/protein analyses using ELISA. *Peptides*, *72*, 4-15.
- Bank, R. A., Bayliss, M. T., Lafeber, F. P., Maroudas, A., & Tekoppele, J. M. (1998). Ageing and zonal variation in post-translational modification of collagen in normal human articular cartilage. The age-related increase in non-enzymatic glycation affects biomechanical properties of cartilage. *Biochem J*, *330* ( Pt 1), 345-351.
- Baragi, V. M., Renkiewicz, R. R., Jordan, H., Bonadio, J., Hartman, J. W., & Roessler, B. J. (1995). Transplantation of transduced chondrocytes protects articular cartilage from interleukin 1-induced extracellular matrix degradation. *J Clin Invest*, *96*(5), 2454-2460.
- Bauge, C., Duval, E., Ollitrault, D., Girard, N., Leclercq, S., Galera, P., & Boumediene, K. (2013). Type II TGFbeta receptor modulates chondrocyte phenotype. *Age (Dordr)*, *35*(4), 1105-1116.
- Bayliss, M. T., Venn, M., Maroudas, A., & Ali, S. Y. (1983). Structure of proteoglycans from different layers of human articular cartilage. *Biochem J*, *209*(2), 387-400.
- Beekman, B., Verzijl, N., Bank, R. A., von der Mark, K., & TeKoppele, J. M. (1997). Synthesis of collagen by bovine chondrocytes cultured in alginate; posttranslational modifications and cell-matrix interaction. *Exp Cell Res*, *237*(1), 135-141.

- Bergholt, N. L., Lysdahl, H., Lind, M., & Foldager, C. B. (2019). A standardized method of applying toluidine blue metachromatic staining for assessment of chondrogenesis. *Cartilage*, *10*(3), 370-374.
- Bernard, P., & Harley, V. R. (2010). Acquisition of SOX transcription factor specificity through protein-protein interaction, modulation of Wnt signalling and post-translational modification. *Int J Biochem Cell Biol*, *42*(3), 400-410.
- Berns, K. I., & Linden, R. M. (1995). The cryptic life style of adeno-associated virus. *Bioessays*, *17*(3), 237-245.
- Bi, W. M., Deng, J. M., Zhang, Z. P., Behringer, R. R., & de Crombrugge, B. (1999). Sox9 is required for cartilage formation. *Nature Genetics*, *22*(1), 85-89.
- Binette, F., McQuaid, D. P., Haudenschild, D. R., Yaeger, P. C., McPherson, J. M., & Tubo, R. (1998). Expression of a stable articular cartilage phenotype without evidence of hypertrophy by adult human articular chondrocytes in vitro. *J Orthop Res*, *16*(2), 207-216.
- Blaney Davidson, E. N., Remst, D. F., Vitters, E. L., Van Beuningen, H. M., Blom, A. B., Goumans, M. J., Van den Berg, W. B., & Van der Kraan, P. M. (2009). Increase in ALK1/ALK5 ratio as a cause for elevated MMP-13 expression in osteoarthritis in humans and mice. *J Immunol*, *182*(12), 7937-7945.
- Bohenzky, R. A., LeFebvre, R. B., & Berns, K. I. (1988). Sequence and symmetry requirements within the internal palindromic sequences of the adeno-associated virus terminal repeat. *Virology*, *166*(2), 316-327.
- Bonaventure, J., Kadhom, N., Cohen-Solal, L., Ng, K. H., Bourguignon, J., Lasselin, C., & Freisinger, P. (1994). Reexpression of cartilage-specific genes by dedifferentiated human articular chondrocytes cultured in alginate beads. *Exp Cell Res*, *212*(1), 97-104.
- Bono, N., Ponti, F., Mantovani, D., & Candiani, G. (2020). Non-viral in vitro gene delivery: it is now time to set the bar! *Pharmaceutics*, *12*(2).
- Bouhadir, K. H., Lee, K. Y., Alsberg, E., Damm, K. L., Anderson, K. W., & Mooney, D. J. (2001). Degradation of partially oxidized alginate and its potential application for tissue engineering. *Biotechnol Prog*, *17*(5), 945-950.
- Bratthauer, G. L. (2010). The avidin-biotin complex (ABC) method and other avidin-biotin binding methods. *Methods Mol Biol*, *588*, 257-270.
- Brentjens, R. J., Davila, M. L., Riviere, I., Park, J., Wang, X., Cowell, L. G., Bartido, S., Stefanski, J., Taylor, C., Olszewska, M., Borquez-Ojeda, O., Qu, J., Wasielewska, T., He, Q., Bernal, Y., Rijo, I. V., Hedvat, C., Kobos, R., Curran, K., Steinherz, P., Jurcic, J., Rosenblat, T., Maslak, P., Frattini, M., & Sadelain, M. (2013). CD19-targeted T cells rapidly induce molecular remissions in adults with chemotherapy-refractory acute lymphoblastic leukemia. *Sci Transl Med*, *5*(177), 177ra138.
- Brittberg, M. (2010). Cell carriers as the next generation of cell therapy for cartilage repair: a review of the matrix-induced autologous chondrocyte implantation procedure. *Am J Sports Med*, *38*(6), 1259-1271.
- Buckwalter, J. A., & Mankin, H. J. (1998a). Articular cartilage: tissue design and chondrocyte-matrix interactions. *Instr Course Lect*, *47*, 477-486.
- Buckwalter, J. A., & Mankin, H. J. (1998b). Articular cartilage repair and transplantation. *Arthritis Rheum*, *41*(8), 1331-1342.
- Buckwalter, J. A., & Brown, T. D. (2004). Joint injury, repair, and remodeling: roles in post-traumatic osteoarthritis. *Clin Orthop Relat Res* (423), 7-16.
- Carballo-Pedrares, N., Kattar, A., Concheiro, A., Alvarez-Lorenzo, C., Rey-Rico, A. (2021) Niosomes-based gene delivery systems for effective transfection of human mesenchymal stem cells. *Mater Sci Eng C Mater Biol Appl*, *128*, 112307.
- Cai, X., Venkatesan, J. K., Schmitt, G., Reda, B., Cucchiari, M., Hannig, M., & Madry, H. (2023). Cytotoxic effects of different mouthwash solutions on primary human articular chondrocytes and normal human articular cartilage - an in vitro study. *Clin Oral Investig*, *27*(9), 4987-5000.
- Caron, M. M., Emans, P. J., Coolen, M. M., Voss, L., Surtel, D. A., Cremers, A., Van Rhijn, L. W., & Welting, T. J. (2012). Redifferentiation of dedifferentiated human articular chondrocytes: comparison of 2D and 3D cultures. *Osteoarthritis Cartilage*, *20*(10), 1170-1178.
- Chan, J. K. (2014). The wonderful colors of the hematoxylin-eosin stain in diagnostic surgical pathology. *Int J Surg Pathol*, *22*(1), 12-32.
- Charlier, E., Deroyer, C., Ciregia, F., Malaise, O., Neuville, S., Plener, Z., Malaise, M., & de Seny, D. (2019). Chondrocyte dedifferentiation and osteoarthritis (OA). *Biochem Pharmacol*, *165*, 49-65.

- Chen, K. L., Mylon, S. E., & Elimelech, M. (2007). Enhanced aggregation of alginate-coated iron oxide (hematite) nanoparticles in the presence of calcium, strontium, and barium cations. *Langmuir*, *23*(11), 5920-5928.
- Chen, C. G., Thuillier, D., Chin, E. N., & Alliston, T. (2012). Chondrocyte-intrinsic Smad3 represses Runx2-inducible matrix metalloproteinase 13 expression to maintain articular cartilage and prevent osteoarthritis. *Arthritis Rheum*, *64*(10), 3278-3289.
- Chen, H., He, Y., Wen, X., Shao, S., Liu, Y., & Wang, J. (2021). SOX9: advances in gynecological malignancies. *Front Oncol*, *11*, 768264.
- Cheng, T., Maddox, N. C., Wong, A. W., Rahnama, R., & Kuo, A. C. (2012). Comparison of gene expression patterns in articular cartilage and dedifferentiated articular chondrocytes. *J Orthop Res*, *30*(2), 234-245.
- Chirmule, N., Propert, K., Magosin, S., Qian, Y., Qian, R., & Wilson, J. (1999). Immune responses to adenovirus and adeno-associated virus in humans. *Gene Ther*, *6*(9), 1574-1583.
- Chuang, C. Y., Shahin, K., Lord, M. S., Melrose, J., Doran, P. M., & Whitelock, J. M. (2012). The cartilage matrix molecule components produced by human foetal cartilage rudiment cells within scaffolds and the role of exogenous growth factors. *Biomaterials*, *33*(16), 4078-4088.
- Coates, E., & Fisher, J. P. (2012). Gene expression of alginate-embedded chondrocyte subpopulations and their response to exogenous IGF-1 delivery. *J Tissue Eng Regen Med*, *6*(3), 179-192.
- Cohen, S. B., Meirisch, C. M., Wilson, H. A., & Diduch, D. R. (2003). The use of absorbable co-polymer pads with alginate and cells for articular cartilage repair in rabbits. *Biomaterials*, *24*(15), 2653-2660.
- Cohen, J., Zaleski, K. L., Nourissat, G., Julien, T. P., Randolph, M. A., & Yaremchuk, M. J. (2011). Survival of porcine mesenchymal stem cells over the alginate recovered cellular method. *J Biomed Mater Res A*, *96*(1), 93-99.
- Colowick, N. P., Kaplan, N. P., & Cunningham, L. W. (1987). Extracellular matrix. In L. W. Cunningham (Ed.), *Structural and contractile proteins* (1st ed., Vol. 144, pp. 1-561). Academic Press.
- Cooke, M. E., Pearson, M. J., Moakes, R. J. A., Weston, C. J., Davis, E. T., Jones, S. W., & Grover, L. M. (2017). Geometric confinement is required for recovery and maintenance of chondrocyte phenotype in alginate. *APL Bioeng*, *1*(1), 016104.
- Cottard, V., Valvason, C., Falgarone, G., Lutomski, D., Boissier, M. C., & Bessis, N. (2004). Immune response against gene therapy vectors: influence of synovial fluid on adeno-associated virus mediated gene transfer to chondrocytes. *J Clin Immunol*, *24*(2), 162-169.
- Cucchiari, M., Ren, X. L., Perides, G., & Terwilliger, E. F. (2003). Selective gene expression in brain microglia mediated via adeno-associated virus type 2 and type 5 vectors. *Gene Ther*, *10*(8), 657-667.
- Cucchiari, M., & Madry, H. (2005). Gene therapy for cartilage defects. *J Gene Med*, *7*(12), 1495-1509.
- Cucchiari, M., Thurn, T., Weimer, A., Kohn, D., Terwilliger, E. F., & Madry, H. (2007). Restoration of the extracellular matrix in human osteoarthritic articular cartilage by overexpression of the transcription factor SOX9. *Arthritis Rheum*, *56*(1), 158-167.
- Cucchiari, M., Terwilliger, E. F., Kohn, D., & Madry, H. (2009). Remodelling of human osteoarthritic cartilage by FGF-2, alone or combined with Sox9 via rAAV gene transfer. *J Cell Mol Med*, *13*(8B), 2476-2488.
- Cucchiari, M., & Madry, H. (2010). Genetic modification of mesenchymal stem cells for cartilage repair. *Biomed Mater Eng*, *20*(3), 135-143.
- Cucchiari, M., Ekici, M., Schetting, S., Kohn, D., & Madry, H. (2011). Metabolic activities and chondrogenic differentiation of human mesenchymal stem cells following recombinant adeno-associated virus-mediated gene transfer and overexpression of fibroblast growth factor 2. *Tissue Eng Part A*, *17*(15-16), 1921-1933.
- Cucchiari, M., Orth, P., & Madry, H. (2013). Direct rAAV SOX9 administration for durable articular cartilage repair with delayed terminal differentiation and hypertrophy in vivo. *J Mol Med (Berl)*, *91*(5), 625-636.
- Cucchiari, M., & Madry, H. (2014a). Use of tissue engineering strategies to repair joint tissues in osteoarthritis: viral gene transfer approaches. *Curr Rheumatol Rep*, *16*(10), 449.
- Cucchiari, M., & Madry, H. (2014b). Overexpression of human IGF-I via direct rAAV-mediated gene transfer improves the early repair of articular cartilage defects in vivo. *Gene Ther*, *21*(9), 811-819.
- Cucchiari, M., Henrionnet, C., Mainard, D., Pinzano, A., & Madry, H. (2015). New trends in articular cartilage repair. *J Exp Orthop*, *2*(1), 8.

- Cucchiari, M., & Rey-Rico, A. (2017). Controlled gene delivery systems for articular cartilage repair. In *Advances in Biomaterials for Biomedical Applications* (pp. 261-300). Springer.
- Cucchiari, M., Asen, A. K., Goebel, L., Venkatesan, J. K., Schmitt, G., Zurakowski, D., Menger, M. D., Laschke, M. W., & Madry, H. (2018). Effects of TGF-beta overexpression via rAAV gene transfer on the early repair processes in an osteochondral defect model in minipigs. *Am J Sports Med*, *46*(8), 1987-1996.
- Cucchiari, M., & Madry, H. (2019). Biomaterial-guided delivery of gene vectors for targeted articular cartilage repair. *Nat Rev Rheumatol*, *15*(1), 18-29.
- Dallas, S. L., Rosser, J. L., Mundy, G. R., & Bonewald, L. F. (2002). Proteolysis of latent transforming growth factor-beta (TGF-beta )-binding protein-1 by osteoclasts. A cellular mechanism for release of TGF-beta from bone matrix. *J Biol Chem*, *277*(24), 21352-21360.
- Daniels, O., Frisch, J., Venkatesan, J. K., Rey-Rico, A., Schmitt, G., & Cucchiari, M. (2019). Effects of rAAV-mediated sox9 overexpression on the biological activities of human osteoarthritic articular chondrocytes in their intrinsic three-dimensional environment. *J Clin Med*, *8*(10).
- Darling, E. M., & Athanasiou, K. A. (2005). Rapid phenotypic changes in passaged articular chondrocyte subpopulations. *J Orthop Res*, *23*(2), 425-432.
- Daya, S., & Berns, K. I. (2008). Gene therapy using adeno-associated virus vectors. *Clin Microbiol Rev*, *21*(4), 583-593.
- De Ceuninck, F., Lesur, C., Pastoureaux, P., Caliez, A., & Sabatini, M. (2004). Culture of chondrocytes in alginate beads. *Methods Mol Med*, *100*, 15-22.
- Demoor-Fossard, M., Redini, F., Boittin, M., & Pujol, J. P. (1998). Expression of decorin and biglycan by rabbit articular chondrocytes. Effects of cytokines and phenotypic modulation. *Biochim Biophys Acta*, *1398*(2), 179-191.
- Demoor-Fossard, M., Boittin, M., Redini, F., & Pujol, J. P. (1999). Differential effects of interleukin-1 and transforming growth factor beta on the synthesis of small proteoglycans by rabbit articular chondrocytes cultured in alginate beads as compared to monolayers. *Mol Cell Biochem*, *199*(1-2), 69-80.
- Dente, L., Cesareni, G., & Cortese, R. (1983). pEMBL: a new family of single stranded plasmids. *Nucleic Acids Res*, *11*(6), 1645-1655.
- DeRamos, C., Irwin, A., Nauss, J., & Stout, B. (1997). 13C NMR and molecular modeling studies of alginic acid binding with alkaline earth and lanthanide metal ions. *Inorganica chimica acta*, *256*(1), 69-75.
- Diaz-Rodriguez, P., Rey-Rico, A., Madry, H., Landin, M., & Cucchiari, M. (2015). Effective genetic modification and differentiation of hMSCs upon controlled release of rAAV vectors using alginate/poloxamer composite systems. *Int J Pharm*, *496*(2), 614-626.
- DiCesare, P. E., Morgelin, M., Carlson, C. S., Pasumarti, S., & Paulsson, M. (1995). Cartilage oligomeric matrix protein: isolation and characterization from human articular cartilage. *J Orthop Res*, *13*(3), 422-428.
- Diduch, D. R., Jordan, L. C., Mierisch, C. M., & Balian, G. (2000). Marrow stromal cells embedded in alginate for repair of osteochondral defects. *Arthroscopy*, *16*(6), 571-577.
- Doege, K. J., Sasaki, M., Kimura, T., & Yamada, Y. (1991). Complete coding sequence and deduced primary structure of the human cartilage large aggregating proteoglycan, aggrecan. Human-specific repeats, and additional alternatively spliced forms. *J Biol Chem*, *266*(2), 894-902.
- Doherty, P. J., Zhang, H., Tremblay, L., Manolopoulos, V., & Marshall, K. W. (1998). Resurfacing of articular cartilage explants with genetically-modified human chondrocytes in vitro. *Osteoarthritis Cartilage*, *6*(3), 153-159.
- Dom, C., Schunke, M., Steinhagen, J., Freitag, S., & Kurz, B. (2004). Influence of various alginate brands on the redifferentiation of dedifferentiated bovine articular chondrocytes in alginate bead culture under high and low oxygen tension. *Tissue Eng*, *10*(11-12), 1796-1805.
- Dornish, M., Kaplan, D., & Skaugrud, O. (2001). Standards and guidelines for biopolymers in tissue-engineered medical products: ASTM alginate and chitosan standard guides. American Society for Testing and Materials. *Ann N Y Acad Sci*, *944*, 388-397.
- Dowthwaite, G. P., Bishop, J. C., Redman, S. N., Khan, I. M., Rooney, P., Evans, D. J., Houghton, L., Bayram, Z., Boyer, S., Thomson, B., Wolfe, M. S., & Archer, C. W. (2004). The surface of articular cartilage contains a progenitor cell population. *J Cell Sci*, *117*(Pt 6), 889-897.
- Drury, J. L., Dennis, R. G., & Mooney, D. J. (2004). The tensile properties of alginate hydrogels. *Biomaterials*, *25*(16), 3187-3199.
- Du, B., Wu, P., Boldt-Houle, D. M., & Terwilliger, E. F. (1996). Efficient transduction of human neurons with an adeno-associated virus vector. *Gene Ther*, *3*(3), 254-261.

- Enobakhare, B., Bader, D. L., & Lee, D. A. (2006). Concentration and M/G ratio influence the physiochemical and mechanical properties of alginate constructs for tissue engineering. *J Appl Biomater Biomech*, 4(2), 87-96.
- Evans, C. H., & Huard, J. (2015). Gene therapy approaches to regenerating the musculoskeletal system. *Nat Rev Rheumatol*, 11(4), 234-242.
- Fan, Y., Li, Y., Yao, X., Jin, J., Scott, A., Liu, B., Wang, S., Huo, L., Wang, Y., Wang, R., Pool Pizzi, M., Ma, L., Shao, S., Sewastjanow-Silva, M., Waters, R., Chatterjee, D., Liu, B., Shanbhag, N., Peng, G., Calin, G. A., Mazur, P. K., Hanash, S. M., Ishizawa, J., Hirata, Y., Nagano, O., Wang, Z., Wang, L., Xian, W., McKeon, F., Ajani, J. A., & Song, S. (2023). Epithelial SOX9 drives progression and metastases of gastric adenocarcinoma by promoting immunosuppressive tumour microenvironment. *Gut*, 72(4), 624-637.
- Fellows, C. R., Williams, R., Davies, I. R., Gohil, K., Baird, D. M., Fairclough, J., Rooney, P., Archer, C. W., & Khan, I. M. (2017). Characterisation of a divergent progenitor cell sub-populations in human osteoarthritic cartilage: the role of telomere erosion and replicative senescence. *Sci Rep*, 7, 41421.
- Flannery, C. R., Hughes, C. E., Schumacher, B. L., Tudor, D., Aydelotte, M. B., Kuettner, K. E., & Caterson, B. (1999). Articular cartilage superficial zone protein (SZP) is homologous to megakaryocyte stimulating factor precursor and is a multifunctional proteoglycan with potential growth-promoting, cytoprotective, and lubricating properties in cartilage metabolism. *Biochem Biophys Res Commun*, 254(3), 535-541.
- Flotte, T. R. (2004). Gene therapy progress and prospects: recombinant adeno-associated virus (rAAV) vectors. *Gene Ther*, 11(10), 805-810.
- Focaroli, S., Teti, G., Salvatore, V., Orienti, I., & Falconi, M. (2016). Calcium/cobalt alginate beads as functional scaffolds for cartilage tissue engineering. *Stem Cells Int*, 2016, 2030478.
- Frenkel, S. R., & Di Cesare, P. E. (1999). Degradation and repair of articular cartilage. *Front Biosci*, 4, D671-685.
- Frisch, J., Venkatesan, J. K., Rey-Rico, A., Schmitt, G., Madry, H., & Cucchiari, M. (2014). Determination of the chondrogenic differentiation processes in human bone marrow-derived mesenchymal stem cells genetically modified to overexpress transforming growth factor-beta via recombinant adeno-associated viral vectors. *Hum Gene Ther*, 25(12), 1050-1060.
- Frisch, J., Rey-Rico, A., Venkatesan, J. K., Schmitt, G., Madry, H., & Cucchiari, M. (2016a). rAAV-mediated overexpression of sox9, TGF-beta and IGF-I in minipig bone marrow aspirates to enhance the chondrogenic processes for cartilage repair. *Gene Ther*, 23(3), 247-255.
- Frisch, J., Rey-Rico, A., Venkatesan, J. K., Schmitt, G., Madry, H., & Cucchiari, M. (2016b). TGF-beta gene transfer and overexpression via rAAV vectors stimulates chondrogenic events in human bone marrow aspirates. *J Cell Mol Med*, 20(3), 430-440.
- Frisch, J., Orth, P., Venkatesan, J. K., Rey-Rico, A., Schmitt, G., Kohn, D., Madry, H., & Cucchiari, M. (2017). Genetic modification of human peripheral blood aspirates using recombinant adeno-associated viral vectors for articular cartilage repair with a focus on chondrogenic transforming growth factor-beta gene delivery. *Stem Cells Transl Med*, 6(1), 249-260.
- Gagne, T. A., Chappell-Afonso, K., Johnson, J. L., McPherson, J. M., Oldham, C. A., Tubo, R. A., Vaccaro, C., & Vasios, G. W. (2000). Enhanced proliferation and differentiation of human articular chondrocytes when seeded at low cell densities in alginate in vitro. *J Orthop Res*, 18(6), 882-890.
- Garza-Veloz, I., Romero-Diaz, V. J., Martinez-Fierro, M. L., Marino-Martinez, I. A., Gonzalez-Rodriguez, M., Martinez-Rodriguez, H. G., Espinoza-Juarez, M. A., Bernal-Garza, D. A., Ortiz-Lopez, R., & Rojas-Martinez, A. (2013). Analyses of chondrogenic induction of adipose mesenchymal stem cells by combined co-stimulation mediated by adenoviral gene transfer. *Arthritis Res Ther*, 15(4), R80.
- Gaumann, A., Laudes, M., Jacob, B., Pommersheim, R., Laue, C., Vogt, W., & Schrezenmeir, J. (2000). Effect of media composition on long-term in vitro stability of barium alginate and polyacrylic acid multilayer microcapsules. *Biomaterials*, 21(18), 1911-1917.
- Gelse, K., von der Mark, K., Aigner, T., Park, J., & Schneider, H. (2003). Articular cartilage repair by gene therapy using growth factor-producing mesenchymal cells. *Arthritis Rheum*, 48(2), 430-441.
- Gelse, K., Muhle, C., Knaup, K., Swoboda, B., Wiesener, M., Hennig, F., Olk, A., & Schneider, H. (2008). Chondrogenic differentiation of growth factor-stimulated precursor cells in cartilage repair tissue is associated with increased HIF-1alpha activity. *Osteoarthritis Cartilage*, 16(12), 1457-1465.

- Glass, K. A., Link, J. M., Brunger, J. M., Moutos, F. T., Gersbach, C. A., & Guilak, F. (2014). Tissue-engineered cartilage with inducible and tunable immunomodulatory properties. *Biomaterials*, *35*(22), 5921-5931.
- Glukhova, S. A., Molchanov, V. S., Lokshin, B. V., Rogachev, A. V., Tsarenko, A. A., Patsaev, T. D., Kamyshinsky, R. A., & Philippova, O. E. (2021). Printable alginate hydrogels with embedded network of halloysite nanotubes: effect of polymer cross-linking on rheological properties and microstructure. *Polymers (Basel)*, *13*(23), 4130-4145.
- Goh, C. H., Heng, P. W. S., & Chan, L. W. (2012). Alginates as a useful natural polymer for microencapsulation and therapeutic applications. *Carbohydrate Polymers*, *88*(1), 1-12.
- Goh, D., Yang, Y., Lee, E. H., Hui, J. H. P., & Yang, Z. (2023). Managing the heterogeneity of mesenchymal stem cells for cartilage regenerative therapy: a review. *Bioengineering (Basel)*, *10*(3).
- Goins, W. F., Hall, B., Cohen, J. B., & Glorioso, J. C. (2016). Retargeting of herpes simplex virus (HSV) vectors. *Curr Opin Virol*, *21*, 93-101.
- Goncalves Junior, R., Pinheiro Ada, R., Schoichet, J. J., Nunes, C. H., Goncalves, R., Bonato, L. L., Quinelato, V., Antunes, L. S., Kuchler, E. C., Lobo, J., Villas-Boas Rde, M., Vieira, A. R., Granjeiro, J. M., & Casado, P. L. (2016). MMP13, TIMP2 and TGFB3 gene polymorphisms in Brazilian chronic periodontitis and periimplantitis subjects. *Braz Dent J*, *27*(2), 128-134.
- Goomer, R. S., Maris, T. M., Gelberman, R., Boyer, M., Silva, M., & Amiel, D. (2000). Nonviral in vivo gene therapy for tissue engineering of articular cartilage and tendon repair. *Clin Orthop Relat Res*(379 Suppl), S189-200.
- Gouze, E., Pawliuk, R., Pilapil, C., Gouze, J. N., Fleet, C., Palmer, G. D., Evans, C. H., Leboulch, P., & Ghivizzani, S. C. (2002). In vivo gene delivery to synovium by lentiviral vectors. *Mol Ther*, *5*(4), 397-404.
- Grandolfo, M., D'Andrea, P., Paoletti, S., Martina, M., Silvestrini, G., Bonucci, E., & Vittur, F. (1993). Culture and differentiation of chondrocytes entrapped in alginate gels. *Calcif Tissue Int*, *52*(1), 42-48.
- Grogan, S. P., Chen, X., Sovani, S., Taniguchi, N., Colwell, C. W., Jr., Lotz, M. K., & D'Lima, D. D. (2014). Influence of cartilage extracellular matrix molecules on cell phenotype and neocartilage formation. *Tissue Eng Part A*, *20*(1-2), 264-274.
- Grunder, T., Gaissmaier, C., Fritz, J., Stoop, R., Hortschansky, P., Mollenhauer, J., & Aicher, W. K. (2004). Bone morphogenetic protein (BMP)-2 enhances the expression of type II collagen and aggrecan in chondrocytes embedded in alginate beads. *Osteoarthritis Cartilage*, *12*(7), 559-567.
- Guilak, F., Nims, R. J., Dicks, A., Wu, C. L., & Meulenbelt, I. (2018). Osteoarthritis as a disease of the cartilage pericellular matrix. *Matrix Biol*, *71-72*, 40-50.
- Guo, J. F., Jourdan, G. W., & MacCallum, D. K. (1989). Culture and growth characteristics of chondrocytes encapsulated in alginate beads. *Connect Tissue Res*, *19*(2-4), 277-297.
- Hacein-Bey-Abina, S., Garrigue, A., Wang, G. P., Soulier, J., Lim, A., Morillon, E., Clappier, E., Caccavelli, L., Delabesse, E., Beldjord, K., Asnafi, V., MacIntyre, E., Dal Cortivo, L., Radford, I., Brousse, N., Sigaux, F., Moshous, D., Hauer, J., Borkhardt, A., Belohradsky, B. H., Wintergerst, U., Velez, M. C., Leiva, L., Sorensen, R., Wulffraat, N., Blanche, S., Bushman, F. D., Fischer, A., & Cavazzana-Calvo, M. (2008). Insertional oncogenesis in 4 patients after retrovirus-mediated gene therapy of SCID-X1. *J Clin Invest*, *118*(9), 3132-3142.
- Hall, A. C., Horwitz, E. R., & Wilkins, R. J. (1996). The cellular physiology of articular cartilage. *Exp Physiol*, *81*(3), 535-545.
- Hanahan, D. (1983). Studies on transformation of Escherichia coli with plasmids. *J Mol Biol*, *166*(4), 557-580.
- Hasson, P., DeLaurier, A., Bennett, M., Grigorieva, E., Naiche, L. A., Papaioannou, V. E., Mohun, T. J., & Logan, M. P. (2010). Tbx4 and tbx5 acting in connective tissue are required for limb muscle and tendon patterning. *Dev Cell*, *18*(1), 148-156.
- Hattori, T., Muller, C., Gebhard, S., Bauer, E., Pausch, F., Schlund, B., Bosl, M. R., Hess, A., Surmann-Schmitt, C., von der Mark, H., de Crombrughe, B., & von der Mark, K. (2010a). SOX9 is a major negative regulator of cartilage vascularization, bone marrow formation and endochondral ossification. *Development*, *137*(6), 901-911.
- Hattori, T., Muller, C., Gebhard, S., Bauer, E., Pausch, F., Schlund, B., Bosl, M. R., Hess, A., Surmann-Schmitt, C., von der Mark, H., de Crombrughe, B., & von der Mark, K. (2010b). SOX9 is a major negative regulator of cartilage vascularization, bone marrow formation and endochondral ossification. *Development*, *137*(6), 901-911.
- Hauselmann, H. J., Aydelotte, M. B., Schumacher, B. L., Kuettner, K. E., Gitelis, S. H., & Thonar, E. J. (1992). Synthesis and turnover of proteoglycans by human and bovine adult articular chondrocytes cultured in alginate beads. *Matrix*, *12*(2), 116-129.
- Hauselmann, H. J., Fernandes, R. J., Mok, S. S., Schmid, T. M., Block, J. A., Aydelotte, M. B., Kuettner, K. E., & Thonar, E. J. (1994). Phenotypic stability of bovine articular chondrocytes after long-term culture in alginate beads. *J Cell Sci*, *107* ( Pt 1), 17-27.

- Hauselmann, H. J., Masuda, K., Hunziker, E. B., Neidhart, M., Mok, S. S., Michel, B. A., & Thonar, E. J. (1996). Adult human chondrocytes cultured in alginate form a matrix similar to native human articular cartilage. *Am J Physiol*, 271(3 Pt 1), C742-752.
- Hayashi, M., Ninomiya, Y., Parsons, J., Hayashi, K., Olsen, B. R., & Trelstad, R. L. (1986). Differential localization of mRNAs of collagen types I and II in chick fibroblasts, chondrocytes, and corneal cells by in situ hybridization using cDNA probes. *J Cell Biol*, 102(6), 2302-2309.
- Hayes, A. J., Hall, A., Brown, L., Tubo, R., & Caterson, B. (2007). Macromolecular organization and in vitro growth characteristics of scaffold-free neocartilage grafts. *J Histochem Cytochem*, 55(8), 853-866.
- Heiligenstein, S., Cucchiari, M., Laschke, M. W., Bohle, R. M., Kohn, D., Menger, M. D., & Madry, H. (2011a). In vitro and in vivo characterization of nonbiomedical- and biomedical-grade alginates for articular chondrocyte transplantation. *Tissue Eng Part C Methods*, 17(8), 829-842.
- Heiligenstein, S., Cucchiari, M., Laschke, M. W., Bohle, R. M., Kohn, D., Menger, M. D., & Madry, H. (2011b). Evaluation of nonbiomedical and biomedical grade alginates for the transplantation of genetically modified articular chondrocytes to cartilage defects in a large animal model in vivo. *J Gene Med*, 13(4), 230-242.
- Hernandez, Y. J., Wang, J., Kearns, W. G., Loiler, S., Poirier, A., & Flotte, T. R. (1999). Latent adeno-associated virus infection elicits humoral but not cell-mediated immune responses in a nonhuman primate model. *J Virol*, 73(10), 8549-8558.
- Herzog, W., & Federico, S. (2006). Considerations on joint and articular cartilage mechanics. *Biomech Model Mechanobiol*, 5(2-3), 64-81.
- Hicks, D. L., Sage, A. B., Shelton, E., Schumacher, B. L., Sah, R. L., & Watson, D. (2007). Effect of bone morphogenetic proteins 2 and 7 on septal chondrocytes in alginate. *Otolaryngol Head Neck Surg*, 136(3), 373-379.
- Hodgkinson, T., Wignall, F., Hoyland, J. A., & Richardson, S. M. (2020). High BMP2 expression leads to enhanced SMAD1/5/8 signalling and GDF6 responsiveness in human adipose-derived stem cells: implications for stem cell therapies for intervertebral disc degeneration. *J Tissue Eng*, 11, 2041731420919334.
- Homicz, M. R., Chia, S. H., Schumacher, B. L., Masuda, K., Thonar, E. J., Sah, R. L., & Watson, D. (2003). Human septal chondrocyte redifferentiation in alginate, polyglycolic acid scaffold, and monolayer culture. *Laryngoscope*, 113(1), 25-32.
- Honda, H., Fujimoto, M., Serada, S., Urushima, H., Mishima, T., Lee, H., Ohkawara, T., Kohno, N., Hattori, N., Yokoyama, A., & Naka, T. (2017). Leucine-rich alpha-2 glycoprotein promotes lung fibrosis by modulating TGF-beta signaling in fibroblasts. *Physiol Rep*, 5(24).
- Hu, K., Xu, L., Cao, L., Flahiff, C. M., Brussiau, J., Ho, K., Setton, L. A., Youn, I., Guilak, F., Olsen, B. R., & Li, Y. (2006). Pathogenesis of osteoarthritis-like changes in the joints of mice deficient in type IX collagen. *Arthritis Rheum*, 54(9), 2891-2900.
- Hu, Y., Wang, Q., Yu, J., Zhou, Q., Deng, Y., Liu, J., Zhang, L., Xu, Y., Xiong, W., & Wang, Y. (2022). Tartrate-resistant acid phosphatase 5 promotes pulmonary fibrosis by modulating beta-catenin signaling. *Nat Commun*, 13(1), 114.
- Huang, C. Y., Reuben, P. M., & Cheung, H. S. (2005). Temporal expression patterns and corresponding protein inductions of early responsive genes in rabbit bone marrow-derived mesenchymal stem cells under cyclic compressive loading. *Stem Cells*, 23(8), 1113-1121.
- Huang, T., Long, M., & Huo, B. (2010). Competitive binding to Cuprous ions of protein and BCA in the bicinchoninic acid protein assay. *Open Biomed Eng J*, 4, 271-278.
- Huang, C. C., Ravindran, S., Kang, M., Cooper, L. F., & George, A. (2020). Engineering a self-assembling leucine zipper hydrogel system with function-specific motifs for tissue regeneration. *ACS Biomater Sci Eng*, 6(5), 2913-2928.
- Hunt, N. C., & Grover, L. M. (2010). Cell encapsulation using biopolymer gels for regenerative medicine. *Biotechnol Lett*, 32(6), 733-742.
- Hunziker, E. B. (2002). Articular cartilage repair: basic science and clinical progress. A review of the current status and prospects. *Osteoarthritis Cartilage*, 10(6), 432-463.
- Hwang, N. S., Varghese, S., & Elisseeff, J. (2007). Cartilage tissue engineering: directed differentiation of embryonic stem cells in three-dimensional hydrogel culture. *Methods Mol Biol*, 407, 351-373.
- Ibraheem, D., Elaissari, A., & Fessi, H. (2014). Gene therapy and DNA delivery systems. *Int J Pharm*, 459(1-2), 70-83.

- Ikeda, T., Kamekura, S., Mabuchi, A., Kou, I., Seki, S., Takato, T., Nakamura, K., Kawaguchi, H., Ikegawa, S., & Chung, U. I. (2004). The combination of SOX5, SOX6, and SOX9 (the SOX trio) provides signals sufficient for induction of permanent cartilage. *Arthritis Rheum*, *50*(11), 3561-3573.
- Ishikawa, K., Ueyama, Y., Mano, T., Koyama, T., Suzuki, K., & Matsumura, T. (1999). Self-setting barrier membrane for guided tissue regeneration method: initial evaluation of alginate membrane made with sodium alginate and calcium chloride aqueous solutions. *J Biomed Mater Res*, *47*(2), 111-115.
- Jang, J., Seol, Y. J., Kim, H. J., Kundu, J., Kim, S. W., & Cho, D. W. (2014). Effects of alginate hydrogel cross-linking density on mechanical and biological behaviors for tissue engineering. *J Mech Behav Biomed Mater*, *37*, 69-77.
- Jay, F. T., Laughlin, C. A., & Carter, B. J. (1981). Eukaryotic translational control: adeno-associated virus protein synthesis is affected by a mutation in the adenovirus DNA-binding protein. *Proc Natl Acad Sci U S A*, *78*(5), 2927-2931.
- Jedidi, I., Ouchari, M., & Yin, Q. (2018). Autosomal single-gene disorders involved in human infertility. *Saudi J Biol Sci*, *25*(5), 881-887.
- Jiang, S., Guo, W., Tian, G., Luo, X., Peng, L., Liu, S., Sui, X., Guo, Q., & Li, X. (2020). Clinical application status of articular cartilage regeneration techniques: tissue-engineered cartilage brings new hope. *Stem Cells Int*, *2020*, 5690252.
- Jin, X., Sun, Y., Zhang, K., Wang, J., Shi, T., Ju, X., & Lou, S. (2007). Ectopic neocartilage formation from predifferentiated human adipose derived stem cells induced by adenoviral-mediated transfer of hTGF beta2. *Biomaterials*, *28*(19), 2994-3003.
- Johnstone, B., Hering, T. M., Caplan, A. I., Goldberg, V. M., & Yoo, J. U. (1998). In vitro chondrogenesis of bone marrow-derived mesenchymal progenitor cells. *Exp Cell Res*, *238*(1), 265-272.
- Jonitz, A., Lochner, K., Peters, K., Salamon, A., Pasold, J., Mueller-Hilke, B., Hansmann, D., & Bader, R. (2011). Differentiation capacity of human chondrocytes embedded in alginate matrix. *Connect Tissue Res*, *52*(6), 503-511.
- Kaul, G., Cucchiari, M., Arntzen, D., Zurakowski, D., Menger, M. D., Kohn, D., Trippel, S. B., & Madry, H. (2006). Local stimulation of articular cartilage repair by transplantation of encapsulated chondrocytes overexpressing human fibroblast growth factor 2 (FGF-2) in vivo. *J Gene Med*, *8*(1), 100-111.
- Kavanagh, E., & Ashhurst, D. E. (1999). Development and aging of the articular cartilage of the rabbit knee joint: Distribution of biglycan, decorin, and matrilin-1. *J Histochem Cytochem*, *47*(12), 1603-1616.
- Kempson, G. E., Muir, H., Pollard, C., & Tuke, M. (1973). The tensile properties of the cartilage of human femoral condyles related to the content of collagen and glycosaminoglycans. *Biochim Biophys Acta*, *297*(2), 456-472.
- Khalid, S., Ekram, S., Salim, A., Chaudhry, G. R., & Khan, I. (2022). Transcription regulators differentiate mesenchymal stem cells into chondroprogenitors, and their in vivo implantation regenerated the intervertebral disc degeneration. *World J Stem Cells*, *14*(2), 163-182.
- Khan, F., & Ahmad, S. R. (2013). Polysaccharides and their derivatives for versatile tissue engineering application. *Macromol Biosci*, *13*(4), 395-421.
- Knarston, I. M., Robevska, G., Van den Bergen, J. A., Eggers, S., Croft, B., Yates, J., Hersmus, R., Looijenga, L. H. J., Cameron, F. J., Monhike, K., Ayers, K. L., & Sinclair, A. H. (2019). NR5A1 gene variants repress the ovarian-specific WNT signaling pathway in 46,XX disorders of sex development patients. *Hum Mutat*, *40*(2), 207-216.
- Knight, M. M., Van de Breevaart Bravenboer, J., Lee, D. A., Van Osch, G. J., Weinans, H., & Bader, D. L. (2002). Cell and nucleus deformation in compressed chondrocyte-alginate constructs: temporal changes and calculation of cell modulus. *Biochim Biophys Acta*, *1570*(1), 1-8.
- Knudson, C. B. (1993). Hyaluronan receptor-directed assembly of chondrocyte pericellular matrix. *J Cell Biol*, *120*(3), 825-834.
- Kobayashi, A., Chang, H., Chaboissier, M. C., Schedl, A., & Behringer, R. R. (2005). Sox9 in testis determination. *Ann N Y Acad Sci*, *1061*, 9-17.
- Kokenyesi, R., Tan, L., Robbins, J. R., & Goldring, M. B. (2000). Proteoglycan production by immortalized human chondrocyte cell lines cultured under conditions that promote expression of the differentiated phenotype. *Arch Biochem Biophys*, *383*(1), 79-90.
- Komai, T., Okamura, T., Inoue, M., Yamamoto, K., & Fujio, K. (2018). Reevaluation of pluripotent cytokine TGF-beta3 in immunity. *Int J Mol Sci*, *19*(8).
- Kozhemyakina, E., Lassar, A. B., & Zelzer, E. (2015). A pathway to bone: signaling molecules and transcription factors involved in chondrocyte development and maturation. *Development*, *142*(5), 817-831.

- Kuettner, K. E., Aydelotte, M. B., & Thonar, E. J. (1991). Articular cartilage matrix and structure: a minireview. *J Rheumatol Suppl*, 27, 46-48.
- Kuettner, K. E. (1992). Biochemistry of articular cartilage in health and disease. *Clin Biochem*, 25(3), 155-163.
- Kwon, C., Cheng, P., King, I. N., Andersen, P., Shenje, L., Nigam, V., & Srivastava, D. (2011). Notch post-translationally regulates beta-catenin protein in stem and progenitor cells. *Nat Cell Biol*, 13(10), 1244-1251.
- Kwon, D. G., Kim, M. K., Jeon, Y. S., Nam, Y. C., Park, J. S., & Ryu, D. J. (2022). State of the art: the immunomodulatory role of MSCs for osteoarthritis. *Int J Mol Sci*, 23(3).
- Kyostio, S. R., Owens, R. A., Weitzman, M. D., Antoni, B. A., Chejanovsky, N., & Carter, B. J. (1994). Analysis of adeno-associated virus (AAV) wild-type and mutant Rep proteins for their abilities to negatively regulate AAV p5 and p19 mRNA levels. *J Virol*, 68(5), 2947-2957.
- Lange, C., Madry, H., Venkatesan, J. K., Schmitt, G., Speicher-Mentges, S., Zurakowski, D., Menger, M. D., Laschke, M. W., & Cucchiari, M. (2021). rAAV-mediated sox9 overexpression improves the repair of osteochondral defects in a clinically relevant large animal model over time in vivo and reduces perifocal osteoarthritic changes. *Am J Sports Med*, 49(13), 3696-3707.
- Lee, K. Y., & Mooney, D. J. (2012). Alginate: properties and biomedical applications. *Prog Polym Sci*, 37(1), 106-126.
- Lee, R. J., & Huang, L. (1997). Lipidic vector systems for gene transfer. *Crit Rev Ther Drug Carrier Syst*, 14(2), 173-206.
- Lee, H. J. (2018). The role of tripartite motif family proteins in TGF-beta signaling pathway and cancer. *J Cancer Prev*, 23(4), 162-169.
- Lefebvre, V., & Dvir-Ginzberg, M. (2017). SOX9 and the many facets of its regulation in the chondrocyte lineage. *Connect Tissue Res*, 58(1), 2-14.
- Lemare, F., Steimberg, N., Le Griel, C., Demignot, S., & Adolphe, M. (1998). Dedifferentiated chondrocytes cultured in alginate beads: restoration of the differentiated phenotype and of the metabolic responses to interleukin-1beta. *J Cell Physiol*, 176(2), 303-313.
- Li, H., Li, X., Jing, X., Li, M., Ren, Y., Chen, J., Yang, C., Wu, H., & Guo, F. (2018). Hypoxia promotes maintenance of the chondrogenic phenotype in rat growth plate chondrocytes through the HIF-1alpha/YAP signaling pathway. *Int J Mol Med*, 42(6), 3181-3192.
- Li, L., Yu, F., Zheng, L., Wang, R., Yan, W., Wang, Z., Xu, J., Wu, J., Shi, D., Zhu, L., Wang, X., & Jiang, Q. (2019). Natural hydrogels for cartilage regeneration: modification, preparation and application. *J Orthop Translat*, 17, 26-41.
- Li, R., Zhao, Y., Zheng, Z., Liu, Y., Song, S., Song, L., Ren, J., Dong, J., & Wang, P. (2023). Bioinks adapted for in situ bioprinting scenarios of defect sites: a review. *RSC Adv*, 13(11), 7153-7167.
- Liu, H., Lee, Y. W., & Dean, M. F. (1998). Re-expression of differentiated proteoglycan phenotype by dedifferentiated human chondrocytes during culture in alginate beads. *Biochim Biophys Acta*, 1425(3), 505-515.
- Liu, C. F., Samsa, W. E., Zhou, G., & Lefebvre, V. (2017). Transcriptional control of chondrocyte specification and differentiation. *Semin Cell Dev Biol*, 62, 34-49.
- Liu, L., Li, Q., Yang, L., Li, Q., & Du, X. (2021). SMAD4 feedback activates the canonical TGF-beta family signaling pathways. *Int J Mol Sci*, 22(18).
- Liu, W., Madry, H., & Cucchiari, M. (2022). Application of alginate hydrogels for next-generation articular cartilage regeneration. *Int J Mol Sci*, 23(3), 1147-1188.
- Loredo, G. A., Koolpe, M., & Benton, H. P. (1996). Influence of alginate polysaccharide composition and culture conditions on chondrocytes in three-dimensional culture. *Tissue Eng*, 2(2), 115-125.
- Loty, S., Sautier, J. M., Loty, C., Boulekbache, H., Kokubo, T., & Forest, N. (1998). Cartilage formation by fetal rat chondrocytes cultured in alginate beads: a proposed model for investigating tissue-biomaterial interactions. *J Biomed Mater Res*, 42(2), 213-222.
- Ma, H. L., Hung, S. C., Lin, S. Y., Chen, Y. L., & Lo, W. H. (2003). Chondrogenesis of human mesenchymal stem cells encapsulated in alginate beads. *J Biomed Mater Res A*, 64(2), 273-281.
- Mackay, A. M., Beck, S. C., Murphy, J. M., Barry, F. P., Chichester, C. O., & Pittenger, M. F. (1998). Chondrogenic differentiation of cultured human mesenchymal stem cells from marrow. *Tissue Eng*, 4(4), 415-428.
- Madry, H., & Trippel, S. B. (2000). Efficient lipid-mediated gene transfer to articular chondrocytes. *Gene Ther*, 7(4), 286-291.

- Madry, H., Cucchiari, M., Terwilliger, E. F., & Trippel, S. B. (2003a). Recombinant adeno-associated virus vectors efficiently and persistently transduce chondrocytes in normal and osteoarthritic human articular cartilage. *Hum Gene Ther*, 14(4), 393-402.
- Madry, H., Cucchiari, M., Stein, U., Remberger, K., Menger, M. D., Kohn, D., & Trippel, S. B. (2003b). Sustained transgene expression in cartilage defects in vivo after transplantation of articular chondrocytes modified by lipid-mediated gene transfer in a gel suspension delivery system. *J Gene Med*, 5(6), 502-509.
- Madry, H., Kaul, G., Cucchiari, M., Stein, U., Zurakowski, D., Remberger, K., Menger, M. D., Kohn, D., & Trippel, S. B. (2005). Enhanced repair of articular cartilage defects in vivo by transplanted chondrocytes overexpressing insulin-like growth factor I (IGF-I). *Gene Ther*, 12(15), 1171-1179.
- Madry, H., Van Dijk, C. N., & Mueller-Gerbl, M. (2010). The basic science of the subchondral bone. *Knee Surg Sports Traumatol Arthrosc*, 18(4), 419-433.
- Madry, H., Grun, U. W., & Knutsen, G. (2011a). Cartilage repair and joint preservation: medical and surgical treatment options. *Dtsch Arztebl Int*, 108(40), 669-677.
- Madry, H., Orth, P., & Cucchiari, M. (2011b). Gene therapy for cartilage repair. *Cartilage*, 2(3), 201-225.
- Madry, H., & Cucchiari, M. (2011). Clinical potential and challenges of using genetically modified cells for articular cartilage repair. *Croat Med J*, 52(3), 245-261.
- Madry, H., Rey-Rico, A., Venkatesan, J. K., Johnstone, B., & Cucchiari, M. (2014). Transforming growth factor Beta-releasing scaffolds for cartilage tissue engineering. *Tissue Eng Part B Rev*, 20(2), 106-125.
- Madry, H., & Cucchiari, M. (2016). Gene therapy for human osteoarthritis: principles and clinical translation. *Expert Opin Biol Ther*, 16(3), 331-346.
- Madry, H., Gao, L., Rey-Rico, A., Venkatesan, J. K., Muller-Brandt, K., Cai, X., Goebel, L., Schmitt, G., Speicher-Mentges, S., Zurakowski, D., Menger, M. D., Laschke, M. W., & Cucchiari, M. (2020a). Thermosensitive hydrogel based on PEO-PPO-PEO poloxamers for a controlled in situ release of recombinant adeno-associated viral vectors for effective gene therapy of cartilage defects. *Adv Mater*, 32(2), e1906508.
- Madry, H., Venkatesan, J. K., Carballo-Pedraes, N., Rey-Rico, A., & Cucchiari, M. (2020b). Scaffold-mediated gene delivery for osteochondral repair. *Pharmaceutics*, 12(10).
- Madry H. (2022). Surgical therapy in osteoarthritis. *Osteoarthritis and cartilage*, 30(8), 1019-1034.
- Maihofer, J., Madry, H., Rey-Rico, A., Venkatesan, J. K., Goebel, L., Schmitt, G., Speicher-Mentges, S., Cai, X., Meng, W., Zurakowski, D., Menger, M. D., Laschke, M. W., & Cucchiari, M. (2021). Hydrogel-guided, rAAV-mediated IGF-I overexpression enables long-term cartilage repair and protection against perifocal osteoarthritis in a large-animal full-thickness chondral defect model at one year in vivo. *Adv Mater*, 33(16), e2008451.
- Makris, E. A., Gomoll, A. H., Malizos, K. N., Hu, J. C., & Athanasiou, K. A. (2015). Repair and tissue engineering techniques for articular cartilage. *Nat Rev Rheumatol*, 11(1), 21-34.
- Mankin, H. J. (1974). The reaction of articular cartilage to injury and osteoarthritis (first of two parts). *N Engl J Med*, 291(24), 1285-1292.
- Mankin, H. J. (1982). The response of articular cartilage to mechanical injury. *J Bone Joint Surg Am*, 64(3), 460-466.
- Marijnissen, W. J., Van Osch, G. J., Aigner, J., Van der Veen, S. W., Hollander, A. P., Verwoerd-Verhoef, H. L., & Verhaar, J. A. (2002). Alginate as a chondrocyte-delivery substance in combination with a non-woven scaffold for cartilage tissue engineering. *Biomaterials*, 23(6), 1511-1517.
- Maroudas, A., Muir, H., & Wingham, J. (1969). The correlation of fixed negative charge with glycosaminoglycan content of human articular cartilage. *Biochim Biophys Acta*, 177(3), 492-500.
- Matheu, A., Collado, M., Wise, C., Manterola, L., Cekaite, L., Tye, A. J., Canamero, M., Bujanda, L., Schedl, A., Cheah, K. S., Skotheim, R. I., Lothe, R. A., Lopez de Munain, A., Briscoe, J., Serrano, M., & Lovell-Badge, R. (2012). Oncogenicity of the developmental transcription factor Sox9. *Cancer Res*, 72(5), 1301-1315.
- Matthew, I. R., Browne, R. M., Frame, J. W., & Millar, B. G. (1995). Subperiosteal behaviour of alginate and cellulose wound dressing materials. *Biomaterials*, 16(4), 275-278.
- Mbita, Z., Hull, R., & Dlamini, Z. (2014). Human immunodeficiency virus-1 (HIV-1)-mediated apoptosis: new therapeutic targets. *Viruses*, 6(8), 3181-3227.

- Meng, W., Rey-Rico, A., Claudel, M., Schmitt, G., Speicher-Mentges, S., Pons, F., Lebeau, L., Venkatesan, J. K., & Cucchiari, M. (2020). rAAV-mediated overexpression of SOX9 and TGF-beta via carbon dot-guided vector delivery enhances the biological activities in human bone marrow-derived mesenchymal stromal cells. *Nanomaterials (Basel)*, *10*(5).
- Mesure, B., Menu, P., Venkatesan, J. K., Cucchiari, M., & Velot, E. (2019). Biomaterials and gene therapy: a smart combination for MSC musculoskeletal engineering. *Curr Stem Cell Res Ther*, *14*(4), 337-343.
- Meyerrose, T. E., Roberts, M., Ohlemiller, K. K., Vogler, C. A., Wirthlin, L., Nolte, J. A., & Sands, M. S. (2008). Lentiviral-transduced human mesenchymal stem cells persistently express therapeutic levels of enzyme in a xenotransplantation model of human disease. *Stem Cells*, *26*(7), 1713-1722.
- Mhanna, R., Ozturk, E., Schlink, P., & Zenobi-Wong, M. (2013). Probing the microenvironmental conditions for induction of superficial zone protein expression. *Osteoarthritis Cartilage*, *21*(12), 1924-1932.
- Mierisch, C. M., Wilson, H. A., Turner, M. A., Milbrandt, T. A., Berthou, L., Hammarskjold, M. L., Rekosh, D., Balian, G., & Diduch, D. R. (2003). Chondrocyte transplantation into articular cartilage defects with use of calcium alginate: the fate of the cells. *J Bone Joint Surg Am*, *85*(9), 1757-1767.
- Miosge, N., Flachsbar, K., Goetz, W., Schultz, W., Kresse, H., & Herken, R. (1994). Light and electron microscopical immunohistochemical localization of the small proteoglycan core proteins decorin and biglycan in human knee joint cartilage. *Histochem J*, *26*(12), 939-945.
- Morscheid, S., Rey-Rico, A., Schmitt, G., Madry, H., Cucchiari, M., & Venkatesan, J. K. (2019a). Therapeutic effects of rAAV-mediated concomitant gene transfer and overexpression of TGF-beta and IGF-I on the chondrogenesis of human bone-marrow-derived mesenchymal stem cells. *Int J Mol Sci*, *20*(10).
- Morscheid, S., Venkatesan, J. K., Rey-Rico, A., Schmitt, G., & Cucchiari, M. (2019b). Remodeling of human osteochondral defects via rAAV-mediated co-overexpression of TGF-beta and IGF-I from implanted human bone marrow-derived mesenchymal stromal cells. *J Clin Med*, *8*(9).
- Muir, H., Bullough, P., & Maroudas, A. (1970). The distribution of collagen in human articular cartilage with some of its physiological implications. *J Bone Joint Surg Br*, *52*(3), 554-563.
- Muir, H. (1995). The chondrocyte, architect of cartilage. Biomechanics, structure, function and molecular biology of cartilage matrix macromolecules. *Bioessays*, *17*(12), 1039-1048.
- Murakami, S., Lefebvre, V., & de Crombrughe, B. (2000). Potent inhibition of the master chondrogenic factor Sox9 gene by interleukin-1 and tumor necrosis factor-alpha. *J Biol Chem*, *275*(5), 3687-3692.
- Murphy, J. M., Fink, D. J., Hunziker, E. B., & Barry, F. P. (2003). Stem cell therapy in a caprine model of osteoarthritis. *Arthritis Rheum*, *48*(12), 3464-3474.
- Nakai, H., Fuess, S., Storm, T. A., Muramatsu, S., Nara, Y., & Kay, M. A. (2005). Unrestricted hepatocyte transduction with adeno-associated virus serotype 8 vectors in mice. *J Virol*, *79*(1), 214-224.
- Naldini, L., Blomer, U., Gallay, P., Ory, D., Mulligan, R., Gage, F. H., Verma, I. M., & Trono, D. (1996). In vivo gene delivery and stable transduction of nondividing cells by a lentiviral vector. *Science*, *272*(5259), 263-267.
- Nam, H. Y., Park, J. H., Kim, K., Kwon, I. C., & Jeong, S. Y. (2009). Lipid-based emulsion system as non-viral gene carriers. *Arch Pharm Res*, *32*(5), 639-646.
- Naso, M. F., Tomkowicz, B., Perry, W. L., 3rd, & Strohl, W. R. (2017). Adeno-associated virus (AAV) as a vector for gene therapy. *BioDrugs*, *31*(4), 317-334.
- Nelson, M. E., Griffin, G. R., Innis, J. W., & Green, G. E. (2011). Campomelic dysplasia: airway management in two patients and an update on clinical-molecular correlations in the head and neck. *Ann Otol Rhinol Laryngol*, *120*(10), 682-685.
- Nelson, L., McCarthy, H. E., Fairclough, J., Williams, R., & Archer, C. W. (2014). Evidence of a viable pool of stem cells within human osteoarthritic cartilage. *Cartilage*, *5*(4), 203-214.
- Newman, A. P. (1998). Articular cartilage repair. *Am J Sports Med*, *26*(2), 309-324.
- Nishimura, R., Hata, K., Takahata, Y., Murakami, T., Nakamura, E., & Yagi, H. (2017). Regulation of cartilage development and diseases by transcription factors. *J Bone Metab*, *24*(3), 147-153.
- Nishimura, R., Hata, K., Nakamura, E., Murakami, T., & Takahata, Y. (2018). Transcriptional network systems in cartilage development and disease. *Histochem Cell Biol*, *149*(4), 353-363.

- Nixon, A. J., Brower-Toland, B. D., Bent, S. J., Saxer, R. A., Wilke, M. J., Robbins, P. D., & Evans, C. H. (2000). Insulinlike growth factor-I gene therapy applications for cartilage repair. *Clin Orthop Relat Res*(379 Suppl), S201-213.
- O'Driscoll, S. W. (1998). The healing and regeneration of articular cartilage. *J Bone Joint Surg Am*, 80(12), 1795-1812.
- Oláh, T., & Madry, H. (2018). The osteochondral unit: the importance of the underlying subchondral bone. In J. Farr & A. H. Gomoll (Eds.), *Cartilage Restoration: Practical Clinical Applications* (pp. 13-22). Springer International Publishing.
- Oláh, T., Kamarul, T., Madry, H., & Murali, M. R. (2021). The illustrative anatomy and the histology of the healthy hyaline cartilage. In D. R. Goyal (Ed.), *The Illustrative Book of Cartilage Repair* (pp. 5-10). Springer International Publishing.
- Oliveira Silva, M., Gregory, J. L., Ansari, N., & Stok, K. S. (2020). Molecular signaling interactions and transport at the osteochondral interface: a review. *Front Cell Dev Biol*, 8, 750.
- Orth, P., Weimer, A., Kaul, G., Kohn, D., Cucchiari, M., & Madry, H. (2008). Analysis of novel nonviral gene transfer systems for gene delivery to cells of the musculoskeletal system. *Mol Biotechnol*, 38(2), 137-144.
- Orth, P., Peifer, C., Goebel, L., Cucchiari, M., & Madry, H. (2015). Comprehensive analysis of translational osteochondral repair: Focus on the histological assessment. *Prog Histochem Cytochem*, 50(3), 19-36.
- Paige, K. T., & Vacanti, C. A. (1995). Engineering new tissue: formation of neo-cartilage. *Tissue Eng*, 1(2), 97-106.
- Paige, K. T., Cima, L. G., Yaremchuk, M. J., Schloo, B. L., Vacanti, J. P., & Vacanti, C. A. (1996). De novo cartilage generation using calcium alginate-chondrocyte constructs. *Plast Reconstr Surg*, 97(1), 168-178.
- Park, H., Kang, S. W., Kim, B. S., Mooney, D. J., & Lee, K. Y. (2009). Shear-reversibly crosslinked alginate hydrogels for tissue engineering. *Macromol Biosci*, 9(9), 895-901.
- Pearle, A. D., Warren, R. F., & Rodeo, S. A. (2005). Basic science of articular cartilage and osteoarthritis. *Clin Sports Med*, 24(1), 1-12.
- Petit, B., Masuda, K., D'Souza, A. L., Otten, L., Pietryla, D., Hartmann, D. J., Morris, N. P., Uebelhart, D., Schmid, T. M., & Thonar, E. J. (1996). Characterization of crosslinked collagens synthesized by mature articular chondrocytes cultured in alginate beads: comparison of two distinct matrix compartments. *Exp Cell Res*, 225(1), 151-161.
- Platt, D., Wells, T., & Bayliss, M. T. (1997). Proteoglycan metabolism of equine articular chondrocytes cultured in alginate beads. *Res Vet Sci*, 62(1), 39-47.
- Podsakoff, G., Wong, K. K., Jr., & Chatterjee, S. (1994). Efficient gene transfer into nondividing cells by adeno-associated virus-based vectors. *J Virol*, 68(9), 5656-5666.
- Ponnazhagan, S., Mukherjee, P., Yoder, M. C., Wang, X. S., Zhou, S. Z., Kaplan, J., Wadsworth, S., & Srivastava, A. (1997). Adeno-associated virus 2-mediated gene transfer in vivo: organ-tropism and expression of transduced sequences in mice. *Gene*, 190(1), 203-210.
- Poole, A. R., Pidoux, I., Reiner, A., & Rosenberg, L. (1982). An immunoelectron microscope study of the organization of proteoglycan monomer, link protein, and collagen in the matrix of articular cartilage. *J Cell Biol*, 93(3), 921-937.
- Poole, C. A., Ayad, S., & Schofield, J. R. (1988). Chondrons from articular cartilage: I. Immunolocalization of type VI collagen in the pericellular capsule of isolated canine tibial chondrons. *J Cell Sci*, 90 ( Pt 4), 635-643.
- Poole, C. A., Glant, T. T., & Schofield, J. R. (1991). Chondrons from articular cartilage. (IV). Immunolocalization of proteoglycan epitopes in isolated canine tibial chondrons. *J Histochem Cytochem*, 39(9), 1175-1187. <https://doi.org/10.1177/39.9.1717545>
- Poole, C. A., Ayad, S., & Gilbert, R. T. (1992). Chondrons from articular cartilage. V. Immunohistochemical evaluation of type VI collagen organisation in isolated chondrons by light, confocal and electron microscopy. *J Cell Sci*, 103 ( Pt 4), 1101-1110.
- Poole, A. R., Rosenberg, L. C., Reiner, A., Ionescu, M., Bogoch, E., & Roughley, P. J. (1996). Contents and distributions of the proteoglycans decorin and biglycan in normal and osteoarthritic human articular cartilage. *J Orthop Res*, 14(5), 681-689.
- Poole, C. A., Gilbert, R. T., Herbage, D., & Hartmann, D. J. (1997). Immunolocalization of type IX collagen in normal and spontaneously osteoarthritic canine tibial cartilage and isolated chondrons. *Osteoarthritis Cartilage*, 5(3), 191-204.
- Poole, A. R., Kojima, T., Yasuda, T., Mwale, F., Kobayashi, M., & Laverty, S. (2001). Composition and structure of articular cartilage: a template for tissue repair. *Clin Orthop Relat Res*(391 Suppl), S26-33.
- Poree, B., Kyriotou, M., Chadjichristos, C., Beauchef, G., Renard, E., Legendre, F., Melin, M., Gueret, S., Hartmann, D. J., Mallein-Gerin, F., Pujol, J. P., Boumediene, K., & Galera, P. (2008). Interleukin-6 (IL-6) and/or soluble IL-6 receptor down-regulation of human type II collagen gene expression in articular chondrocytes requires a decrease of Sp1.Sp3 ratio and of the binding activity of both factors to the COL2A1 promoter. *J Biol Chem*, 283(8), 4850-4865.

- Qadir, A., Gao, Y., Suryaji, P., Tian, Y., Lin, X., Dang, K., Jiang, S., Li, Y., Miao, Z., & Qian, A. (2019). Non-viral delivery system and targeted bone disease therapy. *Int J Mol Sci*, *20*(3).
- Qin, X., Jiang, Q., Nagano, K., Moriishi, T., Miyazaki, T., Komori, H., Ito, K., Mark, K. V., Sakane, C., Kaneko, H., & Komori, T. (2020). Runx2 is essential for the transdifferentiation of chondrocytes into osteoblasts. *PLoS Genet*, *16*(11), e1009169.
- Rabie, M. A., Sayed, R. H., Venkatesan, J. K., Madry, H., Cucchiari, M., & El Sayed, N. S. (2023). Intra-articular injection of rAAV-hFGF-2 ameliorates monosodium iodoacetate-induced osteoarthritis in rats via inhibiting TLR-4 signaling and activating TIMP-1. *Toxicol Appl Pharmacol*, *459*, 116361.
- Ragan, P. M., Chin, V. I., Hung, H. H., Masuda, K., Thonar, E. J., Arner, E. C., Grodzinsky, A. J., & Sandy, J. D. (2000). Chondrocyte extracellular matrix synthesis and turnover are influenced by static compression in a new alginate disk culture system. *Arch Biochem Biophys*, *383*(2), 256-264.
- Rai, M. F., Hashimoto, S., Johnson, E. E., Janiszak, K. L., Fitzgerald, J., Heber-Katz, E., Cheverud, J. M., & Sandell, L. J. (2012). Heritability of articular cartilage regeneration and its association with ear wound healing in mice. *Arthritis Rheum*, *64*(7), 2300-2310.
- Rai, R., Alwani, S., & Badea, I. (2019). Polymeric nanoparticles in gene therapy: new avenues of design and optimization for delivery applications. *Polymers (Basel)*, *11*(4).
- Reinhard, J., Olah, T., Laschke, M. W., Goebel, L. K. H., Schmitt, G., Speicher-Mentges, S., Menger, M. D., Cucchiari, M., Pape, D., & Madry, H. (2024). Modulation of early osteoarthritis by tibiofemoral re-alignment in sheep. *Osteoarthritis Cartilage*.
- Remst, D. F., Blaney Davidson, E. N., Vitters, E. L., Bank, R. A., Van den Berg, W. B., & Van der Kraan, P. M. (2014). TGF- $\beta$  induces Lysyl hydroxylase 2b in human synovial osteoarthritic fibroblasts through ALK5 signaling. *Cell Tissue Res*, *355*(1), 163-171.
- Ren, L., Feng, X., Ma, D., Chen, F., & Ding, Y. (2012). Mechanical properties of alginate hydrogels with different concentrations and their effects on the proliferation chondrocytes in vitro. *Sheng Wu Yi Xue Gong Cheng Xue Za Zhi*, *29*(5), 884-888.
- Rey-Rico, A., Frisch, J., Venkatesan, J. K., Schmitt, G., Madry, H., & Cucchiari, M. (2015a). Determination of effective rAAV-mediated gene transfer conditions to support chondrogenic differentiation processes in human primary bone marrow aspirates. *Gene Ther*, *22*(1), 50-57.
- Rey-Rico, A., Venkatesan, J. K., Sohler, J., Moroni, L., Cucchiari, M., & Madry, H. (2015b). Adapted chondrogenic differentiation of human mesenchymal stem cells via controlled release of TGF- $\beta$ 1 from poly(ethylene oxide)-terephthalate/poly(butylene terephthalate) multiblock scaffolds. *J Biomed Mater Res A*, *103*(1), 371-383.
- Rey-Rico, A., Venkatesan, J. K., Frisch, J., Schmitt, G., Monge-Marcet, A., Lopez-Chicon, P., Mata, A., Semino, C., Madry, H., & Cucchiari, M. (2015c). Effective and durable genetic modification of human mesenchymal stem cells via controlled release of rAAV vectors from self-assembling peptide hydrogels with a maintained differentiation potency. *Acta Biomater*, *18*, 118-127.
- Rey-Rico, A., Venkatesan, J. K., Frisch, J., Rial-Hermida, I., Schmitt, G., Concheiro, A., Madry, H., Alvarez-Lorenzo, C., & Cucchiari, M. (2015d). PEO-PPO-PEO micelles as effective rAAV-mediated gene delivery systems to target human mesenchymal stem cells without altering their differentiation potency. *Acta Biomaterialia*, *27*, 42-52.
- Rey-Rico, A., & Cucchiari, M. (2016a). Controlled release strategies for rAAV-mediated gene delivery. *Acta Biomater*, *29*, 1-10.
- Rey-Rico, A., & Cucchiari, M. (2016b). Recent tissue engineering-based advances for effective rAAV-mediated gene transfer in the musculoskeletal system. *Bioengineered*, *7*(3), 175-188.
- Rey-Rico, A., Madry, H., & Cucchiari, M. (2016a). Hydrogel-based controlled delivery systems for articular cartilage repair. *Biomed Res Int*, *2016*, 1215263-1215275.
- Rey-Rico, A., Frisch, J., Venkatesan, J. K., Schmitt, G., Rial-Hermida, I., Taboada, P., Concheiro, A., Madry, H., Alvarez-Lorenzo, C., & Cucchiari, M. (2016b). PEO-PPO-PEO carriers for rAAV-mediated transduction of human articular chondrocytes in vitro and in a human osteochondral defect model. *ACS Appl Mater Interfaces*, *8*(32), 20600-20613.
- Rey-Rico, A., Venkatesan, J. K., Schmitt, G., Concheiro, A., Madry, H., Alvarez-Lorenzo, C., & Cucchiari, M. (2017). rAAV-mediated overexpression of TGF- $\beta$  via vector delivery in polymeric micelles stimulates the biological and reparative activities of human articular chondrocytes in vitro and in a human osteochondral defect model. *Int J Nanomedicine*, *12*, 6985-6996.
- Rey-Rico, A., Venkatesan, J. K., Schmitt, G., Speicher-Mentges, S., Madry, H., & Cucchiari, M. (2018). Effective remodelling of human osteoarthritic cartilage by sox9 gene transfer and overexpression upon delivery of rAAV vectors in polymeric micelles. *Mol Pharm*, *15*(7), 2816-2826.

- Robbins, P. D., Tahara, H., & Ghivizzani, S. C. (1998). Viral vectors for gene therapy. *Trends Biotechnol*, 16(1), 35-40.
- Robbins, P. D., & Ghivizzani, S. C. (1998). Viral vectors for gene therapy. *Pharmacol Ther*, 80(1), 35-47.
- Ross, K. A., Ferati, S. R., Alaia, M. J., Kennedy, J. G., & Strauss, E. J. (2024). Current and Emerging Techniques in Articular Cartilage Repair. *Bull Hosp Jt Dis* (2013), 82(1), 91-99.
- Saltz, A., & Kandalam, U. (2016). Mesenchymal stem cells and alginate microcarriers for craniofacial bone tissue engineering: A review. *J Biomed Mater Res A*, 104(5), 1276-1284.
- Samuel, S., Ahmad, R. E., Ramasamy, T. S., Manan, F., & Kamarul, T. (2018). Platelet rich concentrate enhances mesenchymal stem cells capacity to repair focal cartilage injury in rabbits. *Injury*, 49(4), 775-783.
- Samulski, R. J., Chang, L. S., & Shenk, T. (1987). A recombinant plasmid from which an infectious adeno-associated virus genome can be excised in vitro and its use to study viral replication. *J Virol*, 61(10), 3096-3101.
- Samulski, R. J., Chang, L. S., & Shenk, T. (1989). Helper-free stocks of recombinant adeno-associated viruses: normal integration does not require viral gene expression. *J Virol*, 63(9), 3822-3828.
- Sandell, L. J., & Aigner, T. (2001). Articular cartilage and changes in arthritis. An introduction: cell biology of osteoarthritis. *Arthritis Res*, 3(2), 107-113.
- Schumacher, B. L., Block, J. A., Schmid, T. M., Aydelotte, M. B., & Kuettner, K. E. (1994). A novel proteoglycan synthesized and secreted by chondrocytes of the superficial zone of articular cartilage. *Arch Biochem Biophys*, 311(1), 144-152.
- Schumacher, B. L., Hughes, C. E., Kuettner, K. E., Caterson, B., & Aydelotte, M. B. (1999). Immunodetection and partial cDNA sequence of the proteoglycan, superficial zone protein, synthesized by cells lining synovial joints. *J Orthop Res*, 17(1), 110-120.
- Schuurman, W., Gawlitta, D., Klein, T. J., ten Hoope, W., Van Rijen, M. H., Dhert, W. J., Van Weeren, P. R., & Malda, J. (2009). Zonal chondrocyte subpopulations reacquire zone-specific characteristics during in vitro redifferentiation. *Am J Sports Med*, 37 Suppl 1, 97S-104S.
- Shakibaei, M., & De Souza, P. (1997). Differentiation of mesenchymal limb bud cells to chondrocytes in alginate beads. *Cell Biol Int*, 21(2), 75-86.
- Shen, J., Li, J., Wang, B., Jin, H., Wang, M., Zhang, Y., Yang, Y., Im, H. J., O'Keefe, R., & Chen, D. (2013). Deletion of the transforming growth factor beta receptor type II gene in articular chondrocytes leads to a progressive osteoarthritis-like phenotype in mice. *Arthritis Rheum*, 65(12), 3107-3119.
- Siczkowski, M., & Watt, F. M. (1990). Subpopulations of chondrocytes from different zones of pig articular cartilage. Isolation, growth and proteoglycan synthesis in culture. *J Cell Sci*, 97 ( Pt 2), 349-360.
- Silva, C. M., Ribeiro, A. J., Figueiredo, I. V., Goncalves, A. R., & Veiga, F. (2006). Alginate microspheres prepared by internal gelation: development and effect on insulin stability. *Int J Pharm*, 311(1-2), 1-10.
- Smidsrød, O., & Skjåk-Braek, G. (1990). Alginate as immobilization matrix for cells. *Trends Biotechnol*, 8(3), 71-78.
- Sophia Fox, A. J., Bedi, A., & Rodeo, S. A. (2009). The basic science of articular cartilage: structure, composition, and function. *Sports Health*, 1(6), 461-468.
- Steinert, A. F., Palmer, G. D., Pilapil, C., Noth, U., Evans, C. H., & Ghivizzani, S. C. (2009). Enhanced in vitro chondrogenesis of primary mesenchymal stem cells by combined gene transfer. *Tissue Eng Part A*, 15(5), 1127-1139.
- Stockwell, R. A. (1978). Chondrocytes. *J Clin Pathol Suppl (R Coll Pathol)*, 12, 7-13.
- Su, Q., Fan, M., Wang, J., Ullah, A., Ghauri, M. A., Dai, B., Zhan, Y., Zhang, D., & Zhang, Y. (2019). Sanguinarine inhibits epithelial-mesenchymal transition via targeting HIF-1alpha/TGF-beta feed-forward loop in hepatocellular carcinoma. *Cell Death Dis*, 10(12), 939.
- Sum, C. H., Shortall, S. M., Wong, S., & Wettig, S. D. (2018). Non-viral gene delivery. *Exp Suppl*, 110, 3-68.
- Sun, J., & Tan, H. (2013). Alginate-based biomaterials for regenerative medicine applications. *Materials (Basel)*, 6(4), 1285-1309.
- SundarRaj, N., Fite, D., Ledbetter, S., Chakravarti, S., & Hassell, J. R. (1995). Perlecan is a component of cartilage matrix and promotes chondrocyte attachment. *J Cell Sci*, 108 ( Pt 7), 2663-2672.
- Symon, A., & Harley, V. (2017). SOX9: A genomic view of tissue specific expression and action. *Int J Biochem Cell Biol*, 87, 18-22.
- Takahashi, N., Knudson, C. B., Thankamony, S., Ariyoshi, W., Mellor, L., Im, H. J., & Knudson, W. (2010). Induction of CD44 cleavage in articular chondrocytes. *Arthritis Rheum*, 62(5), 1338-1348.

- Takka, S., & Gurel, A. (2010). Evaluation of chitosan/alginate beads using experimental design: formulation and in vitro characterization. *AAPS PharmSciTech*, *11*(1), 460-466.
- Tao, K., Frisch, J., Rey-Rico, A., Venkatesan, J. K., Schmitt, G., Madry, H., Lin, J., & Cucchiari, M. (2016a). Co-overexpression of TGF-beta and SOX9 via rAAV gene transfer modulates the metabolic and chondrogenic activities of human bone marrow-derived mesenchymal stem cells. *Stem Cell Res Ther*, *7*, 20.
- Tao, K., Rey-Rico, A., Frisch, J., Venkatesan, J. K., Schmitt, G., Madry, H., Lin, J., & Cucchiari, M. (2016b). rAAV-mediated combined gene transfer and overexpression of TGF-beta and SOX9 remodels human osteoarthritic articular cartilage. *J Orthop Res*, *34*(12), 2181-2190.
- Tao, K., Rey-Rico, A., Frisch, J., Venkatesan, J. K., Schmitt, G., Madry, H., Lin, J., & Cucchiari, M. (2017). Effects of combined rAAV-mediated TGF-beta and sox9 gene transfer and overexpression on the metabolic and chondrogenic activities in human bone marrow aspirates. *J Exp Orthop*, *4*(1), 4.
- Thielen, N. G. M., Van der Kraan, P. M., & Van Caam, A. P. M. (2019). TGFbeta/BMP signaling pathway in cartilage homeostasis. *Cells*, *8*(9).
- Thomas, C. E., Ehrhardt, A., & Kay, M. A. (2003). Progress and problems with the use of viral vectors for gene therapy. *Nat Rev Genet*, *4*(5), 346-358.
- Tigli, R. S., & Gumusderelioglu, M. (2009). Evaluation of alginate-chitosan semi IPNs as cartilage scaffolds. *J Mater Sci Mater Med*, *20*(3), 699-709.
- Tominaga, K., & Suzuki, H. I. (2019). TGF-beta signaling in cellular senescence and aging-related pathology. *Int J Mol Sci*, *20*(20).
- Tonni, G., Ventura, A., Pattacini, P., Bonasoni, M. P., & Baffico, A. M. (2013). p.His165Pro: a novel SOX9 missense mutation of campomelic dysplasia. *J Obstet Gynaecol Res*, *39*(5), 1085-1091.
- Topuz, F., Henke, A., Richter, W., & Groll, J. (2012). Magnesium ions and alginate do form hydrogels: a rheological study. *Soft Matter*, *8*(18), 4877-4881.
- Tu, L., Lin, Z., Huang, Q., & Liu, D. (2021). USP15 enhances the proliferation, migration, and collagen deposition of hypertrophic scar-derived fibroblasts by deubiquitinating TGF-betaR1 in vitro. *Plast Reconstr Surg*, *148*(5), 1040-1051.
- Ulrich-Vinther, M., Maloney, M. D., Schwarz, E. M., Rosier, R., & O'Keefe, R. J. (2003). Articular cartilage biology. *J Am Acad Orthop Surg*, *11*(6), 421-430.
- Ulrich-Vinther, M., Duch, M. R., Soballe, K., O'Keefe, R. J., Schwarz, E. M., & Pedersen, F. S. (2004). In vivo gene delivery to articular chondrocytes mediated by an adeno-associated virus vector. *J Orthop Res*, *22*(4), 726-734.
- Ulrich, J., Cucchiari, M., & Rey-Rico, A. (2020). Therapeutic delivery of rAAV sox9 via polymeric micelles counteracts the effects of osteoarthritis-associated inflammatory cytokines in human articular chondrocytes. *Nanomaterials (Basel)*, *10*(6).
- Van der Kraan, P. M. (2017). The changing role of TGFbeta in healthy, ageing and osteoarthritic joints. *Nat Rev Rheumatol*, *13*(3), 155-163.
- Van Osch, G. J., Van den Berg, W. B., Hunziker, E. B., & Hauselmann, H. J. (1998a). Differential effects of IGF-1 and TGF beta-2 on the assembly of proteoglycans in pericellular and territorial matrix by cultured bovine articular chondrocytes. *Osteoarthritis Cartilage*, *6*(3), 187-195.
- Van Osch, G. J., Van der Veen, S. W., Buma, P., & Verwoerd-Verhoef, H. L. (1998b). Effect of transforming growth factor-beta on proteoglycan synthesis by chondrocytes in relation to differentiation stage and the presence of pericellular matrix. *Matrix Biol*, *17*(6), 413-424.
- Van Susante, J. L., Buma, P., Van Osch, G. J., Versleyen, D., Van der Kraan, P. M., Van der Berg, W. B., & Homminga, G. N. (1995). Culture of chondrocytes in alginate and collagen carrier gels. *Acta Orthop Scand*, *66*(6), 549-556.
- Vanderploeg, E. J., Wilson, C. G., & Levenston, M. E. (2008). Articular chondrocytes derived from distinct tissue zones differentially respond to in vitro oscillatory tensile loading. *Osteoarthritis Cartilage*, *16*(10), 1228-1236.
- Varshney, R. R., Zhou, R., Hao, J., Yeo, S. S., Chooi, W. H., Fan, J., & Wang, D. A. (2010). Chondrogenesis of synovium-derived mesenchymal stem cells in gene-transferred co-culture system. *Biomaterials*, *31*(26), 6876-6891.
- Vedadghavami, A., Hakim, B., He, T., & Bajpayee, A. G. (2022). Cationic peptide carriers enable long-term delivery of insulin-like growth factor-1 to suppress osteoarthritis-induced matrix degradation. *Arthritis Res Ther*, *24*(1), 172.

- Venkatesan, J. K., Ekici, M., Madry, H., Schmitt, G., Kohn, D., & Cucchiari, M. (2012). SOX9 gene transfer via safe, stable, replication-defective recombinant adeno-associated virus vectors as a novel, powerful tool to enhance the chondrogenic potential of human mesenchymal stem cells. *Stem Cell Res Ther*, 3(3), 22.
- Venkatesan, J. K., Rey-Rico, A., Schmitt, G., Wezel, A., Madry, H., & Cucchiari, M. (2013). rAAV-mediated overexpression of TGF-beta stably restructures human osteoarthritic articular cartilage in situ. *J Transl Med*, 11, 211.
- Venkatesan, J. K., Frisch, J., Rey-Rico, A., Schmitt, G., Madry, H., & Cucchiari, M. (2017). Impact of mechanical stimulation on the chondrogenic processes in human bone marrow aspirates modified to overexpress sox9 via rAAV vectors. *J Exp Orthop*, 4(1), 22.
- Venkatesan, J. K., Gardner, O., Rey-Rico, A., Eglin, D., Alini, M., Stoddart, M. J., Cucchiari, M., & Madry, H. (2018a). Improved chondrogenic differentiation of rAAV SOX9-modified human MSCs seeded in fibrin-polyurethane scaffolds in a hydrodynamic environment. *Int J Mol Sci*, 19(9).
- Venkatesan, J. K., Moutos, F. T., Rey-Rico, A., Estes, B. T., Frisch, J., Schmitt, G., Madry, H., Guilak, F., & Cucchiari, M. (2018b). Chondrogenic differentiation processes in human bone-marrow aspirates seeded in three-dimensional-woven poly(epsilon-caprolactone) scaffolds enhanced by recombinant adeno-associated virus-mediated SOX9 gene transfer. *Hum Gene Ther*, 29(11), 1277-1286.
- Venkatesan, J. K., Meng, W., Rey-Rico, A., Schmitt, G., Speicher-Mentges, S., Falentin-Daudre, C., Leroux, A., Madry, H., Migonney, V., & Cucchiari, M. (2020a). Enhanced chondrogenic differentiation activities in human bone marrow aspirates via sox9 overexpression mediated by pNaSS-grafted PCL film-guided rAAV gene transfer. *Pharmaceutics*, 12(3).
- Venkatesan, J. K., Falentin-Daudre, C., Leroux, A., Migonney, V., & Cucchiari, M. (2020b). Biomaterial-guided recombinant adeno-associated virus delivery from poly(sodium styrene sulfonate)-grafted poly(epsilon-caprolactone) films to target human bone marrow aspirates. *Tissue Eng Part A*, 26(7-8), 450-459.
- Venkatesan, J. K., Cai, X., Meng, W., Rey-Rico, A., Schmitt, G., Speicher-Mentges, S., Falentin-Daudre, C., Leroux, A., Madry, H., Migonney, V., & Cucchiari, M. (2021). pNaSS-grafted PCL film-guided rAAV TGF-beta gene therapy activates the chondrogenic activities in human bone marrow aspirates. *Hum Gene Ther*, 32(17-18), 895-906.
- Venkatesan, J. K., Schmitt, G., Speicher-Mentges, S., Orth, P., Madry, H., & Cucchiari, M. (2022). Effects of recombinant adeno-associated virus-mediated overexpression of bone morphogenetic protein 3 on the chondrogenic fate of human bone marrow-derived mesenchymal stromal cells. *Hum Gene Ther*, 33(17-18), 950-958.
- von der Mark, H., von der Mark, K., & Gay, S. (1976). Study of differential collagen synthesis during development of the chick embryo by immunofluorescence. I. Preparation of collagen type I and type II specific antibodies and their application to early stages of the chick embryo. *Dev Biol*, 48(2), 237-249.
- Wan, L. Q., Jiang, J., Arnold, D. E., Guo, X. E., Lu, H. H., & Mow, V. C. (2008). Calcium concentration effects on the mechanical and biochemical properties of chondrocyte-alginate constructs. *Cell Mol Bioeng*, 1(1), 93-102.
- Wang, L., Shelton, R. M., Cooper, P. R., Lawson, M., Triffitt, J. T., & Barralet, J. E. (2003). Evaluation of sodium alginate for bone marrow cell tissue engineering. *Biomaterials*, 24(20), 3475-3481.
- Wang, Y., De Isla, N., Decot, V., Marchal, L., Cauchois, G., Huselstein, C., Muller, S., Wang, B. H., Netter, P., & Stoltz, J. F. (2008). Influences of construct properties on the proliferation and matrix synthesis of dedifferentiated chondrocytes cultured in alginate gel. *Biorheology*, 45(3-4), 527-538.
- Wang, L., Huang, J., Moore, D. C., Zuo, C., Wu, Q., Xie, L., von der Mark, K., Yuan, X., Chen, D., Warman, M. L., Ehrlich, M. G., & Yang, W. (2017). SHP2 regulates the osteogenic fate of growth plate hypertrophic chondrocytes. *Sci Rep*, 7(1), 12699.
- Wang, S., Wei, X., Sun, X., Chen, C., Zhou, J., Zhang, G., Wu, H., Guo, B., & Wei, L. (2018). A novel therapeutic strategy for cartilage diseases based on lipid nanoparticle-RNAi delivery system. *Int J Nanomedicine*, 13, 617-631.
- Wang, Y. F., Dang, H. F., Luo, X., Wang, Q. Q., Gao, C., & Tian, Y. X. (2021). Downregulation of SOX9 suppresses breast cancer cell proliferation and migration by regulating apoptosis and cell cycle arrest. *Oncol Lett*, 22(1), 517.
- Welton, K. L., Logterman, S., Bartley, J. H., Vidal, A. F., & McCarty, E. C. (2018). Knee cartilage repair and restoration: common problems and solutions. *Clin Sports Med*, 37(2), 307-330.
- Whyte, W. A., Orlando, D. A., Hnisz, D., Abraham, B. J., Lin, C. Y., Kagey, M. H., Rahl, P. B., Lee, T. I., & Young, R. A. (2013). Master transcription factors and mediator establish super-enhancers at key cell identity genes. *Cell*, 153(2), 307-319.

- Widuchowski, W., Widuchowski, J., & Trzaska, T. (2007). Articular cartilage defects: study of 25,124 knee arthroscopies. *Knee*, *14*(3), 177-182.
- Williams, R., Khan, I. M., Richardson, K., Nelson, L., McCarthy, H. E., Anabalsi, T., Singhrao, S. K., Dowthwaite, G. P., Jones, R. E., Baird, D. M., Lewis, H., Roberts, S., Shaw, H. M., Dudhia, J., Fairclough, J., Briggs, T., & Archer, C. W. (2010). Identification and clonal characterisation of a progenitor cell sub-population in normal human articular cartilage. *PLoS One*, *5*(10), e13246.
- Wilusz, R. E., Sanchez-Adams, J., & Guilak, F. (2014). The structure and function of the pericellular matrix of articular cartilage. *Matrix Biol*, *39*, 25-32.
- Wolff, L. I., & Hartmann, C. (2019). A second career for chondrocytes-transformation into osteoblasts. *Curr Osteoporos Rep*, *17*(3), 129-137.
- Wong, M., Wuethrich, P., Eggli, P., & Hunziker, E. (1996). Zone-specific cell biosynthetic activity in mature bovine articular cartilage: a new method using confocal microscopic stereology and quantitative autoradiography. *J Orthop Res*, *14*(3), 424-432.
- Wong, M., Siegrist, M., Wang, X., & Hunziker, E. (2001). Development of mechanically stable alginate/chondrocyte constructs: effects of guluronic acid content and matrix synthesis. *J Orthop Res*, *19*(3), 493-499.
- Wong, M. (2004). Alginates in tissue engineering. *Methods Mol Biol*, *238*, 77-86.
- Wu, S., Suzuki, Y., Tanihara, M., Ohnishi, K., Endo, K., & Nishimura, Y. (2002). Repair of facial nerve with alginate sponge without suturing: an experimental study in cats. *Scand J Plast Reconstr Surg Hand Surg*, *36*(3), 135-140.
- Wu, Z., Asokan, A., & Samulski, R. J. (2006). Adeno-associated virus serotypes: vector toolkit for human gene therapy. *Mol Ther*, *14*(3), 316-327.
- Wu, Q., Kim, K. O., Sampson, E. R., Chen, D., Awad, H., O'Brien, T., Puzas, J. E., Drissi, H., Schwarz, E. M., O'Keefe, R. J., Zuscik, M. J., & Rosier, R. N. (2008). Induction of an osteoarthritis-like phenotype and degradation of phosphorylated Smad3 by Smurf2 in transgenic mice. *Arthritis Rheum*, *58*(10), 3132-3144.
- Wu, Z., Yang, H., & Colosi, P. (2010). Effect of genome size on AAV vector packaging. *Mol Ther*, *18*(1), 80-86.
- Wu, Y., Li, J., Kong, Y., Chen, D., Liu, B., & Wang, W. (2013). HSV-1 based vector mediated IL-1 $\alpha$  gene for knee osteoarthritis in rabbits. *Zhong Nan Da Xue Xue Bao Yi Xue Ban*, *38*(6), 590-596.
- Xu, K., Zhang, Q., Zhu, D., & Jiang, Z. (2024). Hydrogels in Gene Delivery Techniques for Regenerative Medicine and Tissue Engineering. *Macromol Biosci*, e2300577.
- Yamane, S., Cheng, E., You, Z., & Reddi, A. H. (2007). Gene expression profiling of mouse articular and growth plate cartilage. *Tissue Eng*, *13*(9), 2163-2173.
- Yang, X., Guo, L., Fan, Y., & Zhang, X. (2013). Preparation and characterization of macromolecule cross-linked collagen hydrogels for chondrocyte delivery. *Int J Biol Macromol*, *61*, 487-493.
- Yang, R., Chen, F., Guo, J., Zhou, D., & Luan, S. (2020). Recent advances in polymeric biomaterials-based gene delivery for cartilage repair. *Bioact Mater*, *5*(4), 990-1003.
- Yang, W., Zhao, Q., Yao, M., Li, X., Shan, Z., & Wang, Y. (2022). The transformation of atrial fibroblasts into myofibroblasts is promoted by trimethylamine N-oxide via the Wnt3a/beta-catenin signaling pathway. *J Thorac Dis*, *14*(5), 1526-1536.
- Ye, J., Xu, B., Fan, B., Zhang, J., Yuan, F., Chen, Y., Sun, Z., Yan, X., Song, Y., Song, S., Yang, M., & Yu, J. K. (2020). Discovery of selenocysteine as a potential nanomedicine promotes cartilage regeneration with enhanced immune response by text mining and biomedical databases. *Front Pharmacol*, *11*, 1138.
- Yue, Y., & Dongsheng, D. (2002). Development of multiple cloning site cis-vectors for recombinant adeno-associated virus production. *Biotechniques*, *33*(3), 672, 674, 676-678.
- Zhang, W., Xia, Y., Ling, Y., Yang, W., Dong, Z. X., Wang, D. A., & Fan, C. (2020). A transcriptome sequencing study on genome-wide gene expression differences of 3D cultured chondrocytes in hydrogel scaffolds with different gel density. *Macromol Biosci*, *20*(5), e2000028.
- Zhang, Y., Sun, L., Liu, X., Zhu, D., Dang, J., Xue, Y., & Fan, H. (2021). Investigating the protective effect of tanshinone IIA against chondrocyte dedifferentiation: a combined molecular biology and network pharmacology approach. *Ann Transl Med*, *9*(3), 249.
- Zhao, Q., Eberspaecher, H., Lefebvre, V., & De Crombrughe, B. (1997). Parallel expression of Sox9 and Col2a1 in cells undergoing chondrogenesis. *Dev Dyn*, *209*(4), 377-386.

- Zhou, Q., Zhang, J. H., Yuan, S., Shao, J. H., Cai, Z. Y., Chen, S., Cao, J., Wu, H. S., & Qian, Q. R. (2019). A new insight of kartogenin induced the mesenchymal stem cells (MSCs) selectively differentiate into chondrocytes by activating the bone morphogenetic protein 7 (BMP-7)/Smad5 pathway. *Med Sci Monit*, 25, 4960-4967.
- Zmora, S., Glicklis, R., & Cohen, S. (2002). Tailoring the pore architecture in 3-D alginate scaffolds by controlling the freezing regime during fabrication. *Biomaterials*, 23(20), 4087-4094.
- Zou, M. L., Chen, Z. H., Teng, Y. Y., Liu, S. Y., Jia, Y., Zhang, K. W., Sun, Z. L., Wu, J. J., Yuan, Z. D., Feng, Y., Li, X., Xu, R. S., & Yuan, F. L. (2021). The Smad dependent TGF-beta and BMP signaling pathway in bone remodeling and therapies. *Front Mol Biosci*, 8, 593310.

## 11. PUBLICATIONS AND PRESENTATIONS

### 11.1. Publications

**Liu W**, Madry H, Cucchiari M. Application of alginate hydrogels for next-generation articular cartilage regeneration. *International Journal of Molecular Sciences*, 2022, 23(3), 1147. [impact factor: 5.6]

**Liu W**, Venkatesan JK, Amini M, Oláh T, Schmitt G, Madry H, Cucchiari M. Effects of rAAV-mediated overexpression of *sox9* and TGF- $\beta$  via alginate hydrogel-guided vector delivery on the chondroregenerative activities of human bone marrow-derived mesenchymal stromal cells. *Journal of Tissue Engineering and Regenerative Medicine*, 2023, 4495697. [impact factor: 4.3]

Venkatesan JK, **Liu W**, Madry H, Cucchiari M. Alginate hydrogel-guided rAAV-mediated FGF-2 and TGF- $\beta$  delivery and overexpression stimulates the biological activities of human meniscal fibrochondrocytes for meniscus repair. *European Cells and Materials*. 2024, 47, 1-14. [impact factor: 3.1]

Amini M, Venkatesan JK, **Liu W**, Leroux A, Nguyen TN, Madry H, Migonney V, Cucchiari M. Advanced gene therapy strategies for the repair of ACL injuries. *International Journal of Molecular Sciences*. 2022, 23(22), 14467. [impact factor: 5.6]

Amini M, Venkatesan JK, Nguyen TN, **Liu W**, Leroux A, Madry H, Migonney V, Cucchiari M. rAAV TGF- $\beta$  and FGF-2 overexpression via pNaSS-grafted PCL films stimulates the reparative activities of human ACL fibroblasts. *International Journal of Molecular Sciences*, 2023, 24(13), 11140. [impact factor: 5.6]

### 11.2. Oral presentations

**Liu W**, Madry H, Cucchiari M. Application of alginate hydrogels for next-generation articular cartilage regeneration. *Cartilage Net Congress 2023*, Saarbrücken, Saarland, Germany

### 11.3. Poster presentations

**Liu W**, Venkatesan JK, Schmitt G, Sahin E, Dahhan O, Madry H, Cucchiariini M. Stimulation of the reparative activities in human chondral defects upon rAAV-mediated overexpression of *sox9* and TGF- $\beta$  via vector delivery in an alginate-based hydrogel. 70<sup>th</sup> Annual Meeting of the Orthopaedics Research Society (ORS), Poster 658, 2024, Long Beach, CA, USA

**Liu W**, Venkatesan JK, Schmitt G, Madry H, Cucchiariini M. Stimulation of the chondroreparative activities of human osteoarthritic articular chondrocytes upon overexpression of *sox9* and TGF- $\beta$  via rAAV gene vector delivery in an alginate-based hydrogel. *OARSI 2023 World Congress*, S403-404, Denver, CO, USA

**Liu W**, Venkatesan JK, Schmitt G, Speicher-Mentges S, Madry H, Cucchiariini M. Stimulation of the biological and chondroreparative activities of human bone marrow-derived stromal cells upon overexpression of *sox9* and TGF- $\beta$  via rAAV gene vector delivery in an alginate-based hydrogel. *OARSI 2022 World Congress*, S423-S424, Berlin, Germany

**Liu W**, Venkatesan JK, Schmitt G, Speicher-Mentges S, Madry H, Cucchiariini M. rAAV-mediated overexpression of *sox9* and TGF- $\beta$  upon vector delivery in an alginate-based hydrogel stimulates the biological and chondroreparative activities of human bone marrow-derived stromal cells. 68<sup>th</sup> Annual Meeting of the Orthopaedics Research Society (ORS), Poster 648, 2022, Tampa, FL, USA

**Liu W**, Venkatesan JK, Wang D, Schmitt G, Sahin E, Dahhan O, Madry H, Cucchiariini M. Effects of alginate hydrogel-guided rAAV-mediated *sox9* and TGF- $\beta$  overexpression on the repair processes of experimental human chondral defects *in situ*. *OARSI 2024 World Congress*, Vienna, Austria (Accepted)

Wang D, **Liu W**, Venkatesan JK, Schmitt G, Beninatto R, Galesso D, Madry H, Cucchiariini M. Effective and durable genetic modification of reparative human bone marrow-derived stromal cells via photopolymerizable hyaluronic acid hydrogel-guided rAAV-mediated gene therapy. *OARSI 2024 World Congress*, Vienna, Austria (Accepted)

Wang D, **Liu W**, Venkatesan JK, Schmitt G, Beninatto R, Galesso D, Madry H, Cucchiariini M. Stimulation of the activities of human osteoarthritic articular chondrocytes via photopolymerizable hyaluronic acid hydrogel-guided rAAV-mediated overexpression of *sox9* and TGF-beta. *OARSI 2024 World Congress*, Vienna, Austria (Accepted)

Amini M, Shamma RN, **Liu W**, Ali NA, Wang D, Venkatesan JK, Schmitt G, Madry H, Cucchiariini M. Effects of rAAV-mediated gene transfer delivered via a hyalosome-diacerein hydrogel on the activities of human osteoarthritic articular chondrocytes. *OARSI 2024 World Congress*, Vienna, Austria (Accepted)

## 12. ACKNOWLEDGEMENTS

The present research was conducted at the Center of Experimental Orthopaedics at Saarland University.

From the depths of my heart, I express my gratitude to **Prof. Dr. rer. nat. Magali Cucchiarini Madry**. Entrusting me with such an attractive doctoral subject has been a pivotal moment in my academic journey. Her meticulous guidance and steadfast patience illuminated every corner of my research period. Each constructive feedback and consistent scientific dialogue she shared not only enriched the content but also continually fueled my passion for the subject. Moreover, her encouraging personal conversations have been a beacon of hope and motivation, holding a cherished place at the hard time of in my life. My mind is brimming with gratitude for **Prof. Dr. med. Henning Madry**, who generously co-supervised this work. His astute insights and deep expertise were not just guiding lights in my academic career, but his consistent availability for both scientific thinking and personal concerns has been a source of immeasurable comfort and strength. Furthermore, the magnitude of his support to my family is truly immeasurable and he is much more than just a supervisor to me in my heart and mind.

I wish to express my heartfelt gratitude to **Dr. rer. nat. Jagadeesh K. Venkatesan, Dr. rer. nat. Mahnaz Amini, Dr. rer. nat. Tamás Oláh**, and **Dr. rer. nat. Mohammadsaeid Enayati**. Their expertise and invaluable guidance during the experiments were instrumental in achieving my goals. Their warmth and efforts in fostering a nurturing working environment made me feel truly integrated and valued in our laboratory team. Co-working with them making every moment spent in the lab both memorable and fulfilling. I want to express my heartfelt gratitude to **Ms. Gertrud Schmitt, Mrs. Susanne Speicher-Mentges, Ms. Ebrar Sahin**, and **Mrs. Ola Dahhan**. Their unwavering dedication and meticulous approach to laboratory work have not only facilitated my progress but have also been an invaluable learning experience for me. Their timely assistance in the midst of our experiments were instrumental that I will always cherish. I owe an immeasurable debt of gratitude to **Mrs. Sonja Ramin**. Her invaluable assistance in streamlining documentation and formalities lightened my workload and provided me with support in navigating the intricacies of daily tasks.

I would also like to credit my friends, **Dr. Xiaoyu Cai, Dr. Weikun Meng, Dr. Gang Zhong**, and **Dr. Liang Gao** who have consistently gone above and beyond, taking care of me and assisting me in countless ways. Many thanks to my parents, **Jixi Liu** and **Liping Wang**, my wife, **Dr. Dan Wang**: thank you very much for your unwavering support, deep concern, and boundless love in the past few years, which are the sources of my strength. I am forever grateful. Finally, I extend my heartfelt gratitude to the China Scholarship Council (CSC) and the Graduate Center of Saarland University (GradUS) for the funding opportunity to support my research.

## **13. CURRICULUM VITAE**

The curriculum vitae was removed from the electronic version of the doctoral thesis for reasons of data protection.